ACOUSTICALLY DRIVEN AIR VIBRATION IN CAVITY AND ITS APPLICATION TO SOUND BARRIERS

NG HO TING

PhD

The Hong Kong Polytechnic University

2019

The Hong Kong Polytechnic University

Department of Building Services Engineering

Acoustically Driven Air Vibration in Cavity and Its Application to Sound Barriers

Ng Ho Ting

A thesis submitted in partial fulfillment of the requirements for the degree of Doctor of Philosophy

July 2017

Certificate of Originality

I hereby declare that this thesis is my own work and that, to the best of my knowledge and belief, it reproduces no material previously published or written, nor material that has been accepted for the award of any other degree or diploma, except where due acknowledgement has been made in the text.

(Signed)

Ng Ho Ting (Name of Student)

Abstract

Abstract of thesis entitled: Acoustically driven air vibration in cavity and its application to sound barriers

Submitted by : NG HO TING

For the degree of: Doctor of Philosophy

at The Hong Kong Polytechnic University in February 2019.

Recently, due to rapid urban development and increasing population in modern cities, main traffic roads are closed to residential regions and lead to serious noise pollution. The annoyance from traffic noise brings health problems to citizens such as sleep disturbance, hypertension, and even ischemic heart diseases. Thus, road traffic noise becomes one of the critical problems in modern cities.

Many acoustical researchers, environmental engineers and scientists pay more concerns on traffic noise problems and seek related solutions. One of the common solutions is to locate an obstacle between traffic road and residential region, which is so-called noise barrier. Based on the physical phenomenon of sound propagation, noise barrier can achieve high noise attenuation at shadow zone by blocking the direct propagation path from noise source to receiver. However, noise barrier has its limitation on low frequency noise due to the high diffractive efficiency of the latter. Low frequency noise attenuation level is thus poor. Improvement of the noise attenuation of noise barrier has then become a main research focus. Theoretical and experimental investigations have been

conducted for half a century. It is found that barrier dimension and shape of barrier top edge would affect noise attenuation efficiency. Because of space limitation in densely populated cities, increasing the size of noise barrier is not a good solution to improve noise reduction performance of noise barrier. Different barrier top edge designs are then considered to achieve higher noise attenuation.

From recent researches (Maekawa,1968) (Seznec,1980) (Watts,1996) (Ishizuka and Fujiwara,2004), numerical and experimental results also show that the general T-shape, Y-shape and cranked barrier can provide good noise attenuation the same as that of a higher and thicker barrier. If absorption material is added on the top edge of these barriers, noise reduction performance can be further improved. However, the performance of absorption materials always depends on atmospheric conditions and decrease dramatically in a short period after exposing to bad atmospheric environment. Diffusive barrier is then proposed to reduce noise by sound diffraction at barrier leading edge instead of absorption by absorption material. Different diffusive barrier designs are proposed in recent researches (such as Lam, 1994) to optimize the noise reduction performance.

Moreover, studies on resonator (Ingard, 1953) (Tang, 1973) have been conducted for decades. Although the noise attenuation level of resonator is frequency dependent, the effective frequency range can be enlarged by using multiple resonators together (Doria, 1995) (Griffin,2001) (XU,2010). Therefore, a noise barrier associated with resonator is then being considered in this study.

The major objectives of this study are to investigate the spatial behavior of sound behind barrier and noise attenuation performance of noise barrier with acoustic cavities on its top edge. In this research, measurements are carried out to indicate the relation of noise attenuation to the following parameters, which are dimension of cavity, arrangement of cavities, number of cavities used and location of cavity. Numerical computations are done in Chapter 4. The results show that the noise attenuation performance of a conventional vertical barrier is improved by adding a single acoustic cavity on its top edge especially at the resonance frequencies of acoustic cavity. In addition, the results also show that the magnitude of Insertion Loss depends on the location of acoustic cavity. When the distance between barrier leading edge and acoustic cavity is decreased, the magnitude of Insertion Loss is increased without influencing resonance frequency.

Analysis of experimental results is shown in Chapter 5. The noise attenuation performance by different cavity arrangements is then investigated. Transfer function is used in these analyses to obtain the insertion loss. Conclusion can be drawn from overall experimental results that the separation from the cavity to the leading edge affects the magnitude of Insertion Loss significantly. Moreover, the resonance frequency of noise barrier is controlled by cavity depth especially at low frequency.

Acknowledgements

I would like to express my grateful acknowledgement to the persons listed below in the Building Services Engineering Department and Mechanical Engineering Department of the Hong Kong Polytechnic University for their valuable advices and assistance in my research project.

I wish to give a special thanks to my chief supervisor Prof. Tang Siu Keung and co-supervisor Dr. Choy Yat Sze. They always provide me guidelines and suggestions when the problems are encountered during this study.

I also express my sincere thanks to Mr. Chan Kwok Wah and Dr. Ng Chun Hung, the technicians of Acoustic Laboratory, who allocates the instruments for measurements. Moreover, thanks for their advice and assistance on the noise measurement and the instructions for using the apparatus.

Special thanks for the patience and support of my family. Their support and recognition give me strength to finish this thesis.

Table of Contents

List of Figures

List of Tables

Glossary of Terms

Variable	Meaning
Att	The attenuation level of noise
$\mathrm{Att_s}$	The measure of position from receiver to source
$\mathrm{Att_b}$	The measure of the proximity of source or receiver from half plane
$\mathrm{Att_{sb}}$	A measure of proximity of receiver to shadow boundary
$\mathrm{Att_{sp}}$	The diffraction effect of spherical incident wave
c_s	The speed of sound in medium
$\mathrm{H}_1^{(1)}$	The Hankel function of first kind
H(u)	Heaviside step function
I	The strength of pressure perturbation in the incident wave
IL	Insertion Loss
k	The wavenumber of incident sound wave
L	The scaled width if PML
L_i	The sound level at receiver by ith source
$\Delta\mathrm{L_i}$	The sound attenuation of barrier calculated by ith point source
N_r	Engine speed(rpm)

n	The scaling exponent for each PML
p_d	Diffracted sound field
p_i	Incident sound field
p_r	Reflected sound field
p_T	Transmitted sound field
Q	Monopole source
q	The term of dipole source with the dimension of force per volume
r	The distance from enter line of barrier to the surface of barrier
R	The strength of the pressure perturbation in the reflected wave
R_1	The distance between source and image source to the receiver 1
R_2	The distance between source and image source to the receiver 2
R'	The shortest distance from source to receiver through the top edge of wedge
T	The strength of pressure perturbation in transmitted wave
ν	The displacement volume of engine (cm^3)

υ The wedge index

ρ_0 the density of fluid

ς_1 The sign function which corresponding to angle θ and distance R in x direction

ς_2 The sign function which corresponding to angle θ and distance R in y direction

ς_i The sound path between source S_0, image source, S'_0 receiver R_0 and image receiver R'_0

Γ_1 The surface of aperture above the screen

Γ_2 The surface of thin screen

δ_1 Path difference, the difference from direct path from source to receiver and the path from source to receiver via the top edge of barrier

λ The wavelength of the sound wave

ξ The coordinate transformation

ξ_0 The coordinate of the inner PML boundary

Chapter 1: Introduction and Outlines

1.1 Objectives and background

Noise is regarded as unwanted sound. Traffic noise has always been one of the main environmental problems in the communities because of its psychological effects on human living quality (Kryter, 1985). In Ancient Rome and Medieval Europe, there were rules to prevent noise emitted by horse carriages and any ironed wheels battered the stones on pavement during nighttime. Nowadays, Noise Control Ordinance is proposed in many highly populated cities such as Hong Kong to reduce transportation noise. From "Spatial Distribution of Traffic Noise Problem in Hong Kong", published by the Hong Kong Environmental Protection Department in 2015, there are still nearly 1 million residents suffering from excess traffic noise (above 70 dBA in L_{A10} within 1 hour) in Hong Kong. Due to the poor planning in the past in old town and lack of available land space in Hong Kong, main roads and highways are built closed to residential buildings. People are exposed to high noise level, which causes interference with daily activities and even degrades sleep quality of people. Kin (2012) found that 26.2 % of Hong Kong populations are exposed to a noise higher than 65 dBA at their dwellings, with a further 7.9 % and other 4.13 % highly annoyed and highly sleep disturbed. The conclusion indicated that Hong Kong is one of the Asian cities suffering from serious transportation noise.

Traffic noise control has been studied extensively (Rathe, 1969) (Delany, 1972) (Sandberg, 1979) (Hothersall, 1992). There are several ways to attenuate traffic noise. In new developing area, a more careful design on city planning and a complete public transportation system can reduce traffic noise effectively. Other than that, noise attenuation measures are used to limit the spread of noise. The easiest way is to block direct sound propagation path from noise source to receiver to reduce the noise level at receiver side. Construction of roadside noise barriers between sound sources and noise sensitive receivers are then proposed for use in Hong Kong. Noise barrier attenuates noise by extending the propagation path for sound wave travelling from source to receiver and setting up a shadow zone behind barrier by blocking the direct propagation path. It can be seen that a higher barrier can provide better noise attenuation by extending the sound propagation path and enlarging the shadow zone. However, it is impossible to build an infinite barrier. Balance should be made between construction requirements and acoustic concerns. Therefore, different types of roadside noise barrier are developed such as curved edge barriers, inclined barriers, louvered barriers, cylindrical edge barriers and multiple-edge barriers.

In recent studies (Yamamoto, 1989) (Yamashita, 1990) (Watts, 1994) (Ishizuka and Fujiwara, 2004), different mitigation measures, such as absorbing materials, were added on the barrier top edge to improve noise attenuation. It is found that adding absorbing materials can improve the noise attenuation of barrier by 3-5 dB at low frequency. However, absorbing materials are unreliable in practical use. Efficiency of the materials will decrease rapidly in a short period since they are highly sensitive to rain, mist and other air contaminants such as dust. Therefore, people are looking for a barrier design which can provide high attenuation at low frequency and is less environmental dependence.

The major objectives of this research are to investigate the noise attenuation performance of barrier with different acoustic cavities on its top edge and the spatial behavior of sound behind barrier. Numerical studies and scale-model experiments are carried out to determine the performance of different barrier designs. Performance of noise barrier can be indicated by Insertion Loss (IL). To determine the effect of acoustic cavities only, the experiments are conducted in an anechoic chamber to maintain a homogeneous atmosphere so that environmental effects, such as atmosphere reflection and turbulence scattering on the results, can be ignored. Environmental effects are discussed in Chapter 2, but not in the later part of this thesis in detail.

1.2 Structure of thesis

There are six chapters in this thesis. The outline of this thesis is as follows:

In Chapter 1, a brief description on the background of traffic noise problem in Hong Kong is presented. Although noise barrier is commonly used to solve road traffic noise problem, it has poor noise attenuation at low frequencies. Therefore, the main objective of this study is to investigate the noise attenuation performance of barrier with acoustic cavity. It is expected that acoustic cavity can improve noise attenuation performance in low frequency range, which is the weakest link of existing barriers. The findings of present research show that acoustic cavities give a significant improvement (2-6 dB) on noise attenuation at their resonance frequencies. At the last part of this chapter, a summary of the outline of this thesis is provided.

In Chapter 2, literature review on related studies of road traffic noise, modeling methods of noise barrier and the performance of noise barriers in different top edge design are presented. Also, environmental factors, such as ground effect and meteorological effects, on barrier noise attenuation are reviewed in this chapter. In order to investigate the noise attenuation performance of acoustic cavities on noise barrier, scale model experiment and numerical simulation are carried out in a fully anechoic environment to avoid any atmospheric effects on the results in this study.

Chapter 3 introduces the theories used in present study to determine the resonance frequency of acoustic cavity and performance of noise barrier. The basic mechanism on noise attenuation by barrier is mentioned in this chapter. The general analytical formula for calculating resonance frequency of acoustic cavities is given to validate the result obtained from both computations and experiments. At the last part of this chapter, indexes used to analyze noise attenuation performance of barrier in this study are presented.

Chapter 4 gives an introduction of the present numerical study which includes the settings of boundary conditions, testing domain and noise source. A series of simulations has been conducted using two-dimensional Finite Element Method (FEM) by the software Comsol Multiphysic. Investigation on the effect of different acoustic cavity parameters is done. Significant improvements at specific frequency which match the acoustic mode number of cavities can be obtained from results. In addition, the relationship between cavity parameters, such as cavity depth, location of cavity and arrangements of acoustic cavities, and noise attenuation performance of barrier are investigated in detail. These results are also used to compare with experimental results presented in Chapter 5 for further analysis.

In Chapter 5, a detailed introduction of scale model experiments is presented which include the dimension of tested models, configuration of scale-model experiments, instruments connecting network and the detail of instruments used in this study. Several experiments are conducted to investigate the relationship between barrier noise attenuation and different acoustic cavity parameters, and also the spatial behavior of sound by capturing the total sound field behind barrier. Results are then analyzed and verified with the numerical results presented in Chapter 4. A summary of noise attenuation level and spatial behavior of barrier with acoustic cavities is given in the last section in this chapter.

Chapter 6 is the last part of this thesis. Conclusion of the whole study is made. All the findings during this study are summarized and the suggestions and recommendations on further works are discussed.

Chapter 2: Literature Review

In recent years, traffic noise becomes an important concern in most countries and studies about traffic noise have been carried out by many researchers (Canelli, 1974, Ko, 1978, Chakrabarty et.al. 1997, Onuu, 2000, Sommerhoff et. Al., 2004). It is found that excessive noise exposure can affect the human hearing and even permanent damage the hearing threshold (Kryter, 1985). Therefore, studies on barrier are needed to reduce the influence on human being by traffic noise.

2.1 Studies on road traffic noise

In general, road traffic noise is the combination noise of vehicle engine noise, exhaust pipe noise, tire noise and aerodynamic noise. In this Section, the detail of engine noise, tire noise and noise from exhaust pipe are discussed since they are the main source of general road traffic noise.

Engine noise is generated by the vibration at explosion process of vehicle engine during operation. The variation of noise level from engine noise is depending on the operation loading. It can be 10dB higher from full load mode to no-load condition. Although the noise generated by different engine is not same due to various design of engine structure. The common frequency range of engine noise is low frequency which around 100-500 Hz.

Tire noise is another noise source which makes a high contribution to general road traffic noise. It is generated by tire vibration and the contact between tire and road surface. The noise level of tire noise is then directly proportional to the speed of car. Tire noise is found to be dominant at car speed around 40-50 km/h. (Sandberg, 1979). The frequency range of tire noise for normal small vehicle is in the region around 800 to 1000 Hz and about 500 Hz for trucks due to the size difference of these vehicles.

The noise form exhaust pipe is generated by the exhaust air from explosion chamber of engine. Thus, the noise is highly dependent to engine speed. The increase in noise level is around 45 dB when the engine speed increase by 10 times. Priede (1971) found that the noise generated from petrol engine is not only proportion to engine speed, but also engine operating loading where diesel engine is not dependent on the loading condition. Other than that, engine size is also found that to be another important factor to the noise level. When engine size increase, the exhaust noise will also increase. That is why noise from truck is always higher than normal vehicle since the engine size of truck is much larger than others. The estimation on noise level of petrol and diesel engine can follow the Equation as below:

$$\begin{aligned} SPL_{(diesel\ engine)} &= 30\log_{10} N_r + 17.5\log_{10} v + L_0 \\ SPL_{(petrol\ engine\ at\ no\ load\ condition)} &= 50\log_{10} N_r + 17.5\log_{10} v + L_0' \end{aligned} , \text{[dB]} \qquad \text{Eq (2.1)}$$

where L_0 is constant, v represents the displacement volume of engine (cm^3) and N_r is the real engine speed(rpm). It can be observed that exhaust noise is dominated by speed of engine more than size of engine and petrol engine will generate a higher noise level when both petrol and diesel engine are operating in same engine speed.

It is clear that general road traffic noise is a board band noise which is dominated in 100-1000 Hz. And the noise level received at residential area in modern cities from traffic noise is always up to 70-80 dB. When people expose to high noise level for a long time, negative impact on human being is found. Thus, studies on noise mitigation by noise barrier are then started in research field.

2.2 Studies on thin barrier

Studies on noise attenuation performance of noise barrier have been carried out for around 100 years. The reviews on research studies include theoretical and experimental works of previous researchers on different noise barrier will be presented in this chapter.

By summarizing the works of previous researchers (Maekawa,1965) (May,1980) (Yamshita,1990) (Yamamoto,1993) (Muradali,1998) (Ishizuka,2004), there are two general methods to undertake studies on noise attenuation performance of noise barriers. One is full scale test and the other is modelling techniques. Physical scale modelling test in laboratory and numerical modelling computation are the most common methods to determine noise attenuation of noise barrier. Other ultimate test is on-site measurements with realistic ground and atmospheric condition to assess the actual performance of noise barrier. These methods will be reviewed in the following paragraphs.

2.2.1 General Modelling Methods

Studies on noise attenuation performance of noise barriers have been carried out for a long time. Thus, different modelling methods have been established to find out the performance of noise barrier. In this Section, six commonly used methods in research field are listed out and discussed in detail.

2.2.1.1Analytical solutions

The diffraction of plane, cylindrical and spherical waves over the edge of thin half plane has been highly interested and has been studied since the end of eighteenth century. It was suggested that the diffraction of sound over thin half plane can be determined as an optics problem due to the similar wave properties. Therefore, the diffraction pattern behind thin screen is based on the coupling between superposition of wave over the edge of thin screen and incident wave inside the line of sight region.

Sommerfeld (1986) developed a rigorous mathematical solution of this diffraction problem. The partial differential Equations are solved to express a two-dimensional diffraction problem of an incident plane wave propagate over a thin reflecting semi-infinite screen. The solution contains two terms which expressed the contribution of direct wave and diffracted wave alternately. For the first term, it is expressed by the principle of geometrical acoustics. And the second term is expressed in terms of Fresnel integrals. A few years later, Carslaw (1899), Carlas (1920) and MacDonald (1915) presented other solutions for the problems on diffraction of cylindrical and spherical incident wave over edge of thin half plane by extending Sommerfeld's approach.

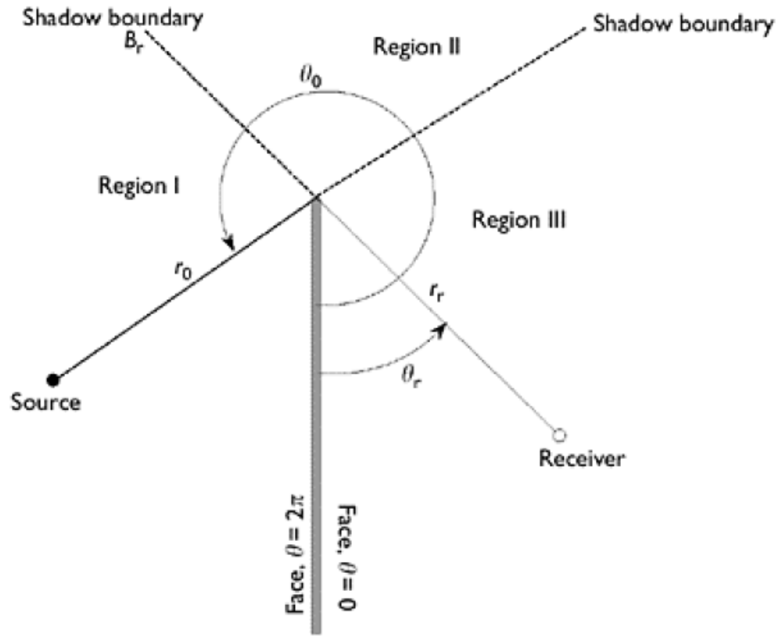

Figure 2.1 Diffraction of sound on a semi-infinite plane

To simplify the complexity of the problem, cylindrical polar coordinate is used to describe the location of sources and receivers. By principle of geometrical acoustics, the sound field in a thin plane problem includes diffracted sound p_d, incident sound p_i and reflected sound p_r. As shown in Figure 2.1, a point source is located at the left-hand side of the thin plane, the thin plane at the middle is of zero thickness and receiver is located at the right-hand side of the thin plane. And the domain is divided into three regions. Region I is the reflected region where the entire reflected wave will confined in region I. Region II is the combined region where diffracted wave and incident wave are occurred in this region. Lastly, region III is the diffracted region which is so-called shadow zone of a barrier. Incident sound wave cannot penetrate in this region since the propagate path is blocked by the thin plate. Therefore, the total sound field p_T in these regions can be expressed as below:

Region I $$p_T = p_i + p_r + p_d \qquad \text{Eq(2.2)}$$

Region II $$p_T = p_i + p_d \qquad \text{Eq(2.3)}$$

Region III $$p_T = p_d \qquad \text{Eq(2.4)}$$

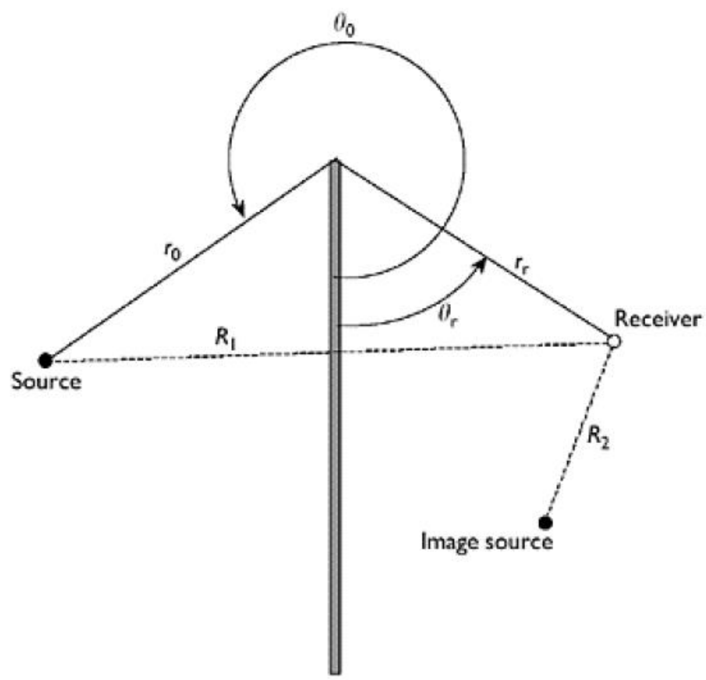

Figure 2.2 The geometry of source, receiver and image source location

MacDonald developed a solution to find out the total sound field in spherical polar coordinate system. The total sound field is expressed as the sum of two contour integrals as:

$$p_T = \frac{ik}{4\pi}\int_{\varsigma_1}^{\infty}\frac{H_1^{(1)}(kR_1+s^2)}{\sqrt{s^2+2kR_1}}ds + \frac{ik}{4\pi}\int_{\varsigma_2}^{\infty}\frac{H_1^{(1)}(kR_2+s^2)}{\sqrt{s^2+2kR_2}}ds \qquad \text{Eq (2.5)}$$

where k is the wavenumber of incident sound wave, $H_1^{(1)}$ is the Hankel function of first kind, R1 and R2 are the distance between source and image source to receiver respectively, ς_1 and ς_2 are the sign function which corresponding to angle θ and distance R. The incident wave, reflected wave and diffracted wave in Region I, II, III can then be expressed as below:

$$p_i = \frac{e^{ikR_1}}{4\pi R_1} \qquad \text{Eq (2.6)}$$

$$p_r = \frac{e^{ikR_2}}{4\pi R_2} \qquad \text{Eq (2.7)}$$

$$p_d = \frac{ik\varsigma_1}{4\pi}\int_{|\varsigma_1|}^{\infty}\frac{H_1^{(1)}(kR_1+s^2)}{\sqrt{s^2+2kR_1}}ds + \frac{ik\varsigma_2}{4\pi}\int_{|\varsigma_2|}^{\infty}\frac{H_1^{(1)}(kR_2+s^2)}{\sqrt{s^2+2kR_2}}ds \qquad \text{Eq (2.8)}$$

If the receiver is located at shadow zone, the solution is then expressed as below:

$$p_T = \frac{e^{ikR_1}}{8\pi R_1} + \frac{ik}{4\pi}\int_{\sqrt{k(R'-R_2)}}^{\infty}\frac{H_1^{(1)}(kR_2+s^2)}{\sqrt{s^2+2kR_2}}ds \qquad \text{Eq (2.9)}$$

Copson (1946), Levine and Schwinger (1948) used a new approach, solve diffraction problems directly like an integral formulation, and also applied the Wiener-Hopf method (Crighton, Doling, Williams, Heckl and Leppington, 1996) (Wright, 2005), which is a technique to solve linear partial differential Equation with mixed boundary condition and semi-infinite geometries to find out the exact solution on diffraction problems. Recently, Tolstoy (1989) obtained an explicit and exact solution for sound waves diffracted by wedges. Since the solution of diffraction sound field is expressed in the sum of infinite series, edge diffractions can be obtained without the need of asymptotic approximation of integrals. However, there is a limitation of this approach due to the slow convergence of the series at high frequency.

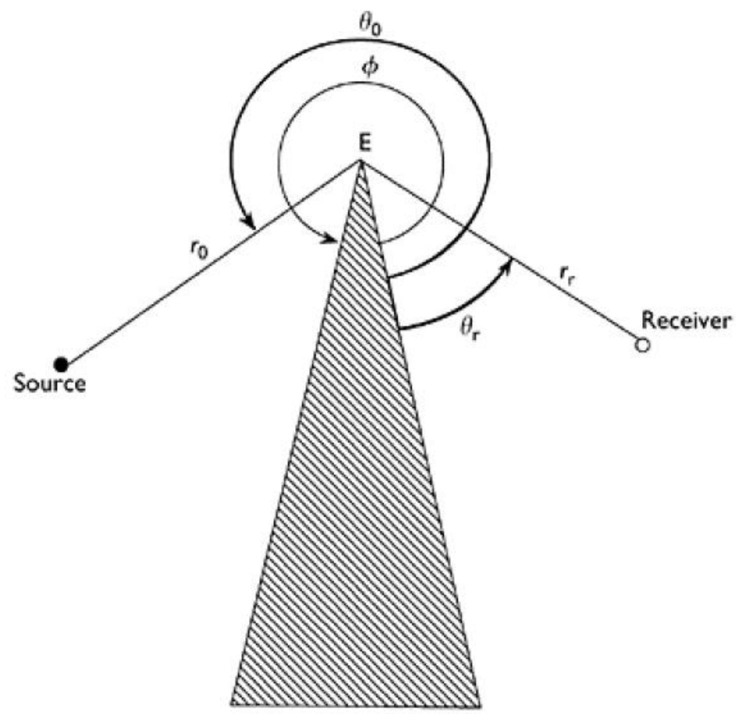

Figure 2.3 Diffraction of spherical sound wave by wedge

From the geometry as shown in Figure 2.3, the solution of diffracted sound field is the combination of incident sound wave and reflected wave of either one surfaces of wedge. However, the incident wave becomes zero since receiver is not directly illuminated to source. And the reflected wave also pays no contribution since the reflected wave can be constructed on either side of the edge to the receiver. Then the diffraction of sound can be expressed in four terms:

$$p_d = \sum_{i=1}^{4} V(\varsigma_i) \qquad \text{Eq (2.10)}$$

where ς_i corresponding to the sound path between source S_0, image source, S'_0 receiver R_0 and image receiver R'_0 as shown in below figure.

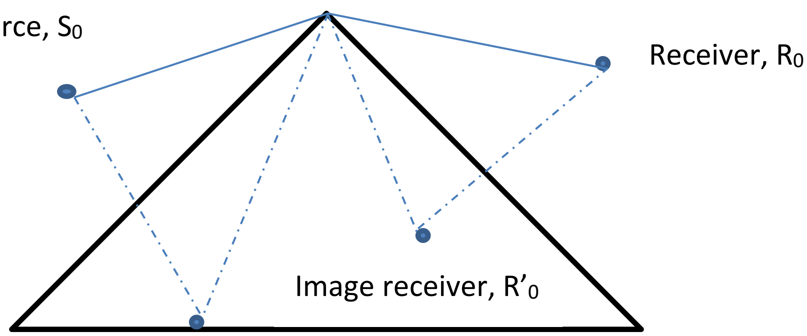

Figure 2.4 Source, image source, receiver and image receiver of wedge

The diffracted field of each path can then be calculated as:

$$V(\varsigma_n) = -\left(\frac{1}{4\pi^2}\right) A_n \left(\frac{e^{ikL}}{R'}\right) F(\varsigma_n) \qquad \text{Eq (2.11)}$$

where

$$A_n = A(\varsigma_n) = \left(\frac{\upsilon}{2}\right)(-\beta - \pi + \varsigma_n) + \pi H(\pi - \varsigma_n) \qquad \text{Eq (2.12)}$$

$$F(\varsigma_n) = \int_0^{\infty} \frac{kR'}{kR' + iy}(1 + \frac{i}{kR' + iy}) q_n e^{-y} dy \qquad \text{Eq (2.13)}$$

$$q_n = \frac{1}{|A_n|} \tan^{-1}(\tan|A_n| \tanh(\upsilon X_n)) \qquad \text{Eq}$$

(2.14)

$$\sinh X_n = \sqrt{\frac{y}{\alpha}\frac{i}{2} - \frac{y}{4kR'}}$$ Eq (2.15)

$$\alpha = \frac{kr_0 r_r}{R'}$$ Eq (2.16)

where R' is the shortest distance from source to receiver through the top edge of wedge and H(u) is the Heaviside step function. The parameter υ is the wedge index. B is a constant and ς_n is $|\theta_r - \theta_0|$.

2.2.1.2 Approximation analytical formulations

Other than solving the diffraction problems of noise barrier by analytical solutions, more simplified methods for predicting noise attenuation of noise barrier is preferred. Young and Fresnel suggested many approximate solutions for the diffraction problems of a half plane with physical interpretation of diffraction. Since the wavelength of high frequency noise compare with barrier is very small, the wave property will be similar to optical light propagate over an obstacle. Thus, a mathematical representation of the Huygens-Fresnel principle, Fresnel-Kirchhoff approximation (Hecht, 1998) (Born and Wolfm, 1975), is developed. By using the solution of Green's theorem, the sound field behind noise barrier can be expressed in surface integral by solving the Helmholtz Equation.

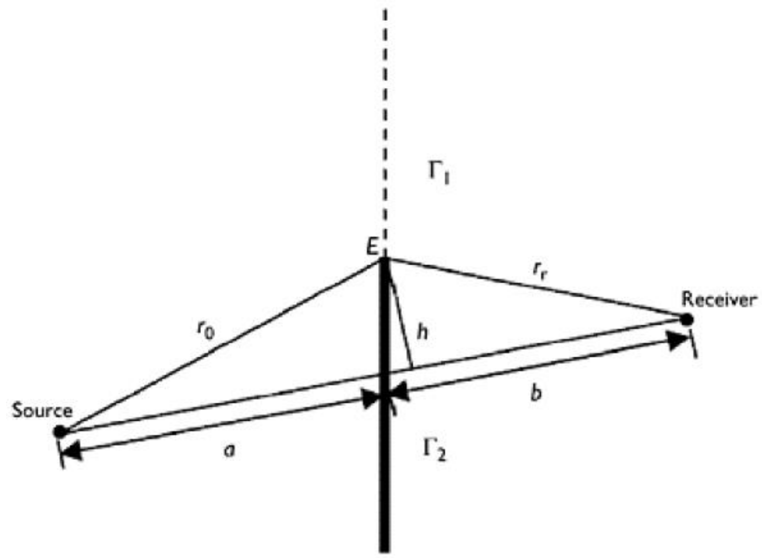

Figure 2.5 Geometry and notation of Fresnel-Kirchhoff approximation

A semi-infinite thin screen is located at the middle of source and receiver as shown in Figure 2.5. Γ_1 represent the surface of aperture above the screen and Γ_2 represent the surface of thin screen. Thus, the sound pressure obtained at receiver point can be determined as below:

$$p_T = \frac{ik}{16\pi^2}\iint_{\Gamma_1} \frac{(\cos\vartheta_0 - \cos\vartheta_r)}{d_0 d_r}\exp[ik(d_0 + d_r)]dA \quad \text{Eq(2.17)}$$

Skudrzyk (1975) extended the Kirchhoff's solution into Rubinowics-Young formula. The diffraction sound field behind noise barrier is then expressed in line integral rather than surface integral which used in Kirchhoff's solution. Besides that, he also decomposed the diffraction sound field into direct sound filed and scattered sound field by the plane and spherical incident wave of Kirchhoff solution.

Another formula expresses the sound diffraction problem of a two-dimensional barrier was derived by Embleton (1980). Two assumptions are made on the Rubinowics-Young formula, the first one is the line integral was along the barrier edge and the second one is that the two ends of barrier edges are connected by a semi-circular arc. The integration variable is then reducing to one dimension so that it becomes more convenient for numerical implementation. The simplified line integral when the barrier is located at the midway between source and receiver is shown below:

$$\Psi(\mathrm{R},\mathrm{t}) = -\frac{\mathrm{A}}{4\pi}\mathrm{e}^{-\mathrm{i}\omega\mathrm{t}}\frac{\sin\theta}{\mathrm{r_r}}\int_0^{\frac{\mathrm{r}}{2}}\frac{\exp(\mathrm{i}2\mathrm{k}\mathrm{r_r}\sec\beta)}{\tan^2\beta+\sin^2(\frac{\theta}{2})}\mathrm{d}\beta \qquad \text{Eq (2.18)}$$

2.2.1.3 Empirical formulations

Engineering chart for predicting the sound attenuation behind noise barrier by a point source had been developed by Redfearn (1940) and Fehr (1951). The sound attenuation estimated in his chart is based on a function with two parameters which are the angle of diffraction and the normalized effective height of barriers by wavelength. However, ground effect and atmospheric effect are not considered or ignored in this chart.

Around 30 years later, Maekawa (1965) (1968) carried out a large amount of measurements to measure the performance of a thin barrier on noise attenuation by using pulsed tone in short duration as a sound source and place the sources and receivers at different positions. Based on the measurement data, he proposed a design chart, which is plotted by sound attenuation against

Fresnel number, to express the shadowing effect of a thin barrier. Ground effect has also been considered in this chart by a correction of 2 dB. In the same period, Rathe (1969) also presented a chart based on his experiment data. Different from Maekawa chart, the sound attenuation obtained in Rathe's chart is in octave bands. In the following few years, researchers developed a few numbers of engineering formulas to represent Maekawa chart (Delany,1972) (Tatge, 1973) (Yamamoto, 1992).

There are two important parameters used in the empirical formula of Maekawa's chart. The first one is path difference δ_1 which is the difference between direct path from source to receiver and the path from source to receiver via the top edge of barrier. It is given by:

$$\delta_1 = (r_0 - r_r) - R_1 \qquad \text{Eq (2.19)}$$

And the other parameter is the wavelength of sound wave, λ. For a sound wave with longer wavelength, the diffraction efficiency becomes larger. These two parameters will then be combined into Fresnel Number:

$$N_1 = \frac{2\delta_1}{\lambda} \qquad \text{Eq (2.20)}$$

The function which well fits the Maekawa's curve is shown below:

$$\mathrm{Att} = 10\log_{10}(3 + 20N) \qquad \text{Eq (2.21)}$$

where Att represent the attenuation level of noise.

Kurze and Anderson (1971) derived empirical formulas for the excess attenuation of barrier. By comparing the difference between the sound attenuation of a point source and line source, including the diffraction angle at source and receiver side, some common feature was found to be consistent with Maekawa chart and Rathe's chart. With the aid of diffraction theory from Keller, the sound attenuation can then be expressed as a function of relative source and receiver positions. The simple formula derived by Kurze and Anderson is shown as below:

$$\mathrm{Att} = 5 + 20\log_{10}\frac{\sqrt{2\pi N_1}}{\tanh\sqrt{2\pi N_1}} \quad \text{Eq (2.22)}$$

Isei et al. (1980) presented a modelling method to estimate the combination effect of barrier and ground which discussed in previous Section. Paths of ground reflected ray have been taken into account in his approach. After that, researchers explored many other analytical methods to calculate the sound insertion loss of barrier on ground (KOERS, 1983) (L'ESPERANCE, A., Nicolas, J., Daigle, G.A., 1989) (L'ESPERANCE, A., 1989) (LEANG, L.K., YAMASHITA, Y., MATSUI, M., 1990) (Lam, 1993) (Lam, 1994). The sound attenuation for the line source of Isei's model is:

$$\mathrm{Att} = 10\log(\sum_{i=1}^{n} 10^{(L_i - \Delta L_i)/10}) \quad \text{Eq (2.23)}$$

where L_i is the sound level at receiver by ith source and ΔL_i is the sound attenuation of barrier calculated by ith point source.

Menounou (2001) modified Makekawa's Chart from one parameter in a single curve into two Fresnel number in a family of curve. The first one is the traditional Fresnel Number which is associated with the location of source and receiver to barrier. The other one is similar to the first one that the Fresnel number is associated with the location of image source and receiver to barrier. Modification has also been done which based on the Kurze-Anderson formula and Kirchhoff solution by considering the situation of plane wave, cylindrical wave and also spherical incident wave. The performance of barrier can then be well determined by the improved Kurze-Anderson formula which includes the effect of image source to the total sound field. The improved Kurze-Anderson formula is shown as below:

$$\mathrm{Att} = \mathrm{Att_s} + \mathrm{Att_b} + \mathrm{Att_{sb}} + \mathrm{Att_{sp}} \qquad \text{Eq (2.24)}$$

where

$$\mathrm{Att_s} = 20\log_{10}\frac{\sqrt{2\pi N_1}}{\tanh\sqrt{2\pi N_1}} - 1 \qquad \text{Eq (2.25)}$$

$$\mathrm{Att_b} = 20\log_{10}\left[1 + \tanh\left(0.6\log\frac{N_2}{N_1}\right)\right] \qquad \text{Eq (2.26)}$$

$$\mathrm{Att_{sb}} = (6\tanh\sqrt{N_2} - 2 - \mathrm{Att_b})(1 - \tanh\sqrt{10N_1} \qquad \text{Eq (2.27)}$$

$$\mathrm{Att_{sp}} = -10\log_{10}\frac{1}{(\frac{R'}{R_1})^2 + (\frac{R'}{R_1})} \qquad \text{Eq (2.28)}$$

where the term $\mathrm{Att_s}$ is the measure of position from receiver to source. The second term $\mathrm{Att_b}$ is the measure of the proximity of source or receiver from half plane. The Third term is the measure of proximity of receiver to shadow boundary and the fourth term is the diffraction effect of spherical incident wave.

2.2.1.4 Numerical Methods

Other than geometrical diffraction, a method which is specific to a certain type of noise barrier design and cannot cope with other barrier in different top edge design, numerical method can provide a higher flexibility to model any shaped noise barrier and also exclude the atmosphere effect on noise attenuation of barrier.

There are two general methods to solve the acoustic problems of a noise barrier in the existed research. The first one is Finite Element Method (FEM) which solves the sound field by discretizing the whole domain. The other is numerical wave-based Boundary Element Method (BEM). In this method, only boundaries of the model are discretized. Muradali and Fyfe (1998) compared the traditional diffraction-based methods to BEM and found that they are in good agreement. Other than that, Salomons (1997) use a traffic noise situation with multi diffraction and reflection of incident sound to compare a ray-based model to numerical method based on BEM. The milestone on numerical modelling of noise barrier is presented by Seznec (1980). It was shown that the numerical model can be applied to a noise barrier problem with arbitrary top edge, shape and also boundary conditions. However, a significant disadvantage of this model is time consuming and a large amount of computational resources is required.

2.2.1.5 Scale Modelling

Other than theoretical solution on the diffraction problems of noise barrier, scale modelling is the most common method to investigate the noise attenuation of noise barrier. The main concept of scale modelling in acoustical problems includes the scaling of physical dimensions in the testing environment, wavelengths and other acoustical properties. Scale factor becomes a main concern in scale modeling method since it is related to the resonance frequency of tested model in the measurement. For a smaller scale factor, the resonance frequency will become higher even further into ultrasonic range which is difficult to detect and generate. Other than that, the environmental effects which affect noise attenuation of barrier are difficult to investigate by this method since the relationship between various environmental effects is complex and further tests are required.

The testing room for scale modelling method should be a well-designed anechoic or semi-anechoic chamber which can provide a reverberation free sound field to neglect the reflection of sound (Andersib, 1993). In order to study noise attenuation of an infinite long barrier with uniform profile, a two-dimensional form anechoic chamber is needed (Fujiara, 1998). An impulsive short duration sound source with fast enough sampling time should be used to ensure only the direct sound is taken into account by reducing the reflection of sound from room boundaries (Maekawa, 1965) (May 1980). Different noise source such as spark source (Koers, 1983) (Hajek, 1984), ultrasonic whistle

(Hutchins, 1984), air jet (Lyon, 1974) (Takagi, 1994) (Yamashita, 1990) and small sized tweeter (Maekawa, 1965) (Leang, 1990) (Lam, 1993) have been used to model a general point source. Other than that, line source will be used in scale modeling method by a series of point sources aligned in a straight line closely.

Different materials have been used to act as similar acoustical properties of model surface in real case. Aluminum was used to model a reflective surface because of its high impedance (Hutchins, 1984) (Takagi, 1994). Other materials, such as acryl, wool (Leang, 1990), plywood (Koyashu and Yamashita, 1973) (Hayek, 1985), fiberglass (Lam, 1994), and pressboard (Lam, 1993) have been used for tested models with different scale factor to determine the acoustic nature of model surface in actual case. The most important parameters for selecting an appropriate material are transmission loss (TL), length and weak point of that material. Sufficient transmission loss is needed to ensure the top diffraction at least 10 dB higher than the noise passing through model. A long enough barrier can highly reduce the interference between top edge diffraction and side edge diffraction. Enhancement should be added on the weak point of the material to reduce sound leakage occurred. Inappropriate material selection in scale modeling method will lead to inaccurate determination on acoustics nature of actual model.

2.2.1.6 Full Scale modelling

Besides scale modelling method, full scale modelling method is also used to determine the field performance of a noise barrier with a real traffic noise

(Watts, 1996) (Yamamoto, 1989). Differ from scale modelling testing, all external factor in the environment such as traffic conditions, atmosphere conditions and also ground condition during the measurement period should be monitored and their effect should also be considered in data analyze process to obtain a more meaningful result. Even though exceed cost and monitoring systems are needed in a full-scale field test, it is the most ultimate test to determine the actual performance of a noise barrier.

2.2.2 Factors affected barrier Performance

Although there are many effects that affect the barrier performance from shielding the receiver form noise source, two main effects will be pointed out in this Section. They are ground effect and atmosphere effect.

2.2.2.1 Ground Effect

As mentioned in the previous Section, ground plays an important on determining the noise attenuation of a noise barrier. Different absorption characteristics and shapes of the ground will lead to a different propagation paths and even different scattering and reflection properties of sound.

Jonasson (1972) showed that the effusiveness of the performance of noise barrier becomes maxima when the noise barrier is located in a place with high ground reflection before the insertion of barrier. For example, the barrier is constructed in a place where an acoustically hard ground located between barrier and receiver.

In previous researches, scale modelling method is commonly used to study the performance of barrier with the presence of different ground surfaces (Hutchins, 1984). If there is an acoustically hard ground, the insertion loss of the barrier will mainly correspond to specific frequencies. The frequencies can be determined as the odd multiples of 1/2 wavelength of the path differences between the direct transfer sound and ground reflected sound. In the result, an increase of insertion loss in specific frequencies is found. Because of high ground reflection, the increase of insertion loss can be explained as the destructive interference between direct and reflected sound due to the configuration of measurements.

For a measurement above an acoustically soft ground, which have noise attenuation around 500 Hz, the beneficial ground effect disappeared in a result of the insertion of barrier. Result showed that the attenuation of acoustically soft ground at low frequency shifted when the barrier existed. However, destructive interference still existed at the frequencies which is the even multiples of 1/2 wavelength of path length difference between direct sound and ground reflected sound at high frequency. Surface roughness also becomes a significant parameter to represent a complex impedance ground surface.

For acoustically hard surface, surface roughness will mainly affect the near grazing sound propagation at low frequency (Boulanger, 1998) (Attenborough, 2000). When noise barrier existed, the maximum ground effect will then shift to other frequency due to interference. From both results, the presence of noise barrier lead to the interference of sound behind the barrier and even frequency shift of sound attenuation. Thus, A careful decision includes the shift of frequency take place should be made before the design stage of barrier performance testing.

2.2.2.2 Meteorological Effects

Although atmospheric conditions are assumed to be unchanged in the barrier modelling tests mentioned in previous Section, it still plays an important role to determine noise attenuation of barrier in actual case. For example, the noise attenuation of barrier will decrease at downwind direction but increase in upwind direction. In fact, refraction and scattering due to atmospheric turbulence are the main environmental effects which influence the performance of noise barrier.

By comparing the results from theory and on-site measurements, it can be found that the performance of noise barrier becomes less effective than expected value. The reason is clear that the sound pressure level behind barrier is higher than predicted value (Dalgle, 1982) because atmospheric turbulence scatters the sound energy from direct sound propagation path. It can increase the sound pressure level for 15-25 dB (A) (Scholes, 1971) in different frequency and lead to the reduction on insertion loss for 15-25 dB (Sutherland, 1998).

In most of previous researches, an assumption that the sound rays travel in a straight path, is made to simplify the sound diffraction problems of noise barrier. In fact, this assumption is not valid in actual environment since uniform atmosphere is not existed. Sound rays travel in a curved path rather than a straight path due to the variation of temperature or fluctuation of wind velocity which is so-called refraction due to air turbulence. Shadow Zone of a barrier is generally known as the area that is not illuminated to sound rays which propagate in a straight path. Therefore, the curved propagation path of sound rays will reduce the size of shadow zone and even the insertion loss of noise barrier since sound can transmit to receiver by curving over the barrier top edge (Sutherland, 1998) which always occurs in a temperature inversions and downwind propagation condition. Thus, a homogenous atmospheric condition is needed to determine the relative performance on different types of noise barrier unless the noise barrier is specifically designed to use under a certain atmospheric condition.

2.2.3 Noise Barrier Types

Many previous researches were focused on straight barrier or a wedge. In fact, the top edge of noise barrier can also enhance noise attenuation of barrier significantly. In order to increase noise attenuation without increasing the height of barrier, different barrier top edged designs added on a normal thin barrier have been developed by researchers. Moreover, cost-effective design, specific resonance frequency design and also the materials used for construction are well investigated. These designs will be reviewed with their physical principles in this Section.

2.2.3.1 Multiple edged Barrier types

Multiple edged barriers represent a noise barrier with more than one top edge. The first BEM approach to the study on such barriers theoretically was done by Hothersall (1991). T-profile, Y-profile and arrow-profile noise barriers were interested in this study. The results from numerical simulation showed that these three types of barrier provide a better noise attenuation than normal straight thin barrier in same height. Moreover, the T-profile barrier performs much better than other two barriers by higher attenuation closed to barrier and ground. A few years later, Watts (1994) conducted a full-scale test of multi edged barriers which showed the average improvement on noise attenuation is around 2.5 dB(A). More tests have then been done by Watts on multiple edged barriers under favorable conditions in the following years. These results double confirmed that the improvement of multiple edged barriers can achieve above 3 dB(A) (Watts, 1996).

The other multiple edged barriers used in high rise cities is cracked barrier. It is a cost-effective design based on Y-profile by increasing the effective height of barrier. Besides that, many barrier top edge designs also benefit to noise attenuation as shown in Figure 2.6. However, when the receiver is far away from noise barrier, noise attenuation by barrier top edge is less effective and the height of barrier becomes the dominant factor of barrier performance again.

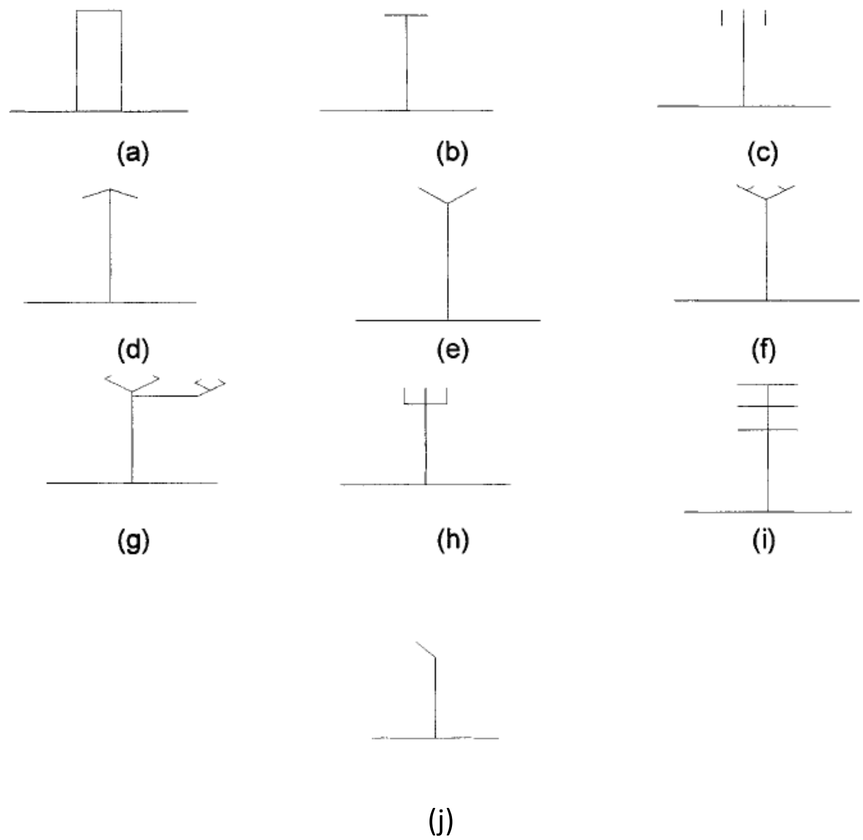

Figure 2.6. Multiple edged barrier configuration: (a) thick barrier, (b) T-profile, (c) bracket attached to barrier, (d) arrow profile, (e) Y-profile, (f) Y-profile with additional edges, (g) branched profile, (h) U-profile, (i) fir tree profile, (j) cracked barrier

2.2.3.2 Absorptive Barriers

To further enhance the performance of multiple edged barriers, absorptive treatment was found to apply on the top edge of barrier to reduce the diffraction of sound. Recent researches showed that there is a significant improvement on noise attenuation when absorption treatment is applied on barrier. The effective height of a 4.2 m high noise barrier with absorption material on its top is found as 0.46 m (Gharabegian, 1995).

On-site and modelling tests were carried out to determine the noise shielding effect of noise barrier with different absorptive treatments on its top. The average improvement on noise attenuation of these designs can be possibly up to 3 dB (Fujiwara, 1991) (Yamamato, 1993). A numerical modeling test was carried out to determine the acoustical performance of T-profile barrier with absorptive material on its top surface. Results indicated that around 2 dB improvement on noise attenuation due to the use of absorption material (Horthersall, 1991). An on-site full-scale testing was conducted and found that the significant effect on insertion loss of a 1m wide T-profile barrier by adding absorptive material is around 0.6 dB (Watts,1994). Besides that, different multiple edged barriers associated with absorption materials shows positive effect on the performance of barrier. Some of them are shown in Figure 2.7.

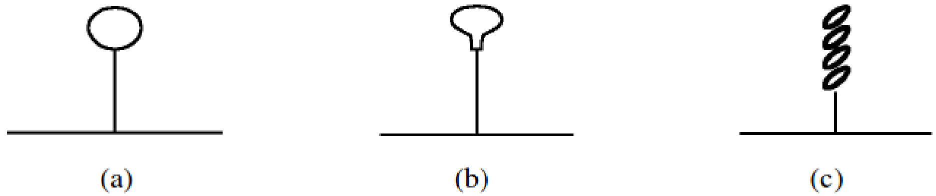

Figure 2.7 Absorptive Barrier, (a) cylindrical cap barrier, (b) mushroom cap barrier, (c) louvered barrier

2.2.3.3 Reactive Barrier/Diffusive Barrier

In fact, absorption materials are not always practical on outdoor noise barrier because of variable environmental conditions at roadside. The efficiency of absorption materials will decrease immediately in a short period because porous absorption materials are highly sensitive to traffic contaminations such as duct, rain mist and fog. Since these traffic contaminations will reduce the effectiveness of absorption materials in a short period, researchers are seeking another design to keep similar noise attenuation enhancement with less sensitive to environmental factors.

Recently, reactive surface on waterwheel and T-profile barrier was presented. Okubo (1992) investigated a noise barrier with waterwheel on its top which provided similar acoustic properties like an acoustical soft cylindrical edge. Waterwheel barrier had an average improvement on noise attenuation around 10 dB in the frequency range it intended for. Fujiwara (1998) conducted a numerical study on noise attenuation of normal rectangular, T-profile and cylindrical edged noise barrier with hard, soft and absorptive top surface. It found that T-profile noise barrier associate with soft upper surface can achieve higher noise attenuation. It also found that T-profile noise barrier with uniform series of wells on its upper surface can provide similar performance to a soft surface in specific frequency range.

Based on above studies, Monazzam (2005) improved the design of uniform wells into wells in different depths in pseudo-stochastic number sequence or pattern to reduce the sound reflection by scattering the incident sound wave in a wide range of direction. The incident wave will excite a wave in each well's opening and propagate to the bottom of the wells. Since the bottom of wells are acoustically hard, the travelling wave will reflect back to the opening of the wells, different phase shift occurred of these waves are then depends on different path length they travelled. Scattering occur when the phase shift is large enough corresponding to the depth of these wells. Results show that the T-profile barrier with quadratic residue diffuser (QRD) provides 0.9 dB more attenuation than noise barrier with absorption materials with same barrier height.

2.2.4 Summary

In this chapter, the components of general road traffic noise are discussed. The frequency range of road traffic noise is dominated at low frequency. Common modelling methods used by researchers and two main factors related to barrier performance are reviewed. Lastly, the evolution of roadside noise barrier and its noise attenuation performance, from traditional conventional vertical barrier, top edged modified barrier, barrier with absorption materials and diffusive barrier are presented. In this study, barrier with finite acoustic cavities are proposed to achieve good noise attenuation as a QRD barrier. In addition, it is expected that the effective noise attenuation frequency range can be enlarged by additional acoustic cavities. Efforts are paid on the noise attenuation performance and spatial behavior of sound on both finite and infinite acoustic cavities in this study.

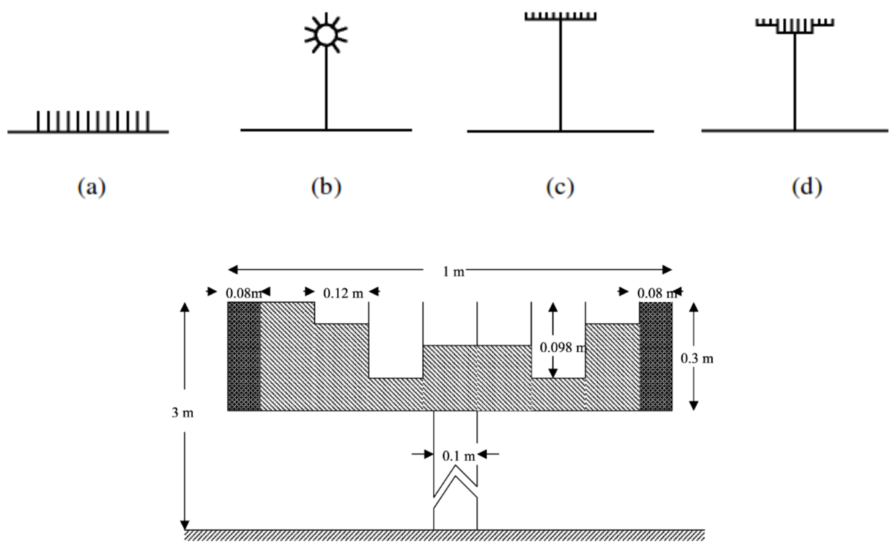

(e)

Figure 2.8 Reactive Barrier. (a) Parallel wells on ground, (b) waterwheel barrier, (c) uniform depth diffusive barrier, (d) variable depth diffusive barrier, (e) quadratic residue diffuser barrier.

Chapter 3. Theory

3.1 Introduction

In this chapter, the general solution of sound diffraction by a conventional vertical barrier is shown. Besides that, the procedure to find out the resonance frequency of an acoustic cavity is also presented. Then, the indexes, which can indicate the noise attenuation performance of a noise barrier used in this study, are listed in the last part of this chapter.

3.2 Diffraction over noise barrier

Noise barrier can be defined as a solid obstacle which is opaque to sound wave, that blocks the line of sight from sound source to receiver, and a sound shadow zone is then created behind noise barrier. In shadow zone, sound wave can only reach receiver form sound source by diffraction at the top edge and side edges of barrier. For considering an infinite long barrier, the diffraction of sound is then only occurred at the top edge of noise barrier.

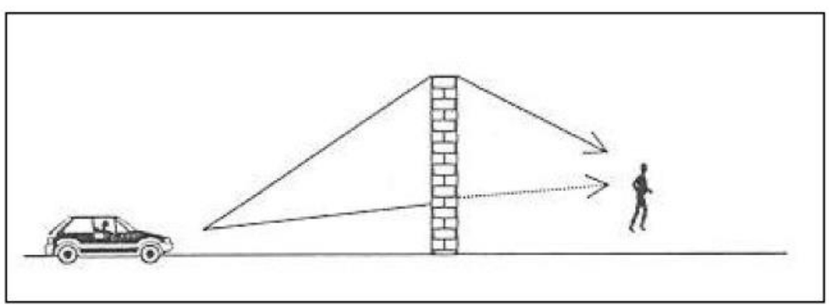

Figure 3.1 Schematic diagram of a roadside barrier

The diffracted pressure at different sound propagation paths can be determined by calculating Maekawa's formula with the aid of geometric diffraction considerations. In this approach, sound diffraction over the edges of noise barrier is calculated by the sum of different diffracted paths over the edges of noise barrier. In general case, a finite barrier is placed on ground, the eight diffracted paths are considered as Figure 3.2:

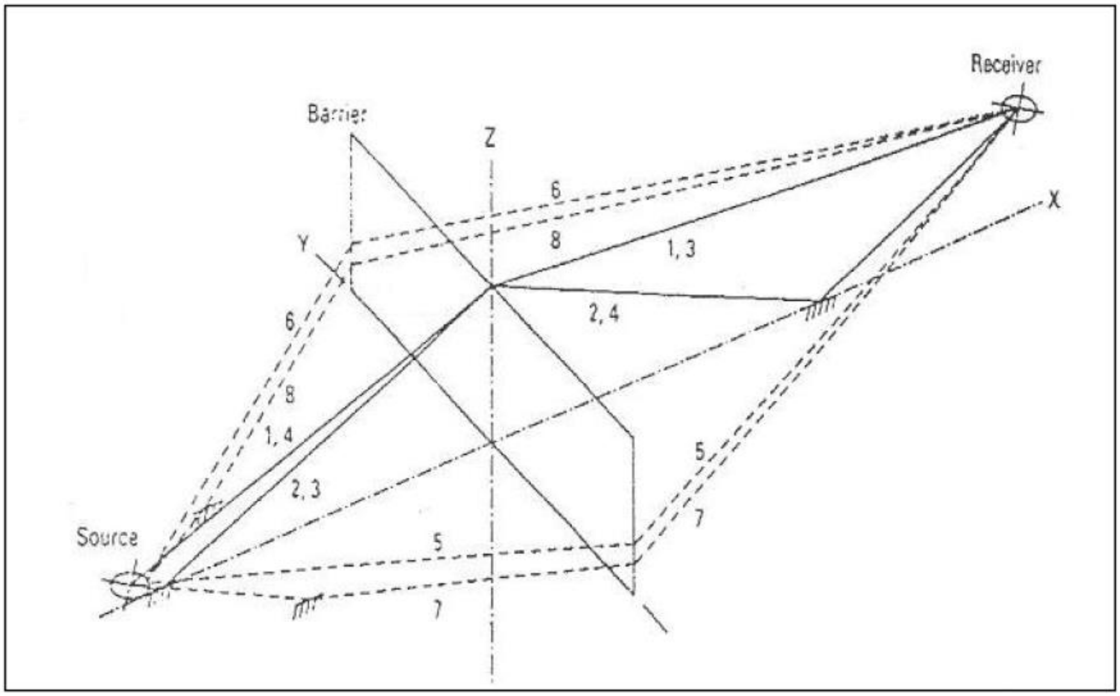

Figure 3.2 Diffraction paths geometry

However, only the effect of sound diffraction by the top edge of noise barrier is interested in this research. The diffraction paths from side edges and ground are not considered in calculation. Only path 8, the direct path from source to the top edge of barrier and then to the receiver is considered. Then the diffraction sound field of the shadow zone can be determined.

3.3 Resonance frequency of cavity

In this thesis, the proposed barrier can be defined as an improved reactive barrier which is mentioned in Chapter 2. By comparing to a conventional vertical barrier, the advantage of an improved reactive barrier is the high noise attenuation in a specific frequency range. This specific frequency range is depended on the depth and width of the acoustic cavity. When sound waves pass over a cavity, the pressure fluctuation due to the incident sound wave will excite a sound wave toward the cavity bottom. Since the cavity bottom surface is acoustically hard, the mechanism of this problem is similar to a plane wave propagate inside an open-close tube and result in the formation of standing wave at certain frequencies. When the excited frequency matches the nature frequency of cavity, impedance at cavity opening becomes very small and the excitation become maximum and standing wave (acoustic mode) will be formed inside cavity. The high excitation of sound will cause absorption and reradiation which interfere with the incident wave. By solving the wave Equation, the resonance frequency of proposed barriers can be estimated as below.

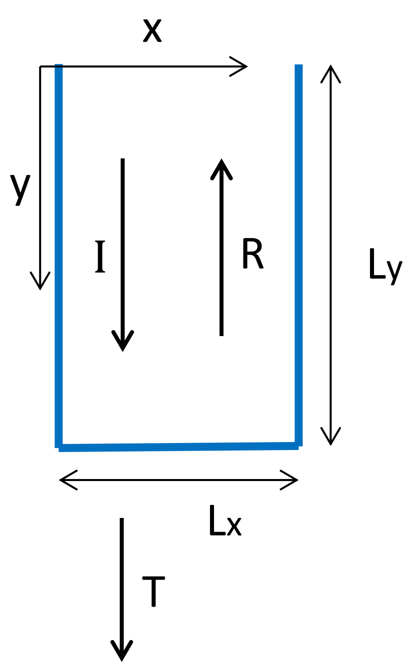

Figure 3.3 Sketch of sound wave propagates inside acoustic cavity

In Cartesian reference system of Figure 3.3, Helmholtz Equation becomes:

$$\left(\frac{\partial^2}{\partial x^2}+\frac{\partial^2}{\partial y^2}+k^2\right)P(x,y)=0 \qquad \text{Eq(3.1)}$$

where k is the wavenumber and P is the pressure perturbation.

Equation 3.1 is then solved by separation of variables approach. Let $P(x,y)=P_x(x)P_y(y)$ and substituting in Equation 3.1 and dividing by P_xP_y, it becomes:

$$\frac{1}{P_x}\frac{\partial^2}{\partial x^2}P_x+k^2=-\frac{1}{P_y}\frac{\partial^2}{\partial y^2}P_y \qquad \text{Eq(3.2)}$$

The left-hand side of Equation 3.2 is independent from y while the right hand side is independent from x. Therefore, this leads to the two coupled ordinary Equation with a separation constant k_y.

$$\left(\frac{\partial^2}{\partial y^2}+k_y^2\right)P_y=0 \qquad \text{Eq(3.3)}$$

$$\left(\frac{\partial^2}{\partial x^2}+k^2-k_y^2\right)P_x=0 \qquad \text{Eq(3.4)}$$

The basis solutions of Equation 3.3 and Equation 3.4 is

$$P_x = A\sin\left(k_x\, x\right) + B\cos(k_x\, x) \quad \text{Eq(3.5)}$$

$$P_y = C\sin\left(k_y\, y\right) + D\cos(k_y\, y) \quad \text{Eq(3.6)}$$

where $k_x = \sqrt{k^2 - k_y^2}$ and k, kx and k_y is not equal to 0.

The boundary conditions of Figure 3.3 are

$$\frac{\partial}{\partial x}P(0, y) = 0 \quad \text{Eq(3.7)}$$

$$\frac{\partial}{\partial x}P(L_x, y) = 0 \quad \text{Eq(3.8)}$$

$$\frac{\partial}{\partial y}P(x, L_y) = 0 \quad \text{Eq(3.9)}$$

$$Z = \frac{P_y}{\frac{\partial}{\partial y}P(x, 0)} = 0 \quad \text{Eq(3.10)}$$

By substituting Equation 3.5 into Equation 3.7 and Equation 3.8, we get

$$A\cos(k_x(0)) - B\sin\left(k_x(0)\right) = 0 \quad \text{Eq(3.11)}$$

$$A\cos(k_x(L_x)) - B\sin\left(k_x(L_x)\right) = 0 \quad \text{Eq(3.12)}$$

From Equation 39, A becomes 0, therefore

$$B\sin\left(k_x(L_x)\right) = 0 \quad \text{Eq(3.13)}$$

$$k_x = \frac{n\pi}{L_x} \quad \text{where } n = 0,1,2,3 \ldots. \quad \text{Eq(3.14)}$$

$$P_x = B\sin\left(\frac{n\pi x}{L_x}\right) \quad \text{Eq(3.15)}$$

Analogously, by substituting Equation 3.6 into Equation 3.9 and 3.10, we get

$$\frac{C\sin\left(k_y(0)\right) + D\cos(k_y(0))}{C\cos\left(k_y(0)\right) - D\sin\left(k_y(0)\right)} = 0 \quad \text{Eq(3.16)}$$

$$C\cos\left(k_y(L_y)\right) - D\sin\left(k_y\left(L_y\right)\right) = 0 \quad \text{Eq(3.17)}$$

From Equation 3.17, we get

$$C = D\tan\left(k_y\left(L_y\right)\right) \quad \text{Eq(3.18)}$$

By substituting Equation 3.18 into Equation 3.16,

$$\frac{1}{\tan\left(k_y(L_y)\right)} = 0 \qquad \text{Eq(3.19)}$$

Therefore,

$$\tan\left(k_y(L_y)\right) = \infty \qquad \text{Eq(3.20)}$$

$$k_y = \frac{(2n-1)\pi}{2L_y} \quad \text{where } n = 0,1,2,3 \ldots \qquad \text{Eq(3.21)}$$

$$P_y = C\cos\left(\frac{(2n-1)\pi y}{2}\right) + D\sin\left(\frac{(2n-1)\pi y}{2}\right) \qquad \text{Eq(3.22)}$$

And the natural mode wavenumber of the acoustic cavity becomes:

$$k(n,m) = \sqrt{k_x^2 + k_y^2} = \sqrt{\left(\frac{n\pi}{L_x}\right)^2 + \left(\frac{(2m-1)\pi}{2L_y}\right)^2} \qquad \text{Eq(3.23)}$$

where m, n =0,1,2,3….

Since k=2 πf/c

The natural mode frequencies of acoustic cavity are

$$f(n,m) = \frac{c}{2\pi}\sqrt{\left(\frac{n\pi}{L_x}\right)^2 + \left(\frac{(2m-1)\pi}{2L_y}\right)^2} \qquad \text{Eq(3.24)}$$

where m, n $= 0,1,2,3 \ldots.$

Based on the above solution, the resonance frequency f(n, m) of different acoustic cavities can be determined.

3.4 Index for noise barrier performance

To compare the noise attenuation performance of different noise barriers, a quantification on the noise attenuation of noise barrier is required. In the past studies, researchers used different index to quantify the performance of noise barrier. In this Section, introductions of three common indexes used to indicate the barrier noise attenuation performance are made.

3.4.1 Insertion Loss (IL)

Insertion Loss (IL) is commonly used to indicate the noise attenuation performance of noise barrier. The definition of Insertion Loss at a receiver point is the sound pressure level difference before and after the barrier is constructed. In general, it is expressed in logarithmic scale as:

$$IL = -20\log_{10} \left| \frac{\text{sound received with barrier}}{\text{sound received without barrier}} \right| \quad \text{Eq(3.25)}$$

The Insertion Loss is defined as sound of board band frequency and 1/3 octave frequency in this study. Since white noise is generated as the noise source in scale model testing, the Insertion Loss cannot reflect the actual performance of the noise barrier to traffic noise. Traffic weighting (BS EN 1793-3) should be considered on the results to access the acoustics performance of noise barrier to general traffic noise. The normalized traffic noise spectrum given by BS EN 1793-3 is shown in Table 3.1:

Table 3.1 Normalized traffic noise spectrum

Table 1. Normalized traffic noise spectrum	
f_i Hz	L_i dB
100	−20
125	−20
160	−18
200	−16
250	−15
315	−14
400	−13
500	−12
630	−11
800	−9
1000	−8
1250	−9
1600	−10
2000	−11
2500	−13
3150	−15
4000	−16
5000	−18

And the traffic weighted Insertion Loss can be calculated as Eq 45:

$$\mathrm{IL_T} = -10\log\frac{\sum_{i=1}^{18} 10^{0.1L_i} \times 10^{-0.1R_i}}{\sum_{i=1}^{18} 10^{0.1L_i}} \qquad \text{Eq(3.26)}$$

Where IL_T is the traffic weighted Insertion Loss, R_i is the Insertion Loss of noise barrier in the i^{th} one third octave band and L_i is the normalized A-weighted sound pressure level of traffic noise in the i^{th} one third octave band defined in BS EN 1793-3.

3.4.2 Effective Height

Effective Height is also called equivalent effective height which is another index for indicating the performance of noise barriers. Since it is simply found that the performance of noise barrier is mainly affected by the path difference, which is the difference of diffraction path and direct path from source to receiver, and results show that increasing the path difference can increase the performance of noise barrier. Therefore, the easiest way to improve the noise attenuation of barrier is to increase the height of barrier. However, it is not a cost-effective solution to increase the height of barrier to achieve the desired performance of noise barrier. Thus, modification on top edge of noise barrier is being considered to increase the diffracting edge along the sound propagating path. By increasing the number of diffracting edges, the noise attenuation of barrier can be improved. The effective height of a barrier is an index to find out the increase of height of a reference barrier to achieve the same acoustic attenuation on the tested barrier with same height to reference barrier. For example, if the tested barrier performs 3 dB better than the reference barrier and the reference barrier should increase its height for 1 m to achieve 3 dB more noise attenuation improvement. The effective height of the tested barrier is 1 m. The noise attenuation performance of different top edge design can be obtained by effective height.

3.4.3 Diffraction angle

Diffraction is the capacity of sound waves to bend at the edges of barrier and it is also the important wave phenomenon to explain the shadow area behind barrier. Thus, it can be one of the indexes to indicate the performance of noise barrier. For the noise barrier with same height, the performance of noise barrier becomes much better when the diffraction angle is smaller. Piechowicz (2011) provides a diffraction index which is the ratio between pressure of incident wave and diffracted wave. It indicates the noise attenuation performance in the total sound field of noise barrier. The disadvantage of this method is that a number of receivers are needed to obtain a more accurate sound field behind barrier. Therefore, diffraction angle is a need to predict the performance of barrier in a simpler way. For the diffraction at the shadow zone, the diffraction angle should be smaller for a better performance of barrier. Then, diffraction angle becomes one of the indexes used to compare the performance of noise barrier in this study.

3.5 Transfer function

Although the performance of noise barrier can be compared by measuring the actual noise level at receiver point behind barrier, an important assumption should be made that the sound source output of each measurement is consistent. It is not easy to ensure the white noise generated at each measurement is uniform since a random noise is generated to perform a white noise from signal generator. Transfer function is then be considered to overcome this problem. In general, Transfer function is always used for data analysis in signal processing. In a problem which the input signals and output is time continuous, the transfer function is defined as the ratio from output signal to input signal. By calculating the insertion loss of each barrier by transfer function, the meaning of transfer function becomes the ratio of sound power at receivers to the sound power of sound source. Since the scale modelling experiments were conducted in a fully anechoic chamber, it can be assumed that no additional sound source was taking into account during measurements, transfer function method can eliminate the error of insertion loss due to the inconsistent of sound source in each measurement.

3.6 Summary

In this chapter, different indexes that commonly used in past researches for comparing the performance of noise barrier are presented. However, extra experiments of barriers in different height should be carried out when using effective height to indicate the noise attenuation performance of barrier. Thus, effective height is not considered in this study. Then, Insertion Loss and diffraction angle are used to analyze the numerical and experimental results in the latter part of this thesis.

Other than that, the general theory for predicting the resonance frequency of tested barrier is introduced. Based on these theories, the experiment data and computation results can be compared with the calculated data to make validation. The details of computation results and analysis are presented in the following chapter.

Chapter 4: Numerical Study on noise barrier

4.1 Introduction

Sound diffraction over a noise barrier top edge has been introduced in Chapter 2. In this chapter, further analysis is done to determine the sound field behind noise barrier. It is well-known that the acoustic cavity can reduce the sound power from source to receiver due to impedance discontinuities at the opening of cavity. The effectiveness of acoustic cavity is frequency dependent therefore the maximum sound attenuation can be obtained only at specific frequencies, which are the resonance frequencies of acoustic cavity.

In general, the advantage of acoustic cavity is its high noise attenuation at specific frequencies and these frequencies are dependent to the depth of acoustic cavity. Numerical models are done first to compute the performance of barrier with addition acoustic cavity. When the numerical results meet the target attenuation level, experiment will be done for validation. In the following sections, acoustic cavities with different depth are placed on the top edge of noise barrier and the noise attenuation performance is computed by using 2D FEM simulation.

4.2 Configuration of numerical model

Finite Element Computational Scheme is used to compute the performance of barriers with different top edge shapes and the coupling effect between acoustic cavities. Commercial software COMSOL Multiphysics 5.1 becomes the operator on computation and even post process the data. The general configuration numerical model is shown as Figure 4.1:

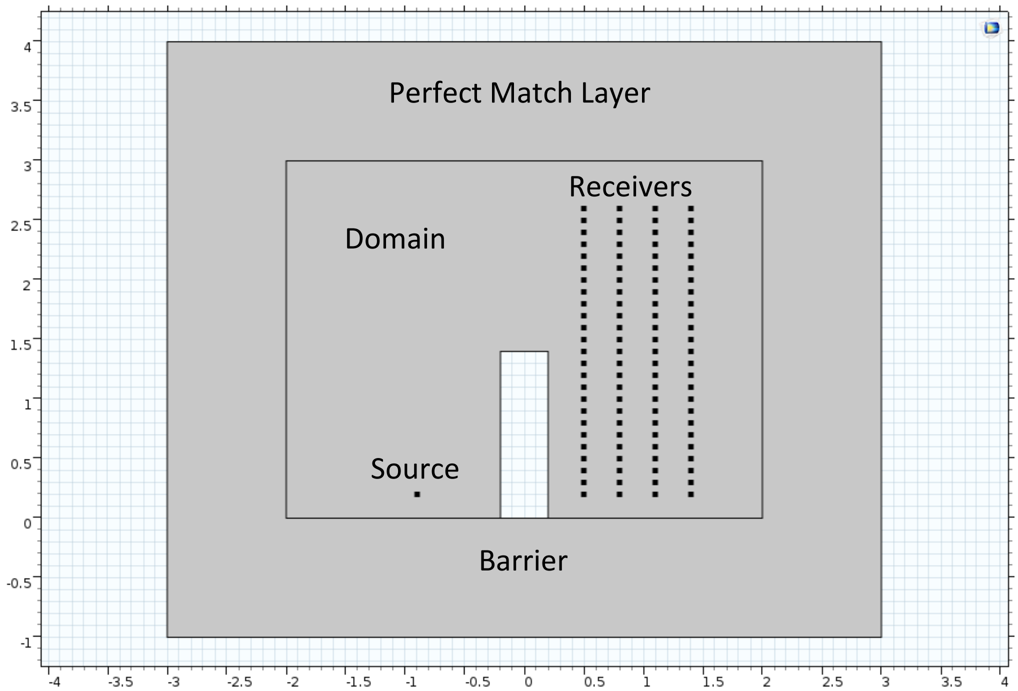

Figure 4.1 General configuration of numerical model

Figure 4.1 shows the detail configuration of numerical model. A two-dimensional numerical model is used in this study to reduce time and computational resource during the process. The numerical model is solved by inhomogeneous Helmholtz Equation in frequency domain and obtains the resonance frequency in target frequency range.

$$\nabla \cdot \left(-\frac{1}{\rho_0} (\nabla p - q) \right) - \frac{\omega^2}{\rho_0 c_s^2} p = Q \quad \text{Eq (4.1)}$$

where ρ_0 refers to the density and c_s denotes the speed of sound in medium, q denotes the dipole source which is zero in this study and Q denotes monopole source.

In Figure 4.1, the rectangle placed at the middle of the model is the computational domain in 4 m x 3 m, the white rectangle at the middle of domain implies the tested barrier in 0.4 m x 1.4 m, the sound source is placed at 0.9 m from the barrier center at left hand side of the barrier and the receivers are placed at 0.5 m, 0.8 m, 1.1 m and 1.4 m form barrier center at the right hand side of the barrier and the height of these receivers are from 0.2 m to 2.5 m with 0.1 m interval.

The outer domain of the model is the Perfect Match Layer (PML) which is used to avoid the reflection of sound by the outer boundary. The detail of PML and boundary conditions of numerical model are introduced in the following Section in this chapter.

4.3 Boundary conditions

In computations, boundary condition is one of the important parts in modelling. A correct boundary condition can reflect the actual acoustic properties of the objects in computational domain. In this Section, the boundary conditions used in this study such as rigid wall condition, outgoing condition and Perfectly Matched Layer will be introduced in detail. The requirement on mesh grid size of COMSOL Multiphysics is also presented at the last part of this Section.

4.3.1 Rigid wall condition

The surface of noise barrier is assumed to be acoustically rigid in this study since the mathematical model becomes more difficult if there is a leakage on the surface of noise barrier. When sound wave impinges on the surface of noise barrier, the normal velocity of the surface is always same as the normal particle velocity of the fluid. For a rigid boundary of noise barrier, the fluid will be stopped on the surface of noise barrier which shown that $v \cdot n = 0$, where v and n are the particle velocity and normal vector of the surface respectively. By conservation of momentum, relationship between particle velocity and pressure gradient is found to be proportional to each other, thus, the rigid boundary condition can be described as Equation 47:

$$\frac{\partial P(r)}{\partial n} = 0 \qquad \text{Eq(4.2)}$$

where r represents the distance from center of barrier to the surface of barrier. The governing Equation transferred in COMSOL Multiphysics 5.1 is:

$$n \cdot \left(\frac{1}{\rho_0} (\nabla P - q) \right) = 0 \qquad \text{Eq(4.3)}$$

where ρ_0 is the density of fluid, q is the term of dipole source with the dimension of force per volume.

4.3.2 Outgoing boundary condition

To focus on the effect of barrier top edge, ground effect is neglected in all computational models in this study by applying an outgoing boundary condition to that surface. Besides the non-reflecting ground surface, the outer boundary of computational domain is also non-reflecting by applying the impedance at boundary where Z=ρc. However, it is not possible to completely attenuate all the reflection of incident sound wave by using an outgoing boundary in most computational method, another setting Perfectly Matched Layer (PML) is used to ensure the reflection from outer boundary is eliminated.

4.3.3 Perfectly Matched Layer (PML)

In numerical model configuration, there is a region, which bounded the outer boundary of computational domain is the location of PML. A PML is strictly not a boundary condition but it is an additional domain that absorbs or even known as losing the wave energy of incident wave without producing reflections. It can provide a good performance for a wide range of incident angle and is not particularly sensitive to the shape of wave. The principle of PML is using a formulation to transform the complex valued coordinate to the actual coordinate without affecting the wave impedance. For the incident wave is in coordinate ξ, the coordinate transformation is shown as below:

$$\xi' = \mathrm{sign}(\xi - \xi_0)|\xi - \xi_0|^{n} \frac{L}{\partial\xi^{n}}(1 - i) \qquad \text{Eq (4.4)}$$

where L is the scaled width of PML, ξ_0 is the coordinate of the inner PML boundary, $\partial\xi$ is the actual width of PML and n is the scaling exponent for each PML. The imaginary coordinate becomes a buffer zone that enlarges the actual width of PML during calculation. The energy of incident sound is then dissipated in this buffer zone and only little or even no reflection is produced by the outer boundary.

4.3.4 Size of mesh grids

According to the user guideline of COMSOL Multiphysics, the mesh grid used in this numerical model is in tetrahedral shape which includes at least six elements in a wavelength of the highest frequency. To capture the modes pattern clearly in the acoustic cavities, the mesh size inside the cavity is twenty elements in a wavelength of highest frequency. The total mesh grids consist in the domain is around 5250000 elements.

4.4 Model of barriers

In this study, there are three kinds of noise barrier tested by numerical method. As described in previous Section, different acoustic cavities are added on the top edge of barrier. The configurations of these barriers are shown as Figure 4.2, Figure 4.3 and Figure 4.4:

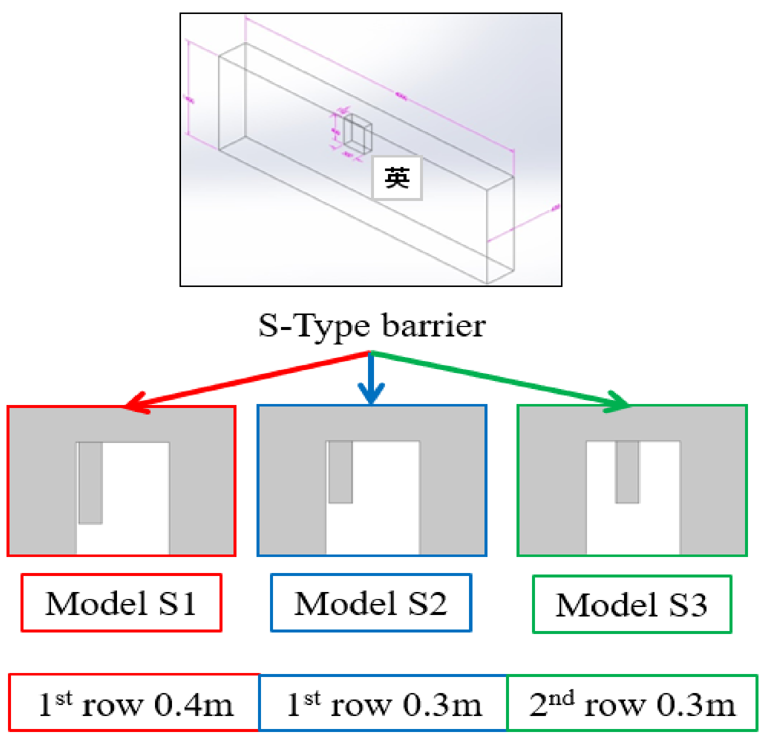

Figure 4.2 Model of single slot barrier

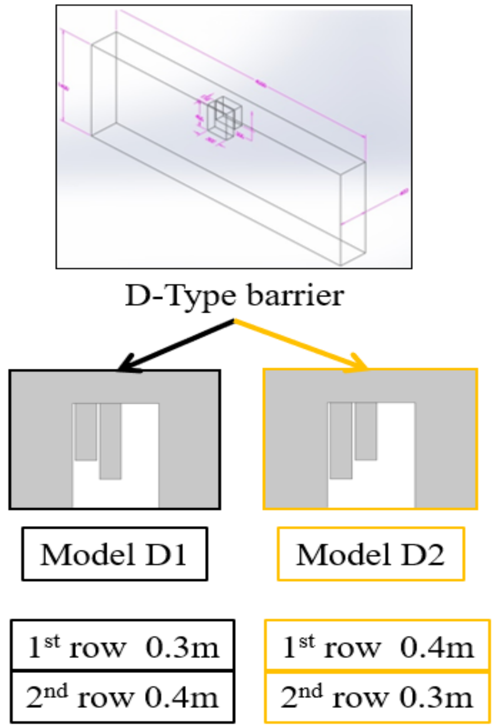

Figure 4.3 Model of double slots barrier

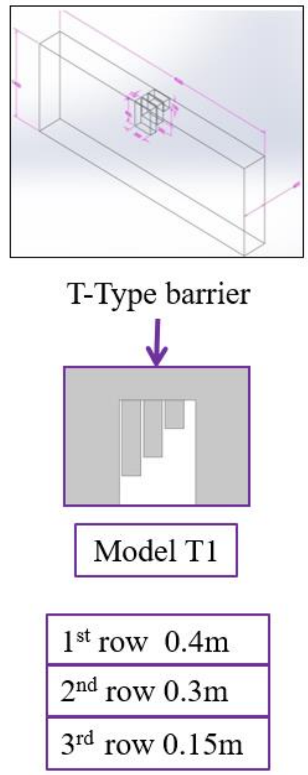

Figure 4.4 Model of triple slots barrier

The widths of these acoustic cavities are in 0.116 m and the depths are 0.4 m, 0.3 m and 0.15 m respectively. The separation between these acoustic cavities are 0.0127 m which same as the separation between the leading edge of barrier to the first slot and the separation between back edge of barrier to the third slot.

4.5 Results and analysis

Before carrying out the numerical study on the noise attenuation performance of barrier with acoustic cavities, agreement should be made with other studies to confirm the boundary condition is correct to provide an accurate result.

4.5.1 Validation

In conventional BEM methods, a large difference is usually found between the exact solution and conventional BEM method at a variety of frequency range. It is likely that these frequencies are close to Eigen frequencies. Ishizuka (2004) proposed an improved technique on BEM by boundary modifications to reduce the bounded area while keeping the barrier configurations. The results from BEM with improved technique coincide well with the exact solution over a wide frequency range. Therefore, it is a valuable reference to validate the results from FEM.Agreement is done by comparing the insertion loss results of a conventional vertical barrier with 3 m high between Ishizuka (2004) and FEM are shown as Figure 4.5.

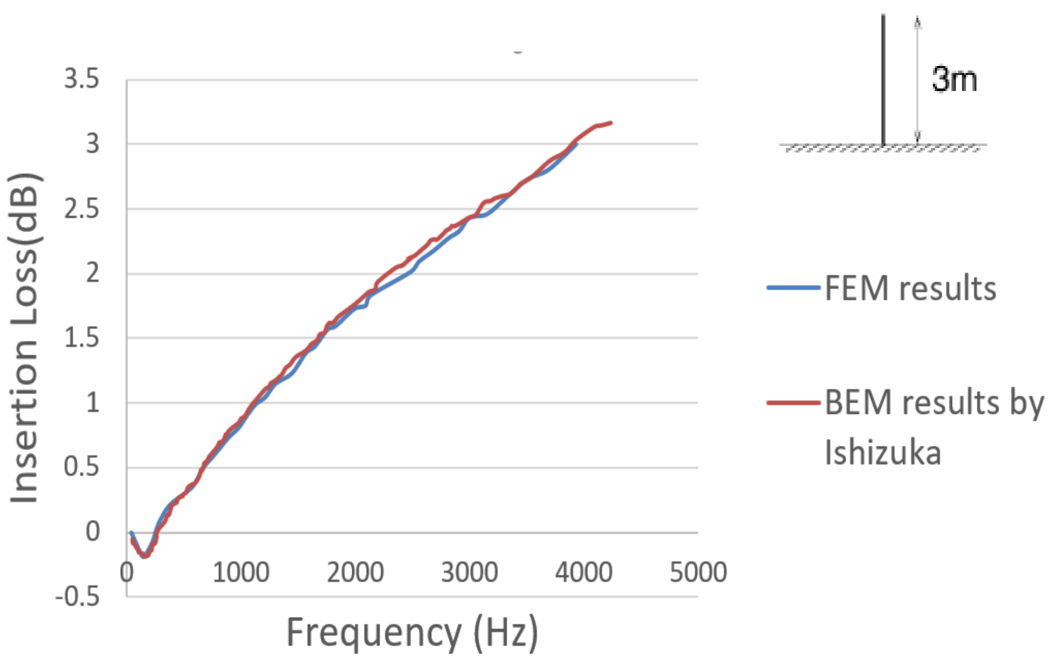

Figure 4.5 Results of Ishizuka using Boundary Element Method and Finite element method

It is clear that there is a drop of Insertion Loss from FEM results at around 100 Hz. After it reaches the local minimum point around 100 Hz, the Insertion Loss is gradually increase with the increase of frequency. From Figure 4.5, Ishizuka's BEM results give a similar result on the Insertion Loss of conventional vertical barrier. Although there is difference after 2000 Hz, the trend of both lines is same. Furthermore, the focal frequency range in this study is just 100-3000 Hz that a good agreement can be obtained at this frequency range. After validating the setting of boundary conditions and mesh quality, computation on noise attenuation performance of barrier with acoustic cavities are carried out in the following Section.

4.5.2 Single slot barrier (S-Type)

At the beginning of numerical model computation, the relationship between performance of noise barrier and two variables are being investigated. They are the depth of acoustic cavity, and the location of acoustic cavity. The noise attenuation of acoustic cavity is compared to the reference barrier. The performance is indicated by total Insertion Loss (dB)of the receivers which are located behind the barrier.

4.5.2.1 Effect on the depth of acoustic cavity

The performance of the single slot barrier is compared with the reference barrier which is so-called a conventional vertical barrier with same height. The resonance frequency of both barriers is given in Figure 4.6:

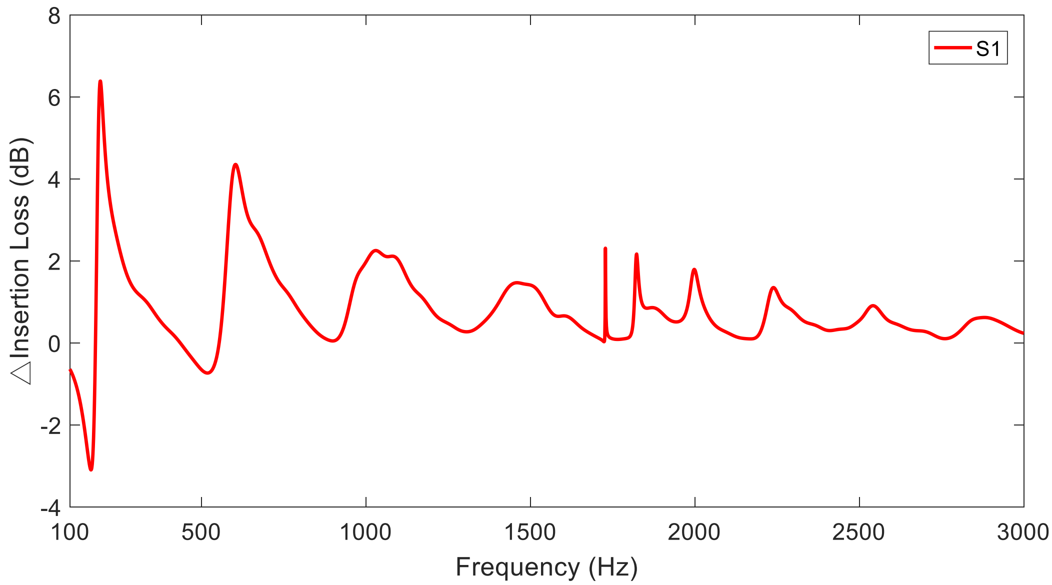

Figure 4.6 Relative Insertion Loss of Model S1

It can be observed that the relative insertion loss of Model S1 is almost positive at whole frequency range which means acoustic cavity gives improvement on the noise attenuation. Moreover, sudden increase or sharp peaks are found at specified frequencies. The magnitude of peaks is inversely proportional to the frequency that it is around 6 dB at low frequency and only 2 dB at high frequency. The decay trend of Insertion Loss stops at the 4th peak and become higher at 5th peak. Although the magnitude of 5th peak is only 2 dB, it produces a new decay trend for the following peaks after 1728 Hz. It is also found that sudden drop appeared at the lower frequency to all resonance frequencies. When the magnitude of peak is higher, the magnitude of drop is also higher. According to the properties of resonator, these sharp peaks are produced by the acoustic cavity on the top edge of barrier due to the sudden impedance change at cavity opening which cause suction of sound and also reradiation of sound at resonance frequencies. To verify the relationship between peaks and acoustic cavity, comparison on the resonance frequency of experimental results and calculation by the formulas described in Chapter 3 are shown in Table 4.1:

Table 4.1 Resonance frequency of Model S1 by calculation and numerical results

Calculated resonance frequencies (Hz)	Resonance frequencies of Model S1 (Hz)
214(0,1)	193
643(0,2)	602
1071(0,3)	1084
1500(0,4)	1466
1728(1,1)	1728
1831(1,2)	1823
1929(0,5)	
2022(1,3)	1998
2278(1,4)	2242
2358(0,6)	
2581(1,5)	2526
2786(0,7)	
2915(1,6)	2915

It can be observed from the Table 4.1 that the resonance frequencies of numerical result are similar to the calculated result. A little shift of the resonance frequency to lower frequency is due to the location of the acoustic cavity. Since the acoustic cavity is not in zero thickness, there is a 12.5 mm thin edge formed by the thickness of acoustic cavity. It produces a little scattering point and affects the diffraction of sound wave pass over the acoustic cavity. It becomes a flanged resonator case that a correction should be added to the depth of cavity which so-called effective length. By adding the effective length to Equation 3.24, the calculated frequencies will shift to lower frequency which same as the numerical results. Other than that, from the observed frequency range, there are two missing resonance frequency 1715 Hz and 2786 Hz. It is because the Insertion Loss at 1728 Hz is too high and too close to 1715 Hz, the peak maybe combines or hides by the sudden increase of Insertion Loss. Another reason for the missing peak at high frequency is that the performance of acoustic cavity becomes weaker when frequency increase since the noise attenuation performance of a conventional vertical barrier is good at high frequency. The relative improvement of acoustic cavity at high frequency becomes weaker, thus, the peak still exists but cannot be observed clearly. In conclude, the result shows that the acoustic cavity has its improvement on sound attenuation at a certain frequency behind the barrier.

To investigate the relation between the performance of acoustic cavities and the noise attenuation behind barrier, the absolute pressure of sound wave inside the acoustic cavity is captured as Figure 4.7. It can be indicated that a significant high acoustic pressure appears at resonance frequency. At 193 Hz which is the first transverse mode of cavity, nearly whole cavity is in high pressure. At 602 Hz, second mode can be seen clearly at the lower part and upper part inside the cavity with high pressure. At 1084 Hz and 1466 Hz, third and fourth modes can be observed respectively. However, the acoustic pressure of modes becomes weaker which is around half the magnitude of second mode. At 1728 Hz, a sharp mode can be found, and the mode shape is not like the first four transverse modes. It is because this is the longitudinal mode but not the transverse mode of cavity. The acoustic pressure of this mode inside the cavity is as high as the first mode at 193 Hz. At 1823 Hz, a combined mode appears which form a cross shape at the middle of cavity. The acoustic pressure keeps its level as 1728 Hz. By calculation using the analytical solution shown in Chapter 3, there should be a peak at 1929 Hz. However, it disappeared at the spectrum presented in previous Section. By observing the acoustic pressure inside the cavity, mode shape cannot be found due to the low pressure. At 1998 Hz, two combined modes are clearly seen. The acoustic pressure keeps as the same level as the first mode at 1728 Hz. At 2242 Hz, 2526 Hz and 2915 Hz, combined modes can be found in these frequencies. The mode order increases while the magnitude of acoustic pressure inside the cavity decrease. For transverse modes, the mode shape cannot be captured clearly after the 4th mode. For the combined mode, since it is still the combination of the first longitudinal mode, the pressure is high enough to form an obviously mode shape for even the 6th combined mode. In general, results show that there is higher order mode inside the acoustic cavity at different resonance frequency. When the frequency is low, mode shape is much obvious inside acoustic cavity than high frequency since the acoustic pressure inside cavity is high enough to observed in lower mode number.

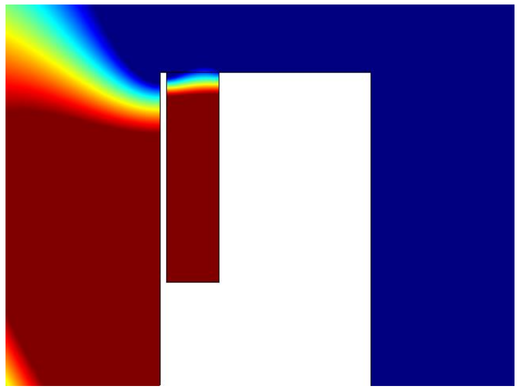

F (0,1) 193 Hz

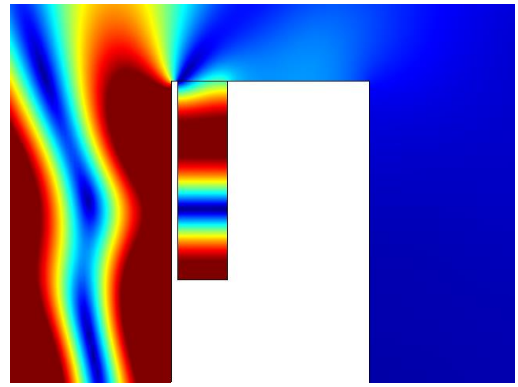

F (0,2) 602 Hz

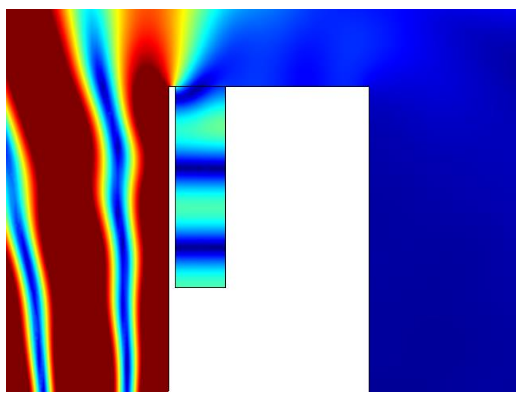

F (0,3) 1084 Hz

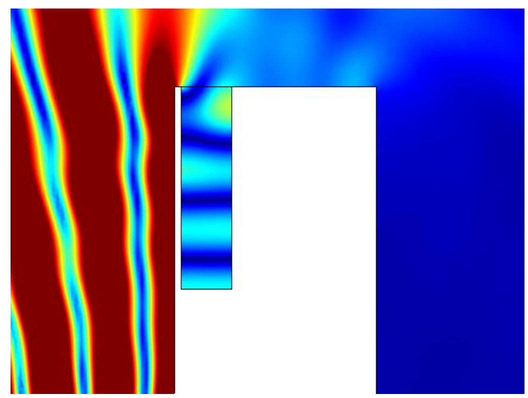

F (0,4) 1466 Hz

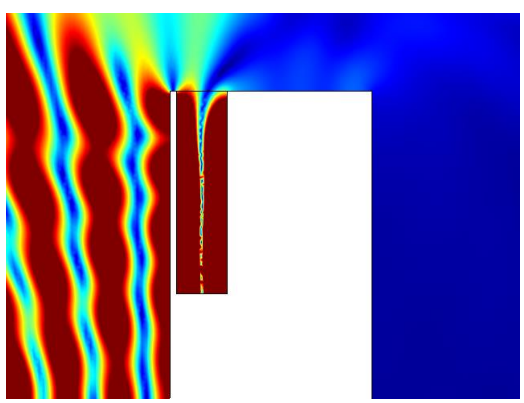

F (1,1) 1728 Hz

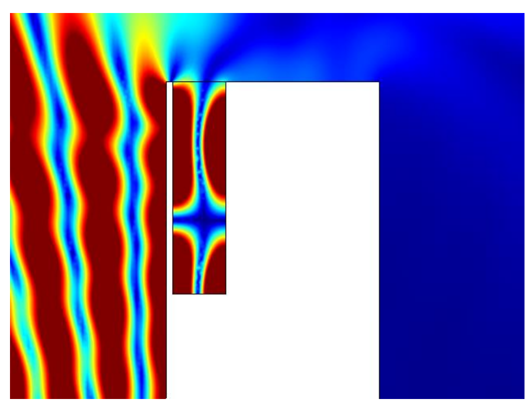

F (1,2) 1823 Hz

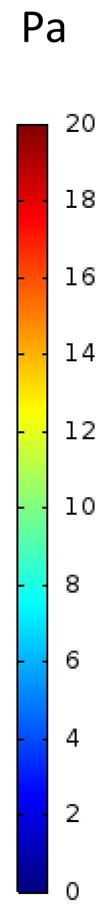

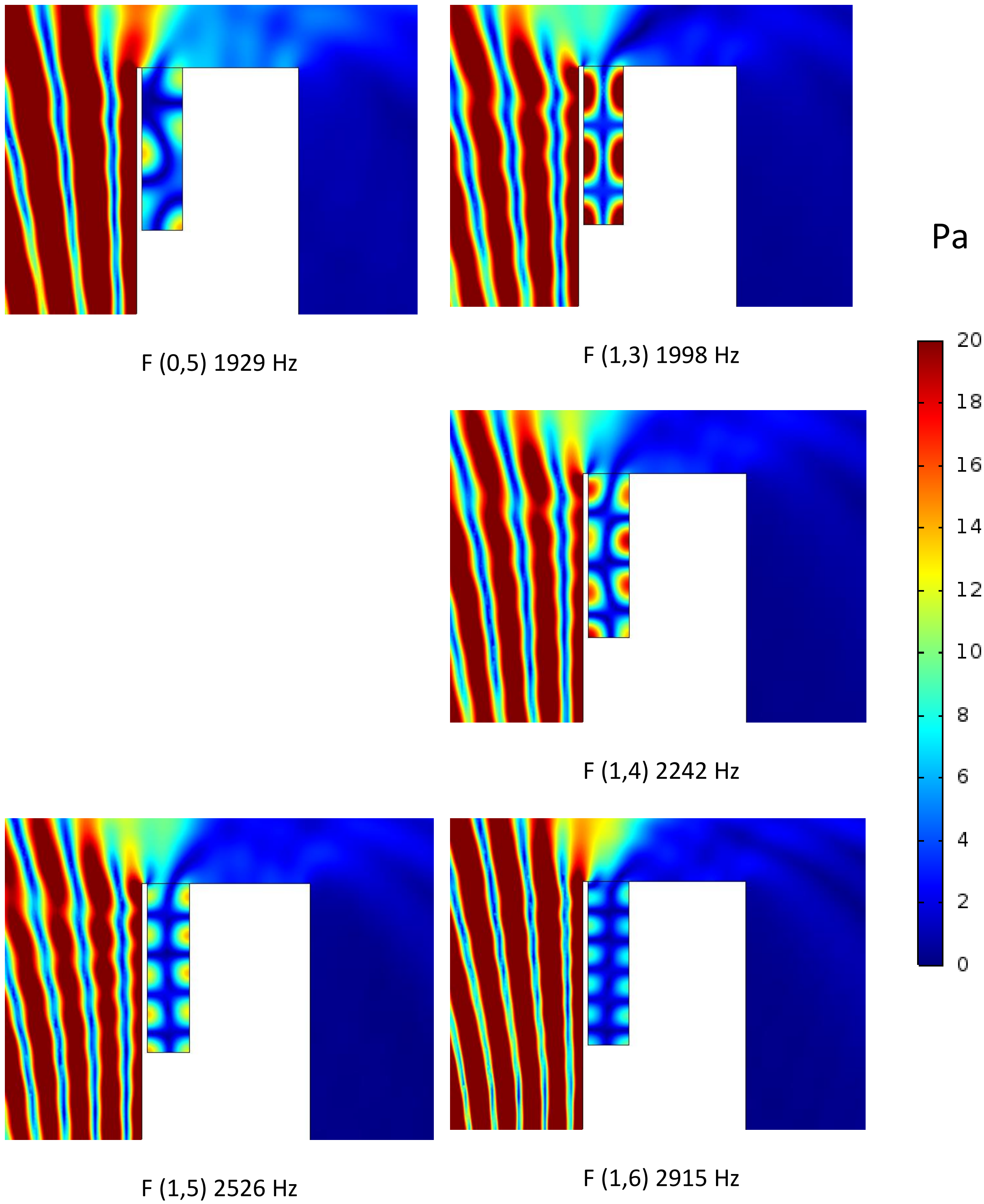

Figure 4.7 Absolute pressure of sound wave inside the acoustic cavity at different resonance frequency

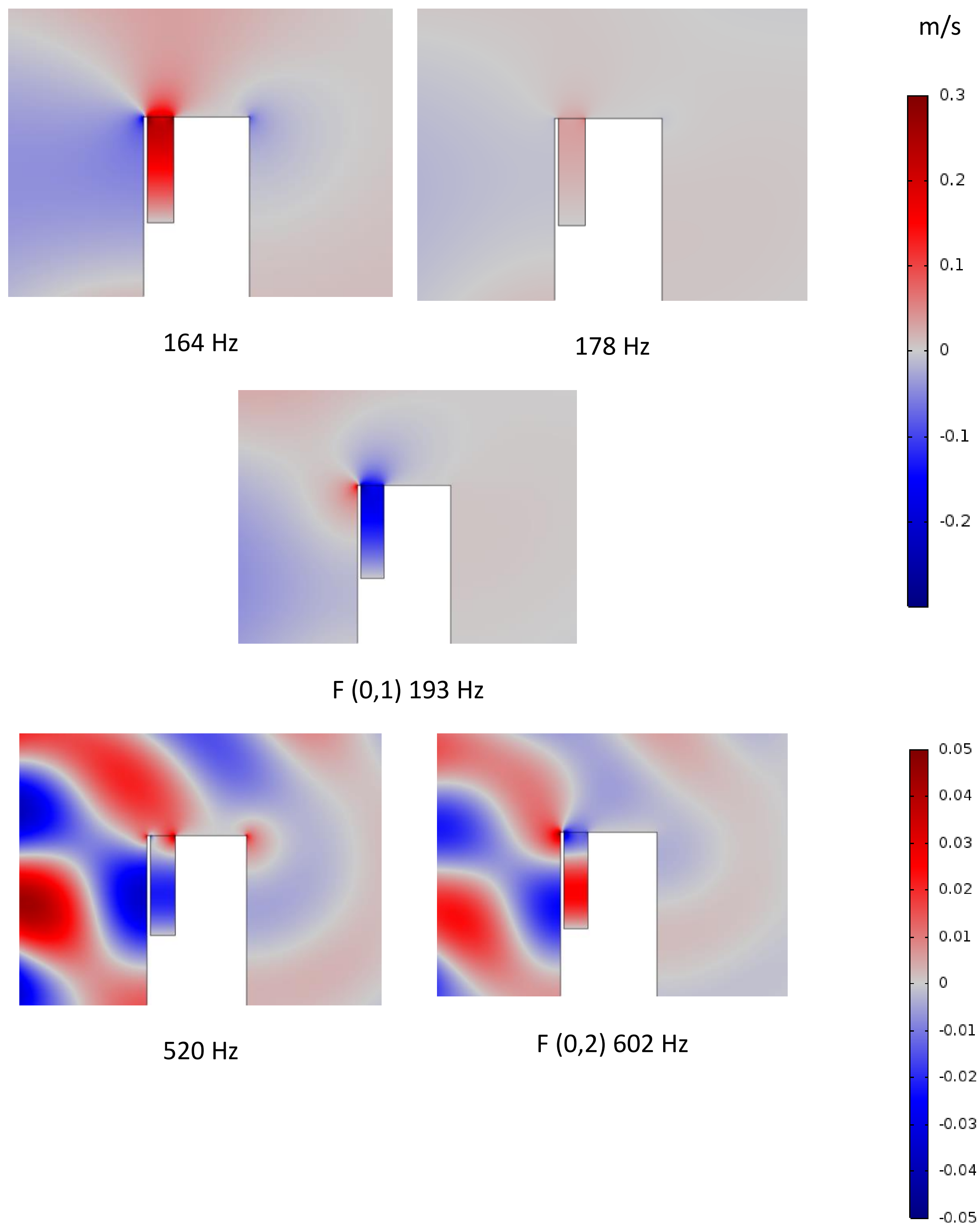
m/s
0.3
0.2
0.1
0
-0.1
-0.2
164 Hz
178 Hz
F (0,1) 193 Hz
520 Hz
F (0,2) 602 Hz
0.05
0.04
0.03
0.02
0.01
0
-0.01
-0.02
-0.03
-0.04
-0.05

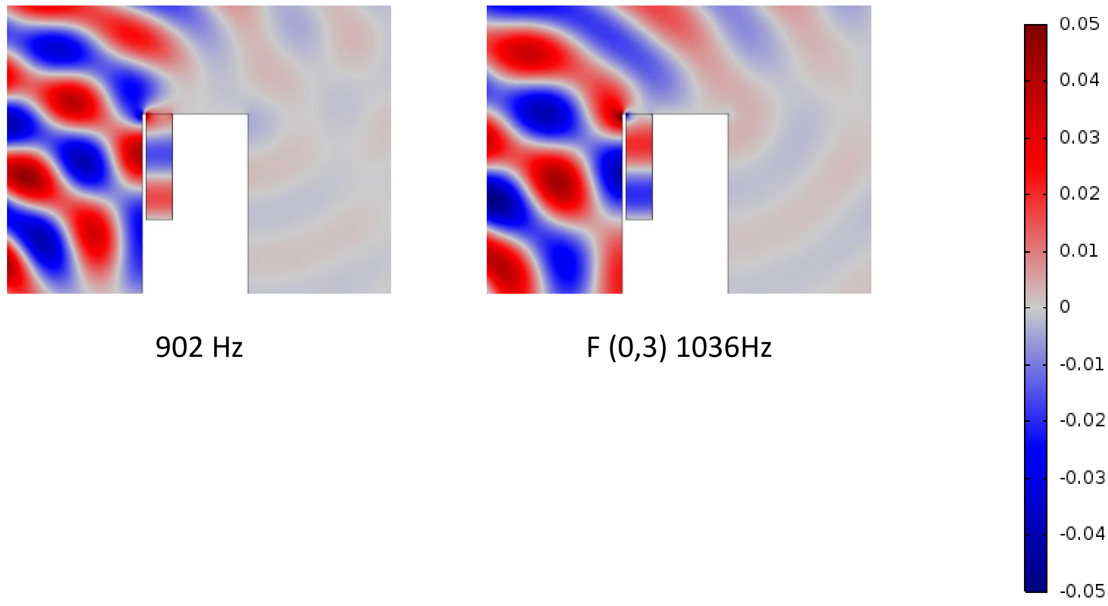

Figure 4.8 Velocity contour at the opening of acoustic cavity

Figure 4.8 shows the velocity contour in y-direction which is the particle velocity at cavity opening at frequency of drops, frequency of peaks and also frequency between drops and peaks with 0 absolute pressure.

At 164 Hz, the frequency of first drop, the particle velocity in y-direction at cavity opening is positive which means sound are reradiated from cavity. At 178 Hz, frequency between first drop and peak with 0 absolute pressure, it is easily to obtain that particle velocity in y-direction is nearly zero which means no motion in cavity. At 193 Hz, the first transverse mode, the particle velocity in y-direction is negative which cause a suction of sound into cavity. At 520 Hz and 902 Hz, it is the second and third drop, particle velocity at cavity opening is positive where the particle velocity at 602 Hz, and 1036 Hz, the second and third peak, are negative at cavity opening. It can be concluded that the drops in total Insertion Loss behind barrier is caused by the reradiation of sound at cavity opening at frequency a little lower than resonance frequencies. And the suction of sound at cavity opening at resonance frequency causes the peaks of Insertion Loss.

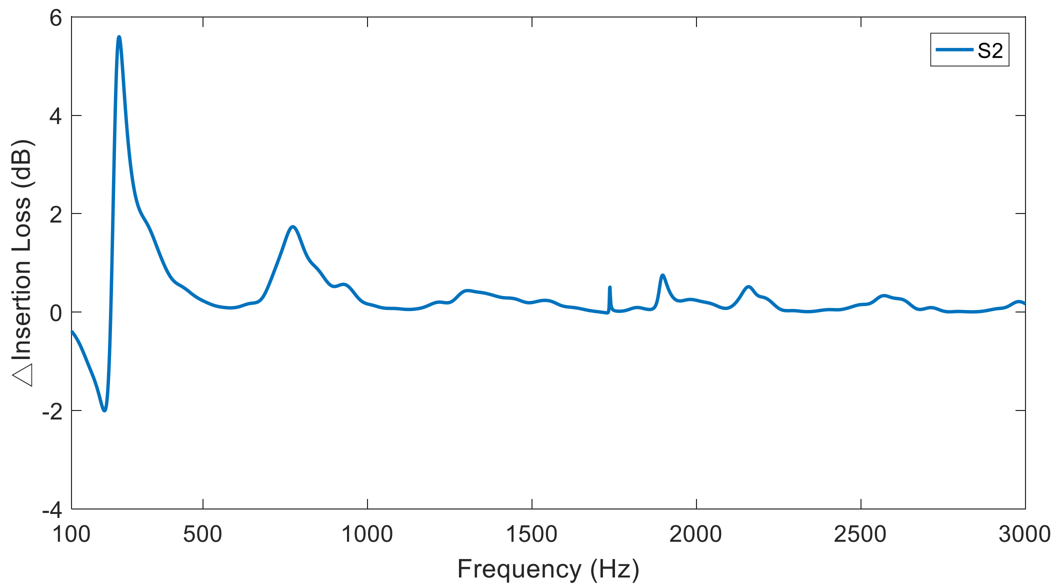

Figure 4.9 Relative Insertion Loss of Model S2

The validation of the relationship between resonance frequency and acoustic cavity is given in the previous Section. Further works are done to investigate the effect on noise attenuation behind barrier by changing the depth of acoustic cavity. A 0.3 m depth acoustic cavity (S2) is used instead of the 0.4 m depth acoustic cavity (S1) used in previous Section. By using the same boundary condition setting, two-dimensional computation is done, and the result is shown as Figure 4.9. It is easy to observe that Insertion Loss of Model S2 is almost positive in whole frequency range. Same as the result in previous Section, a decay trend of insertion loss can be found from first to third transverse modes. In addition, peaks appear at some specific frequencies and a drop is found next to the first resonance frequency. However, the peak and drop frequencies are shifted to higher frequency when compare with Model S1. Other than the shift of sharp peak, the Insertion Loss is also lower than Model S1 especially in high frequency which over 2000 Hz. The performance of Model S2 becomes poor because the separation of resonance frequency is changed. When the separation of sharp peak is close to each other, it can enlarge the effective frequency range and even increase the performance of noise attenuation.

Table 4.2 Resonance frequency of Model S2 by calculation and numerical results

Calculated resonance frequencies (Hz)	Resonance frequencies of Model S2 (Hz)
285 (0,1)	245
857 (0,2)	770
1429 (0,3)	1305
1738 (1,1)	1737
1917 (1,2)	1900
2000 (0,4)	
2232 (1,3)	2167
2572 (0,5)	
2635 (1,4)	2567

From Table 4.2, results show that the shift of resonance frequency becomes larger at low frequency compare with Model S1 and close to the calculated value at high frequency. Investigation on the relationship of the mode pattern in cavity is conducted. It can be observed that the missing frequency at high frequency is the higher order transverse modes (begin at the third mode) .It can be concluded that when the mode order of transverse mode becomes higher, the effectiveness of noise attenuation provided becomes worse unless it is coupled with the first longitudinal mode. It can validate to the performance of resonator that the significant sharp peak is only occurred at the first resonance frequency. Besides that, the top edge of normal straight noise barrier also contributes to the sound diffraction at high frequency. Therefore, the worse performance of acoustic cavity is the result in the coupling effect of sound diffraction of noise barrier and mechanism of resonator, which the diffraction effect of barrier will dominate at high frequency. In Addition, another missing peak at 1715 Hz is produced by the first longitudinal mode. Since it is close to the coupling mode at 1738 Hz, it can be determined that the two peaks are combined to form a significant sharp peak.

Absolute pressure of sound wave inside the acoustic cavity is obtained as Figure 4.10 to found out the relationship between the depth of acoustic cavity and noise attenuation level behind barrier. At 245 Hz, which is the first mode to the depth of cavity, a significant high pressure appears inside the acoustic cavity. At 770Hz, second mode is found inside the cavity with lower acoustics pressure magnitude than first mode. At 1305 Hz, although the patterns of third mode can be observed, the magnitude of acoustic pressure inside the cavity is too low. Noise attenuation cannot be achieved at 1305 Hz since the sound energy haven’t vanish in the acoustic cavity. Thus, peak disappeared in the spectrum shown in previous Section. At 1737 Hz, due to the first longitudinal mode, high pressure is obtained inside the acoustic cavity. At 1900 Hz, 2167 Hz and 2567 Hz, combined mode patterns can be seen clearly. However, the acoustic pressure becomes lower after the third mode (2167 Hz). The peaks of fourth and fifth mode disappeared in spectrum.

Overall results show that, the depth of acoustic cavity is highly related to the resonance frequency of the best noise attenuation behind barrier. When the depth of acoustic cavity increases, the resonance frequencies shift to lower frequency. Moreover, the effect by acoustic cavity depth is dominated in the first two modes of cavity. The peak cannot be shown clearly or even disappeared in the spectrum after the third mode. Therefore, good noise attenuation due to the depth of acoustic cavity is in low frequency range only unless the longitudinal mode appears. The appearance of first longitudinal mode will contribute to transverse mode and even combined to form a peak. However, noise attenuation performance of combined mode also decreases after the third mode. It can be concluded that the noise attenuation performance decrease when frequency increase.

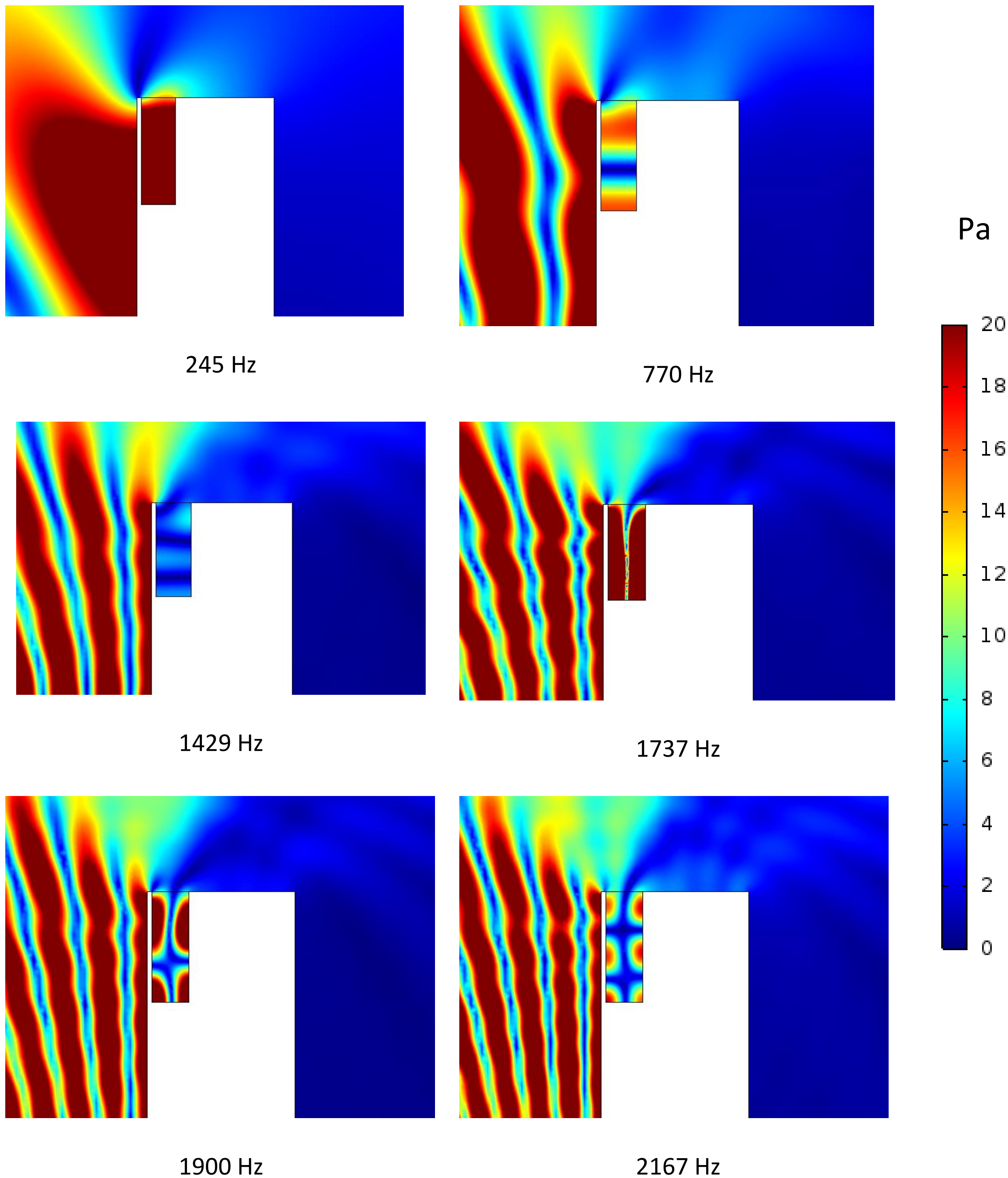
Pa
20
18
16
14
12
10
8
6
4
2
0
245 Hz
770 Hz
1429 Hz
1737 Hz
1900 Hz
2167 Hz

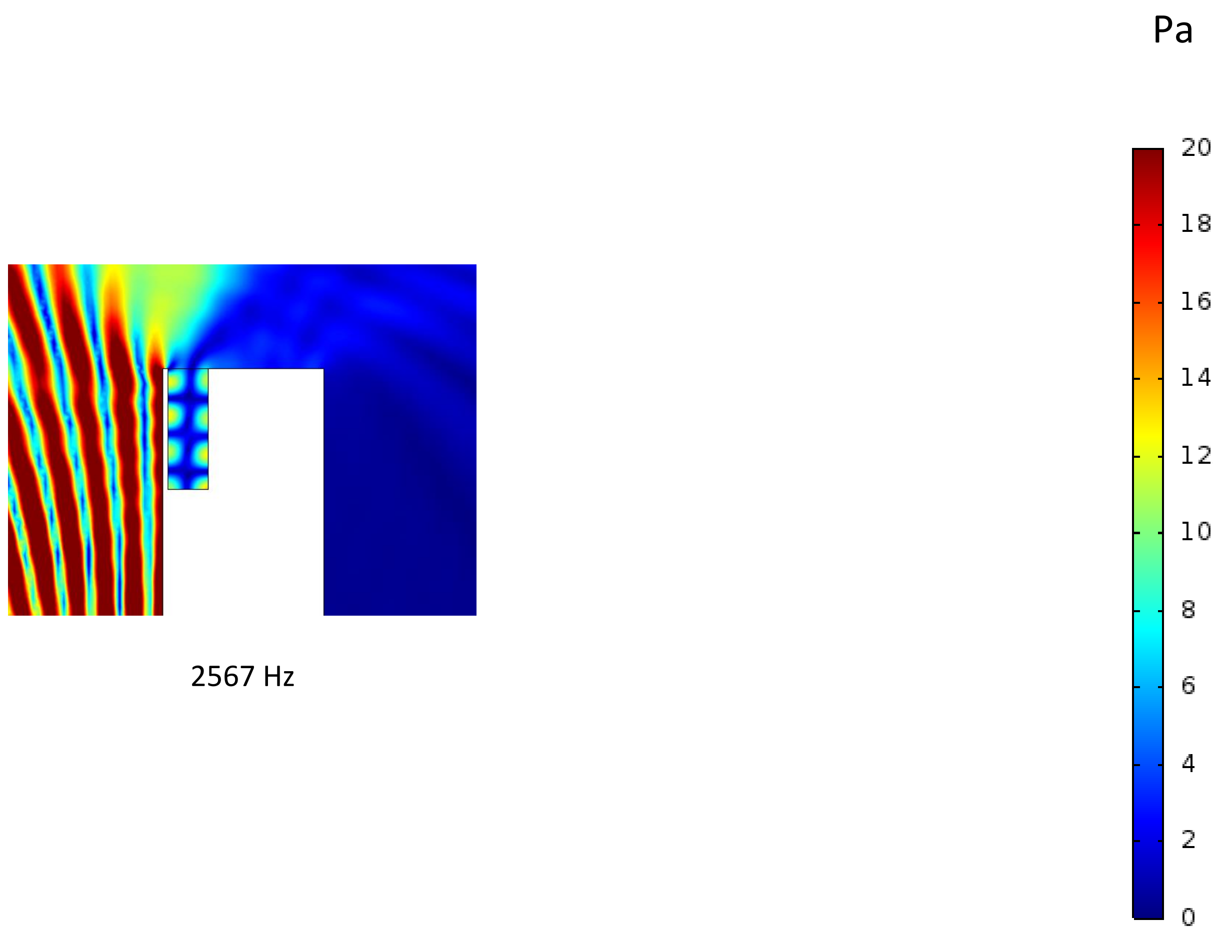

Figure 4.10 Absolute pressure of sound wave inside Model S2 at different resonance frequencies

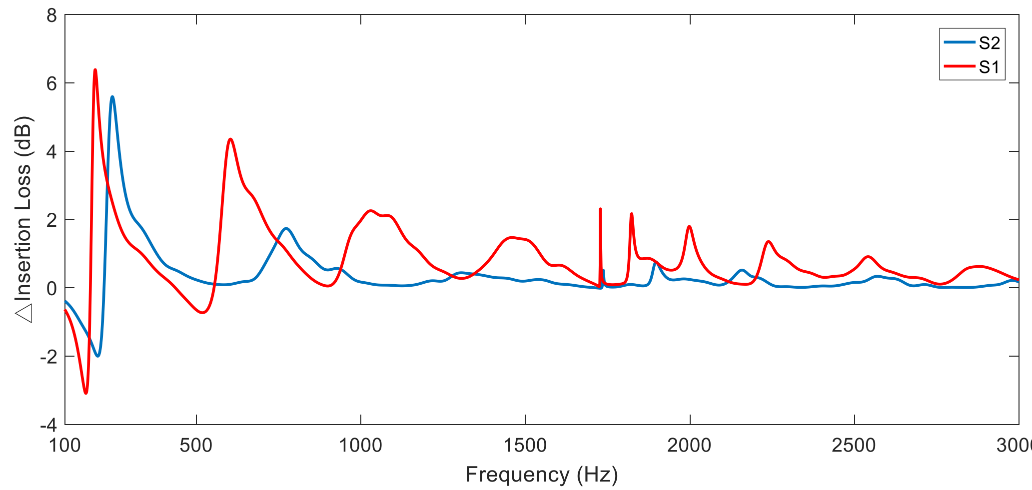

Figure 4.11 Relative Insertion Loss of Model S1 and S2

Figure 4.11 shows the comparison on relative Insertion Loss of Model S1 and S2. It shows clearly that the magnitude of Insertion Loss at first peak is almost the same. After the first peak, the magnitude of Insertion Loss will decay and the decay trend of Model S2 which have shorter cavity depth decrease rapidly at second peak and third peak cannot be observed clearly. Other than that, Model S1 have higher magnitude of first longitudinal mode, it causes the higher magnitude of Insertion Loss of combined peak in high frequency.

In conclude, acoustic cavity can give a great improvement on noise attenuation up to 2-6 dB at specific frequencies. However, the noise attenuation of cavity decreases when the mode number increase. In addition, Equation 3.24 can be used to estimate the resonance frequency of cavity in different depth. Results also finds that cavity depth is related to resonance frequency that it shifts to lower frequency when cavity depth increase.

4.5.2.2 Effect on location of acoustic cavity

From the results of Alfredson and Du (1995), scattering occurred at the edge of barrier so that the performance of barrier increases when number of diffracting edges on the barrier increase. However, the effect on barrier noise attenuation due to the distance between two diffraction edges is not given. Therefore, computation is carried out by moving the acoustic cavity much backward which extend the separation between the first and second diffraction edge. Results are given in Figure 4.12:

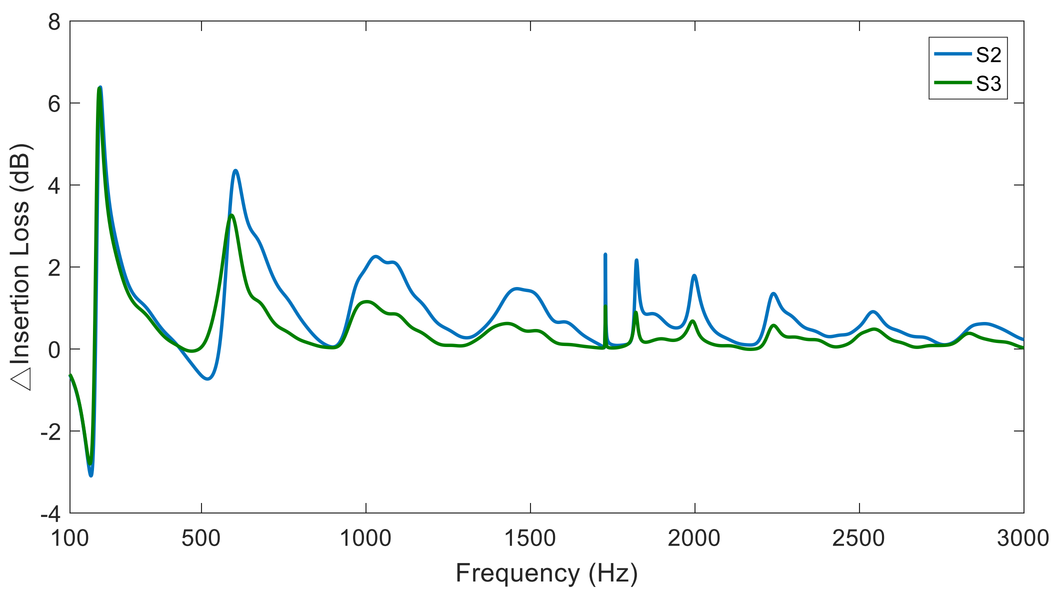

Figure 4.12 Relative Insertion Loss of Model S2 and Model S3

Computations are done by placing the acoustic cavity at original location and center of barrier. When all the dimension of acoustic cavity keeps unchanged, the performance of barrier affected by the location is clearly shown in Figure 4.12 that the Insertion Loss becomes smaller after the first resonance frequency. Nearly 2 dB less on Insertion Loss is found on these resonance frequencies produced by the higher order transverse mode. And 1 dB less on insertion Loss is found on the combined resonance frequencies. Although the magnitude of Insertion Loss becomes lower when the distance from leading edge to the acoustic cavity increase, the pattern of resonance frequency is similar to original one.

Table 4.3 Resonance frequency of Model S2 and Model S3

Calculated resonance frequencies (Hz)	Resonance frequencies of Model S2 (Hz)	Resonance frequencies of Model S3 (Hz)
214 (0,1)	193	189
643 (0,2)	602	589
1071 (0,3)	1082	1085
1500 (0,4)	1466	1409
1929 (0,5)		
2358 (0,6)		
2768 (0,7)		
1715 (1,0)	1728	1728
1728 (1,1)		
1831 (1,2)	1823	1821
2022 (1,3)	1998	1993
2278 (1,4)	2239	2241

2581 (1,5)	2528	2511
2915(1,6)	2893	2925

The detail of resonance frequencies captured in the computation is shown in Table 4.3. There is a little shift to lower frequency on the resonance frequency when the acoustic cavity is moved to the center of barrier. And it can be observed that the pattern of resonance frequency found in both cases is the same. It can be concluded that the location of acoustic cavity does not influence the mechanism of acoustic cavity but only affect the magnitude of the Insertion Loss at resonance frequency.

Model S2

Model S3

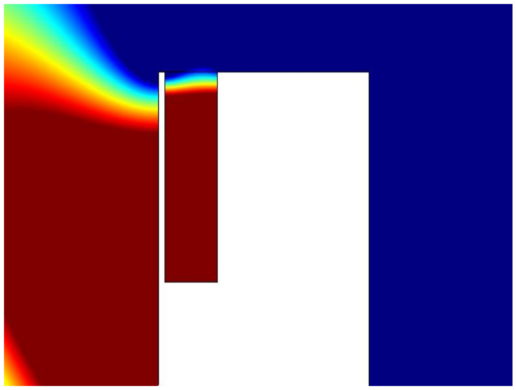

F (0,1) 193 Hz

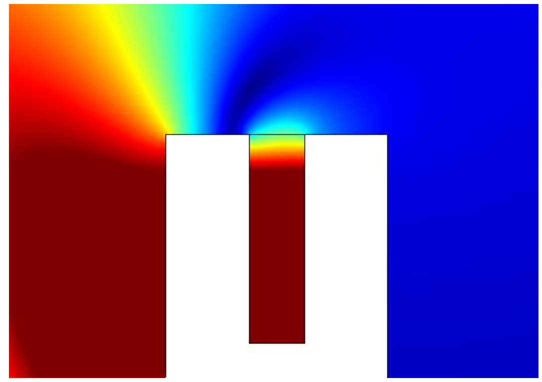

F (0,1) 189 Hz

Pa

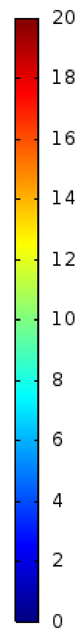

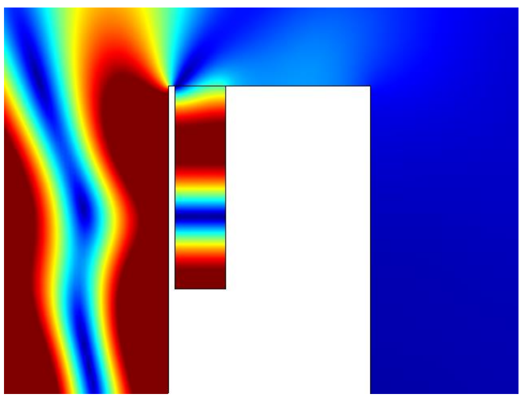

F (0,2) 602Hz

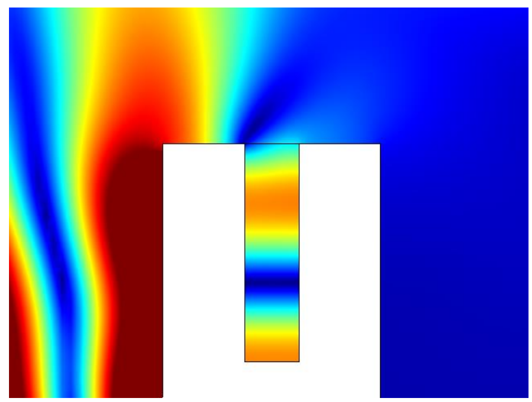

F (0,2) 589 Hz

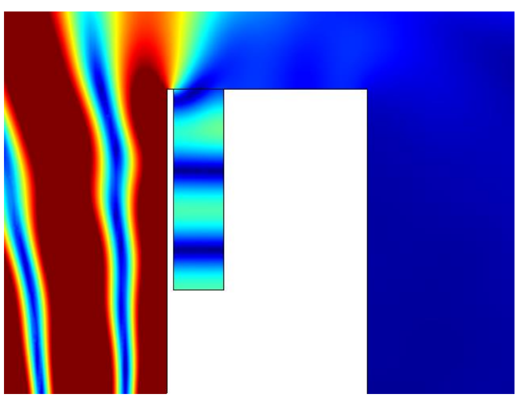

F (0,3) 1082 Hz

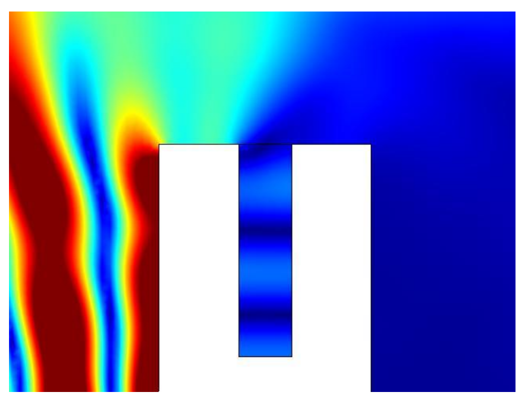

F (0,3) 1085 Hz

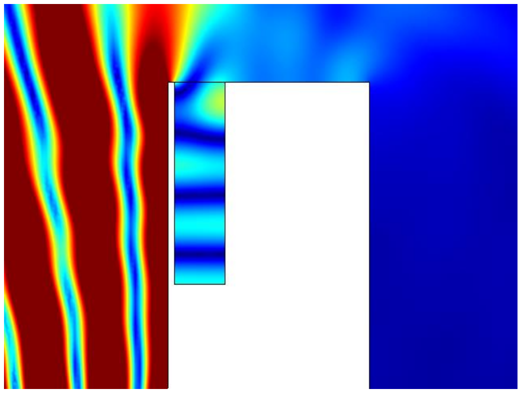

F (0,4) 1466 Hz

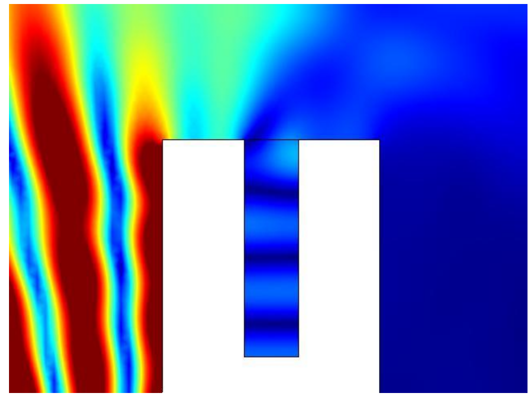

F (0,4) 1409 Hz

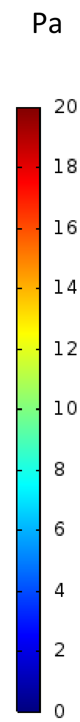

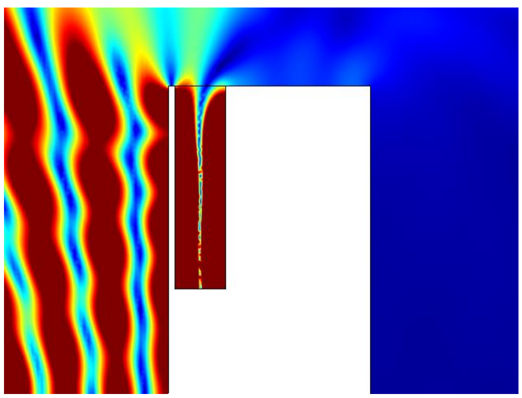

F (1,0) 1728 Hz

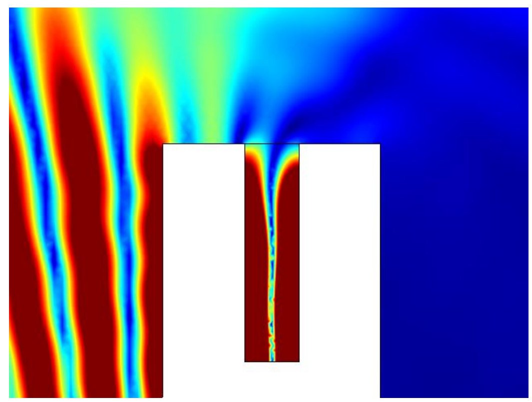

F (1,0) 1728 Hz

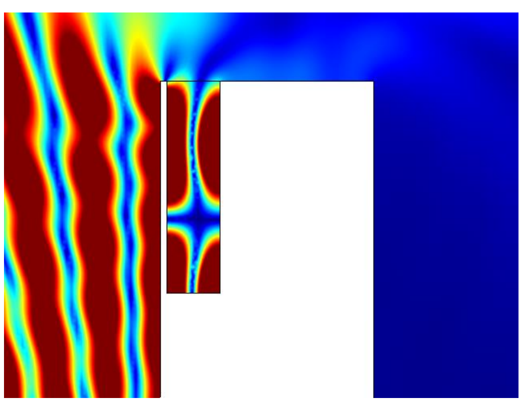

F (1,2) 1823 Hz

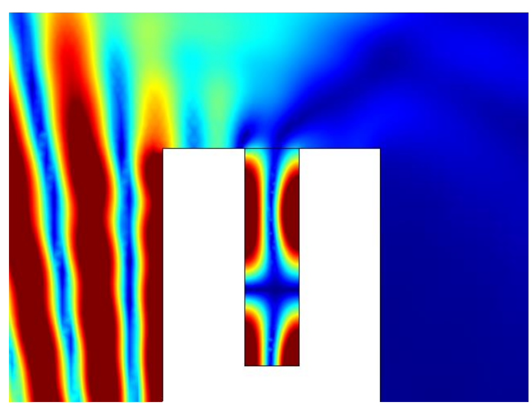

F (1,2) 1821 Hz

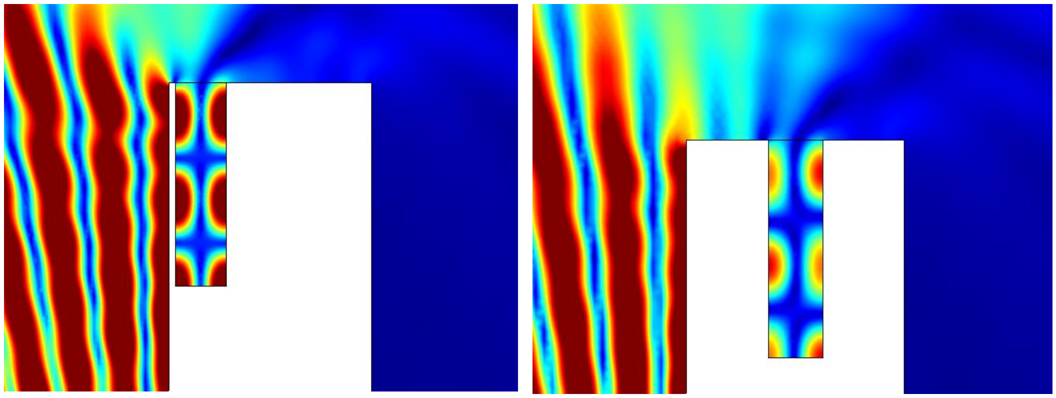

F (1,3) 1998 Hz

F (1,3) 1993 Hz

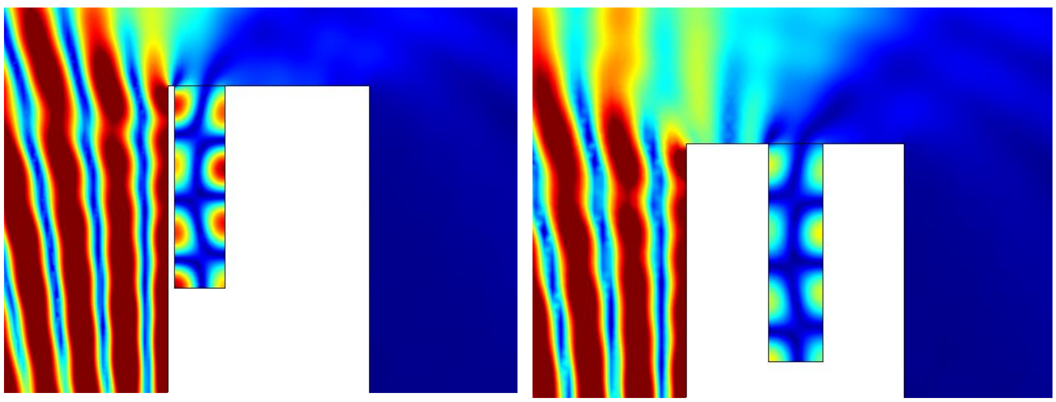

F (1,4) 2239 Hz

F (1,4) 2241 Hz

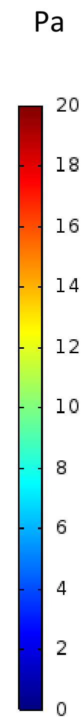

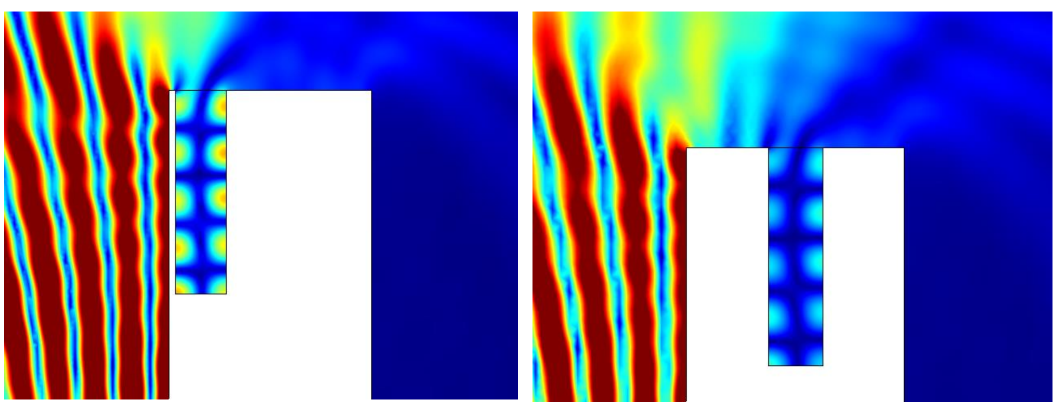

F (1,5) 2528 Hz

F (1,5) 2511 Hz

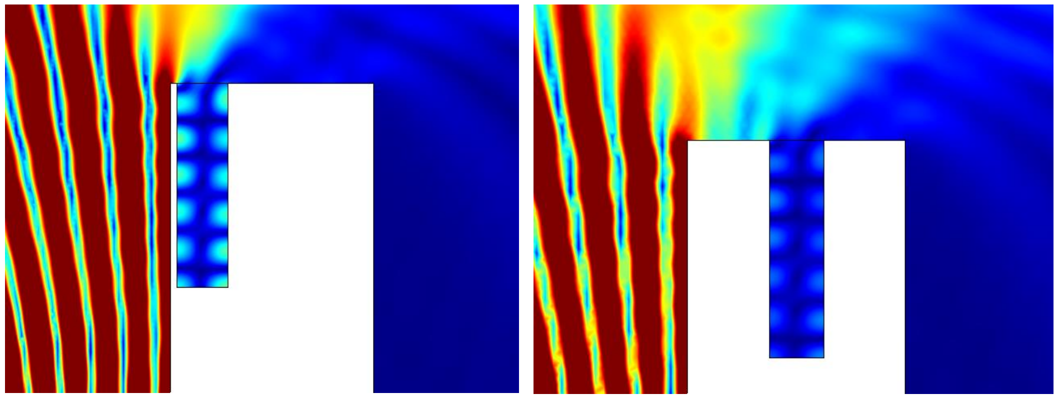

Figure 4.13 Absolute pressure of sound wave inside Model S2 and Model S3

Compare is also done using contour plot of absolute acoustic pressure inside cavity. Although the resonance frequency of Model S3 have a little shift to lower frequency, it is clear that the mode patterns of both Models are similar at these resonance frequencies. The main difference of these two Models is that the magnitude of acoustic pressure in each mode is much lower when the cavity located at the center at all resonance frequencies except the first transverse and longitudinal mode. Therefore, it reflects that the magnitude of Insertion Loss of Model S3 is much lower than Model S2 at resonance frequencies.

4.5.2.3 Summary

Several tests are done by numerical computations in this Section. Results have shown that changing the location and depth of acoustic cavity affect the performance of noise barrier in different ways. By changing the cavity depth, resonance frequency of noise barrier is changed. All the resonance frequencies are shifted to another location following Equation 3.24 mentioned in Chapter 3. Therefore, the effective frequency range of noise barrier can be adjusted by changing the depth of acoustic cavity.

By changing the separation of first and second diffraction edge of noise barrier, it does not affect the resonance frequency of acoustic cavity. However, the magnitudes of Insertion Loss at these resonance frequencies decrease by 1-2 dB especially at high frequency range when separation between acoustic cavity and barrier leading edge becomes longer.

4.5.3 Double slots barrier (D-Type)

After the test of single slot barrier, the relationship between noise attenuation performance and the location and depth of acoustic cavity is found. To further improve the noise attenuation performance of barrier, the use of additional acoustic cavity is considered to enlarge the resonance frequency and magnitude at resonance frequencies. Investigation on the effect of barrier with double acoustic cavities is done by numerical computations in this Section.

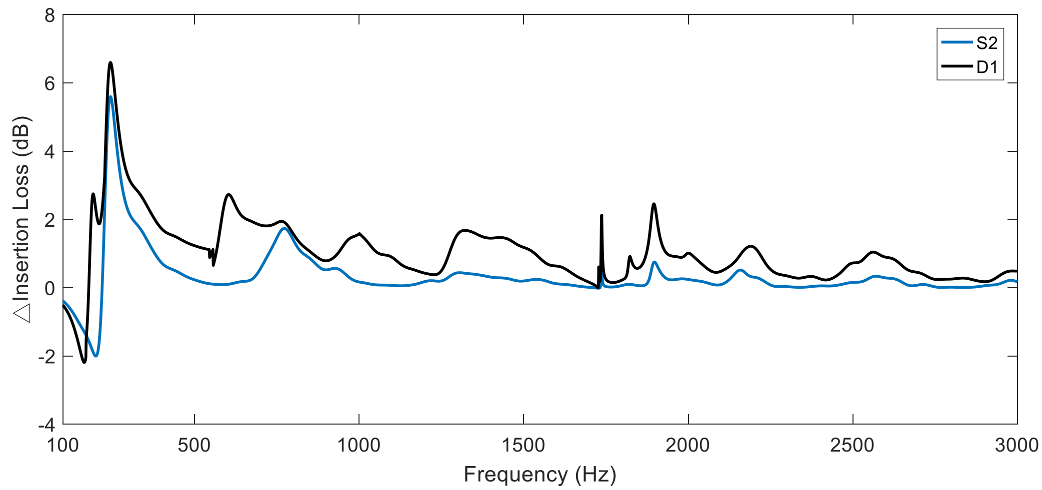

Figure 4.14 Insertion Loss of Model S2 and Model D1

In Figure 4.14, the blue line represents the relative Insertion Loss of barrier with 0.3 m depth cavity. The black line represents the relative Insertion Loss of barrier with 0.3 m depth and 0.4 m depth cavity in first row and second row respectively. Difference can be observed that the number of resonance frequencies of Model D1 is double than Model S2. At around 700 Hz, the effective frequency range of Model D1 is extended from the second resonance frequency of Model S2 which should be 857 Hz. The extended effective frequency range of Model D1 can also be observed at around 1000 Hz and 1350 Hz. In general, these barriers can perform a higher Insertion Loss than a reference barrier in whole frequency range. It is given that the performance of Model D1 at low frequency is better than the performance of Model S2 but give a similar performance in high frequency range.

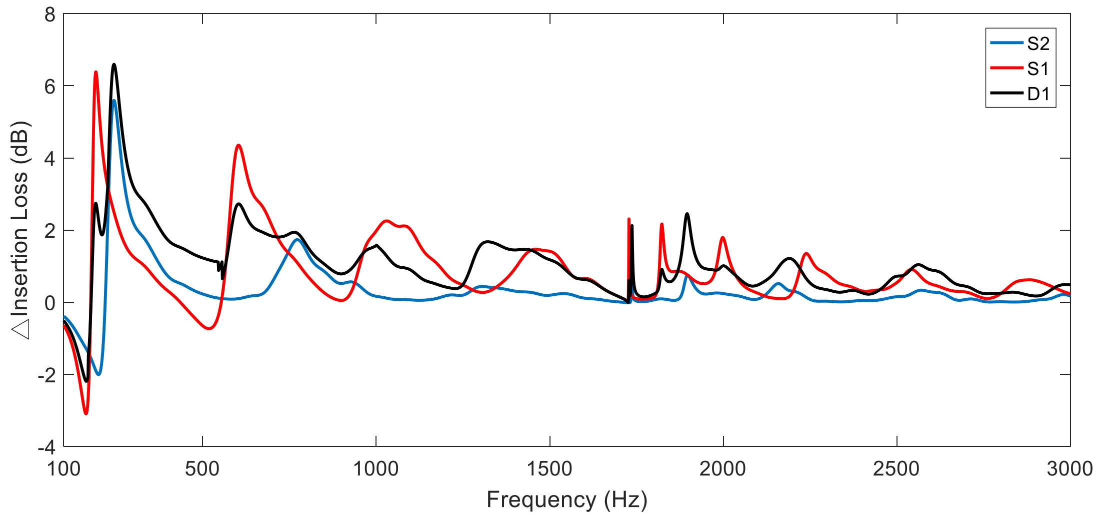

Figure 4.15 Insertion Loss of Model S2, Model S1 and Model D1

In Figure 4.15, the relative Insertion Loss of Model S1 is added in red. It can be found that the extended effective frequency of Model D2 is related to the resonance frequency of Model S1. When there is a resonance frequency of model S1 or Model S2, there is a peak of Model D1 too. By averaging the relative Insertion Loss of Model S1 and Model S2, it equal to the relative Insertion Loss of Model D1 at almost whole frequency range. Therefore, the overall relative Insertion Loss of Model D1 is higher than Model 1 or Model S2 which also shows that additional cavity can improve the noise attenuation of barrier. Other than that, decay trend of Insertion Loss at resonance frequency of Model D1 is found similar to the average decay trend of both Model S1 and S2. However, the noise attenuation performance of Model D1 is still weak at high frequency due to the relative weak performance of acoustic cavity.

Table 4.4 Resonance frequency of Model S1, Model S2 and Model D1

Calculated resonance frequencies (Hz)	Resonance frequencies of Model S1 (Hz)	Resonance frequencies of Model S2 (Hz)	Resonance frequencies of Model D2 (Hz)
F1 (0,1) 214	193		195
F2 (0,1) 285		245	242
F1 (0,2) 643	602		605
F2 (0,2) 857		770	763
F1 (0,3) 1071	1083		1083
F2 (0,3) 1429			
F1 (0,4) 1500	1464		1468
F1,2 (1,0) 1715			1728
F1 (1,1) 1728	1728		1737
F2 (1,1) 1738		1737	1822
F1 (1,2) 1831	1823		1906
F2 (1,2) 1917		1900	1997
F1 (0,5) 1929	1999		
F2 (0,4) 2000			2094
F1 (1,3) 2022	2092		2170

F2 (1,3) 2232		2167	2240
F1 (1,4) 2278	2239		
F1 (0,6) 2358			
F2 (0,5) 2572			
F1 (1,5) 2581	2527		2530
F2 (1,4) 2635		2607	2611
F1 (0,7) 2786			
F1 (1,6) 2915	2912		2912

The resonance frequency of Model D1 is shown in Table 4.4. It is clearly seen that the resonance frequency of Model D1 is nearly same with the combination of both Model S1 and Model S2. And it also keeps the property of acoustic cavity that the effectiveness in higher order transverse mode is still low or even not obvious. It gives a good agreement to our assumption that the performance of barrier can be improved by enlarging the frequency range due to the addition acoustic cavity. Further computations are done to test the effect of performance due to acoustic cavity arrangement change and also the change in cavity depth in both slots.

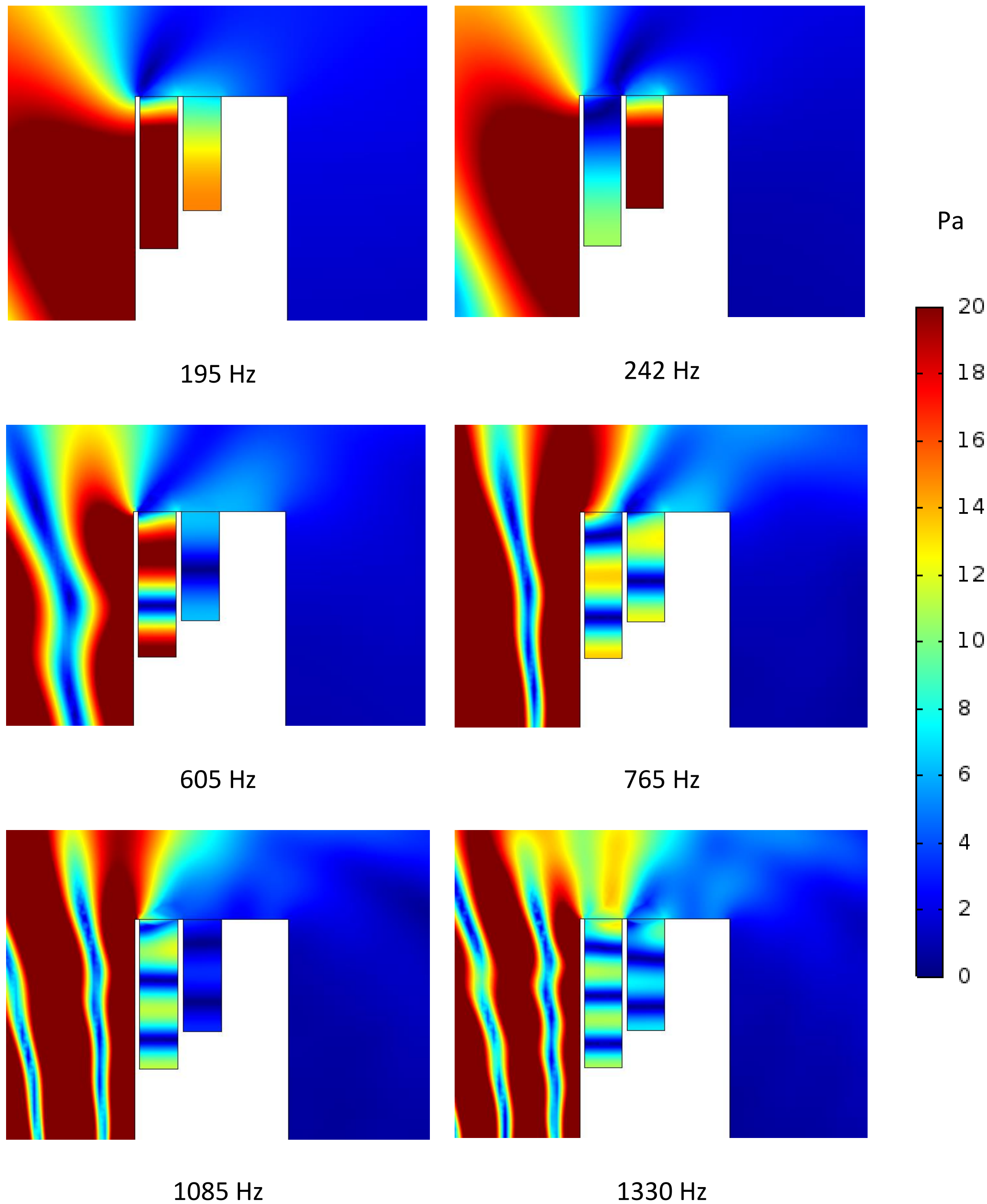

Pa
20
18
16
14
12
10
8
6
4
2
0
195 Hz
242 Hz
605 Hz
765 Hz
1085 Hz
1330 Hz

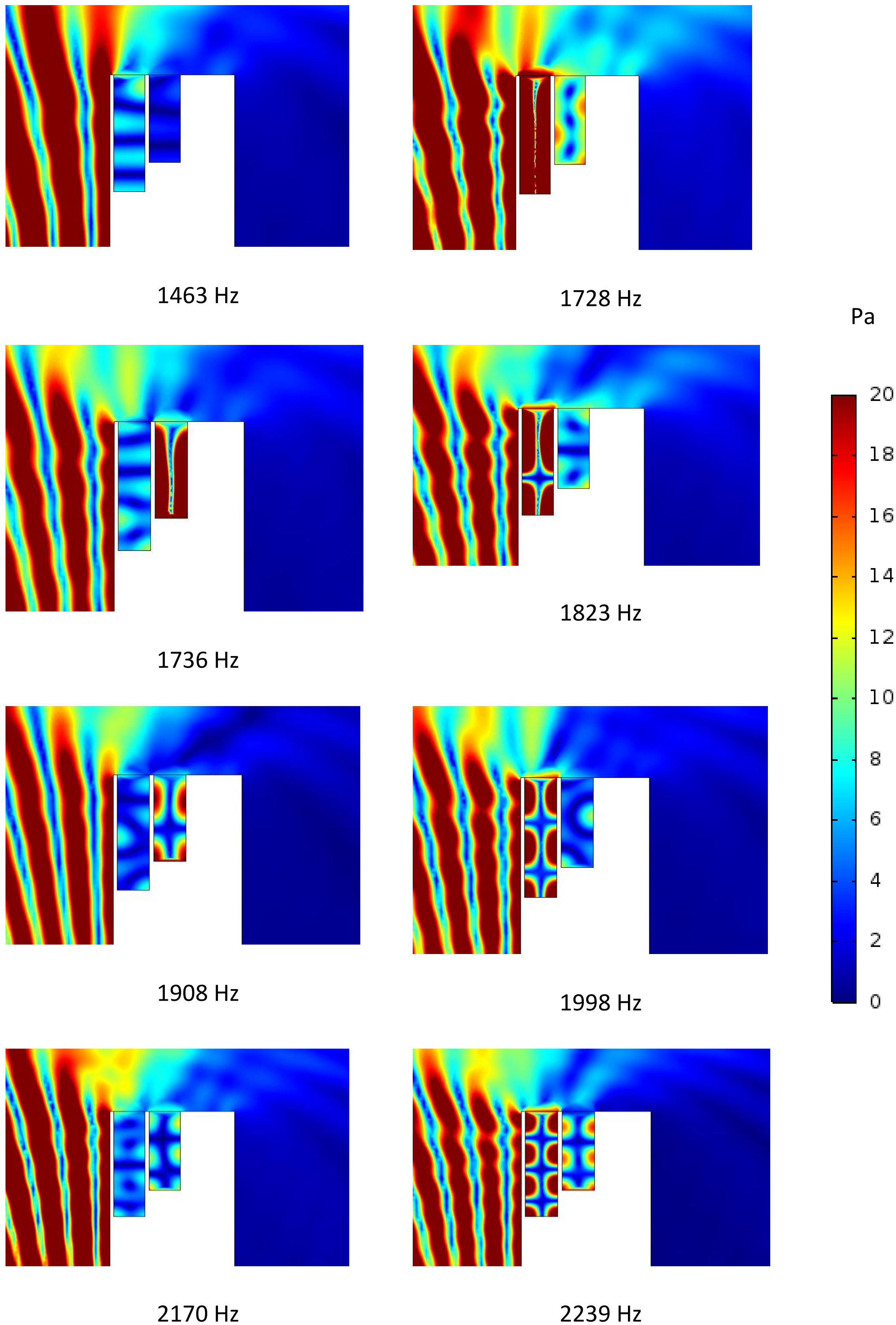
1463 Hz
1728 Hz
Pa
20
18
16
14
12
10
8
6
4
2
0
1736 Hz
1823 Hz
1908 Hz
1998 Hz
2170 Hz
2239 Hz

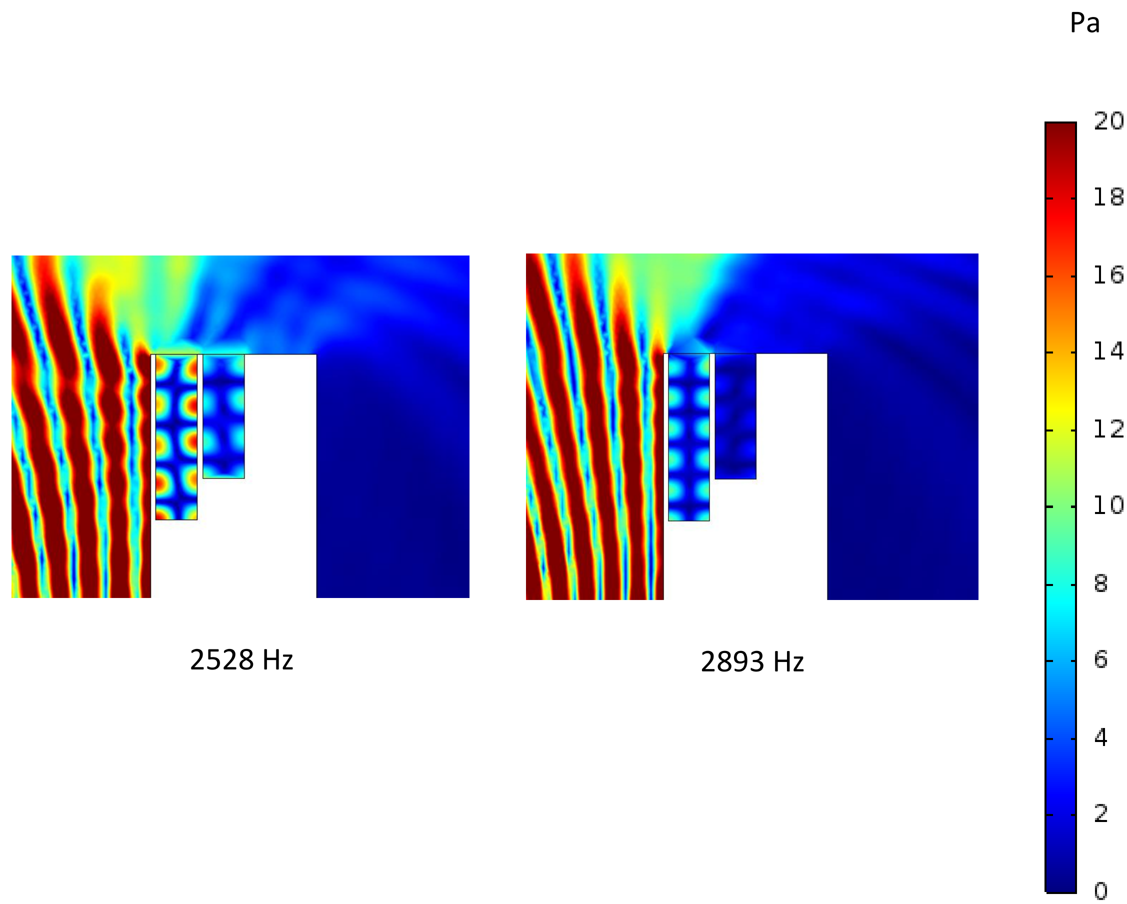

Figure 4.16 Absolute pressure of sound wave inside cavity of Model D1

At 195 and 242 Hz, the first mode of 0.4 m and 0.3 m acoustic cavity appeared so that high acoustic pressure can be found inside these cavities. However, the magnitude of acoustic pressure drops inside the second cavity at 765 Hz where the magnitude of acoustic pressure inside the first cavity remains at similar level at 605 Hz. At 1085 Hz, 1330 Hz and 1463Hz, the magnitude and patterns of first cavity same as Model S1. However, the mode patterns of second cavity at these frequencies cannot be observed clearly as Model S2 since there is diffraction of sound occurred at first cavity and reduce the sound energy enter the second cavity. At 1728 Hz and 1736 Hz, a significant high pressure is shown in both cavities due to the first combined mode of both cavities. The magnitude of acoustic pressure of second cavity is lower than Model S2 at same frequency. At 1823 Hz, 1998 Hz, 2239 Hz, 2528 Hz and 2893 Hz, the combined modes inside the first cavity are clearly seen and the magnitude of acoustic pressure at these frequencies has no big difference to the results of Model S1. However, the combined modes of second cavity are not clear due to the low magnitude of acoustic pressure.

From the overall results, the higher order modes of both acoustic cavities are observed at different resonance frequencies from the Figure 4.16. Although peak can be found at resonance frequency of these cavities, difference is found on the acoustic pressure magnitude in acoustic cavities. It is given that the higher order modes in the first acoustic cavity are clear. However, the acoustics mode pattern in the second cavity are not shown clearly due to the low magnitude of absolute sound pressure inside the cavity. It is because a large amount of sound energy is diffracted at the first cavity and the rest is then propagated over the second slot and diffracted again. Therefore, the magnitude of the sound energy inside the second cavity is lower and it means the performance of noise barrier is less related to the diffraction of sound at its opening.

4.5.3.1 Effect on the depth of acoustic cavity

The last test on double slots barrier is swapping the first and second cavity on the top surface of barrier. In the following numerical computation, the depth of first cavity is change to 0.3 m and the second cavity is change to 0.4 m. According to the results obtained in the previous Section by S-Type barrier, the resonance frequency of the tested barrier should be difference after the swapping acoustic cavities.

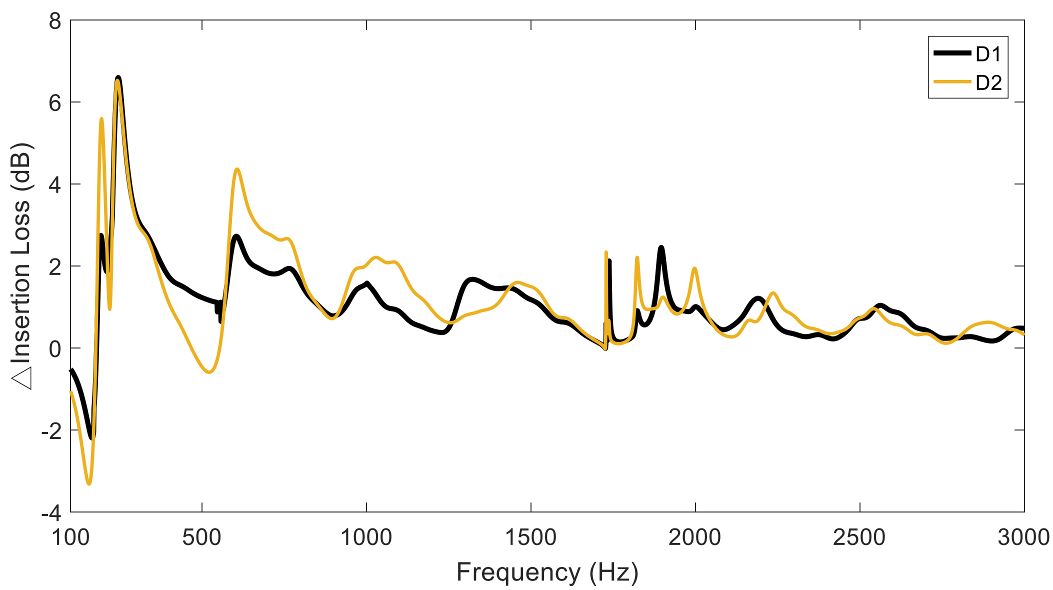

Figure 4.17 Insertion Loss of Model D1 and Model D2

It is observed that the noise attenuation performances of these D-Type barriers are better than the conventional vertical barrier in whole frequency range. Difference is found on the resonance frequency between both barriers as estimation. From Figure 4.17, the resonance frequency of D-Type barriers is dominated by depth of first cavity. For Model D1, the resonance frequency is almost same as the resonance frequency of Model S2. Besides that, the second cavity still contribute to noise attenuation as the extra peaks which can compensate the weakness part of frequency spectrum of Model S2. For example, the Insertion Loss from 600 Hz to 1000 Hz is the weakest part of Model S2. When a 0.4 m depth acoustic cavity is placed at second row, there is an increase in Insertion Loss around 3 dB in this frequency range. The compensation of second cavity is most significant in low frequency range than that in high frequency range since separation of peak is large at low frequency.

Table 4.5 Resonance frequency of Model D1 and Model D2

Calculated resonance frequencies (Hz)	Resonance frequencies of Model D1 (Hz)	Resonance frequencies of Model D2 (Hz)
F1 (0,1) 214	195	200
F2 (0,1) 285	242	246
F1 (0,2) 643	605	625
F2 (0,2) 857	765	772
F1 (0,3) 1071	1085	1085
F2 (0,3) 1429	1330	1300
F1 (0,4) 1500	1463	1474
F1,2 (1,0) 1715	1728	1728
F1 (1,1) 1728		
F2 (1,1) 1738	1736	1737
F1 (1,2) 1831	1823	1823
F2 (1,2) 1917	1908	1896
F1 (0,5) 1929		
F2 (0,4) 2000		2000
F1 (1,3) 2022	1998	
F2 (1,3) 2232	2170	2181
F1 (1,4) 2278	2239	

F1 (0,6) 2358		
F2 (0,5) 2572		2504
F1 (1,5) 2581	2528	
F2 (1,4) 2635		2616
F1 (0,7) 2786		
F1 (1,6) 2915	2893	2900

F1 and F2 in the Table 4.5 represent the resonance frequency of 0.3 m depth cavity and 0.4 m depth cavity. It can be observed that the first four resonance frequencies of both cavities can be obtained in these D-Type barriers. Same as the resonance frequency of S-Type barrier, peak at high frequency cannot be obtained clearly. Besides that, results also show that the resonance frequency of first cavity is more observable than that of second cavity. It is because sound energy is dissipated by the scattering at first cavity which reduces the performance of second cavity.

Compare is done on the absolute acoustic pressure inside cavities to investigate the change in noise attenuation due to different arrangement on the acoustic cavity position. The magnitude of acoustic pressure by the first mode of these cavities is nearly same even the cavity location swapped. At other resonance frequencies, a drop on acoustic pressure is obtained when the cavity swapped.

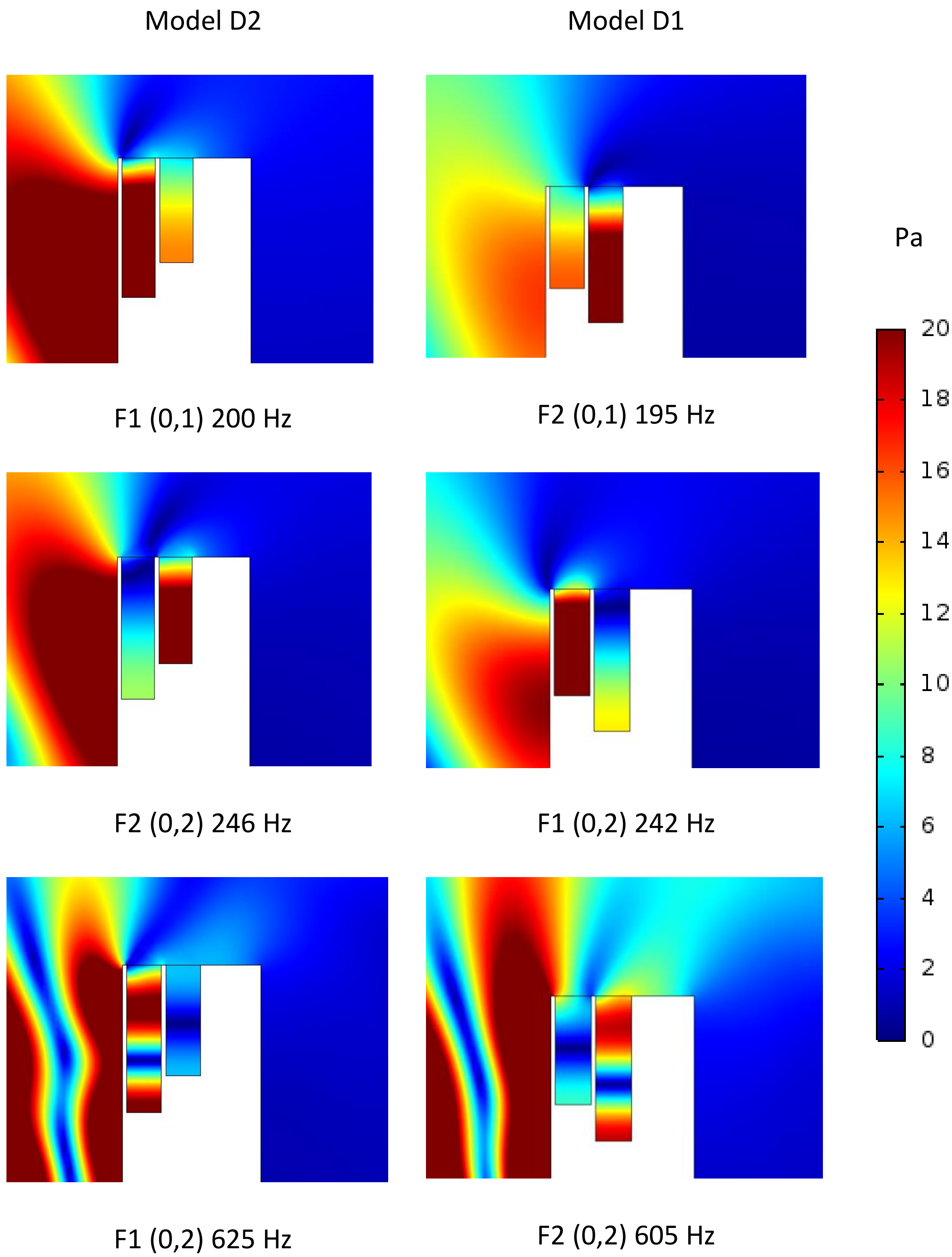
Model D2
Model D1
F1 (0,1) 200 Hz
F2 (0,1) 195 Hz
F2 (0,2) 246 Hz
F1 (0,2) 242 Hz
F1 (0,2) 625 Hz
F2 (0,2) 605 Hz
Pa
20
18
16
14
12
10
8
6
4
2
0

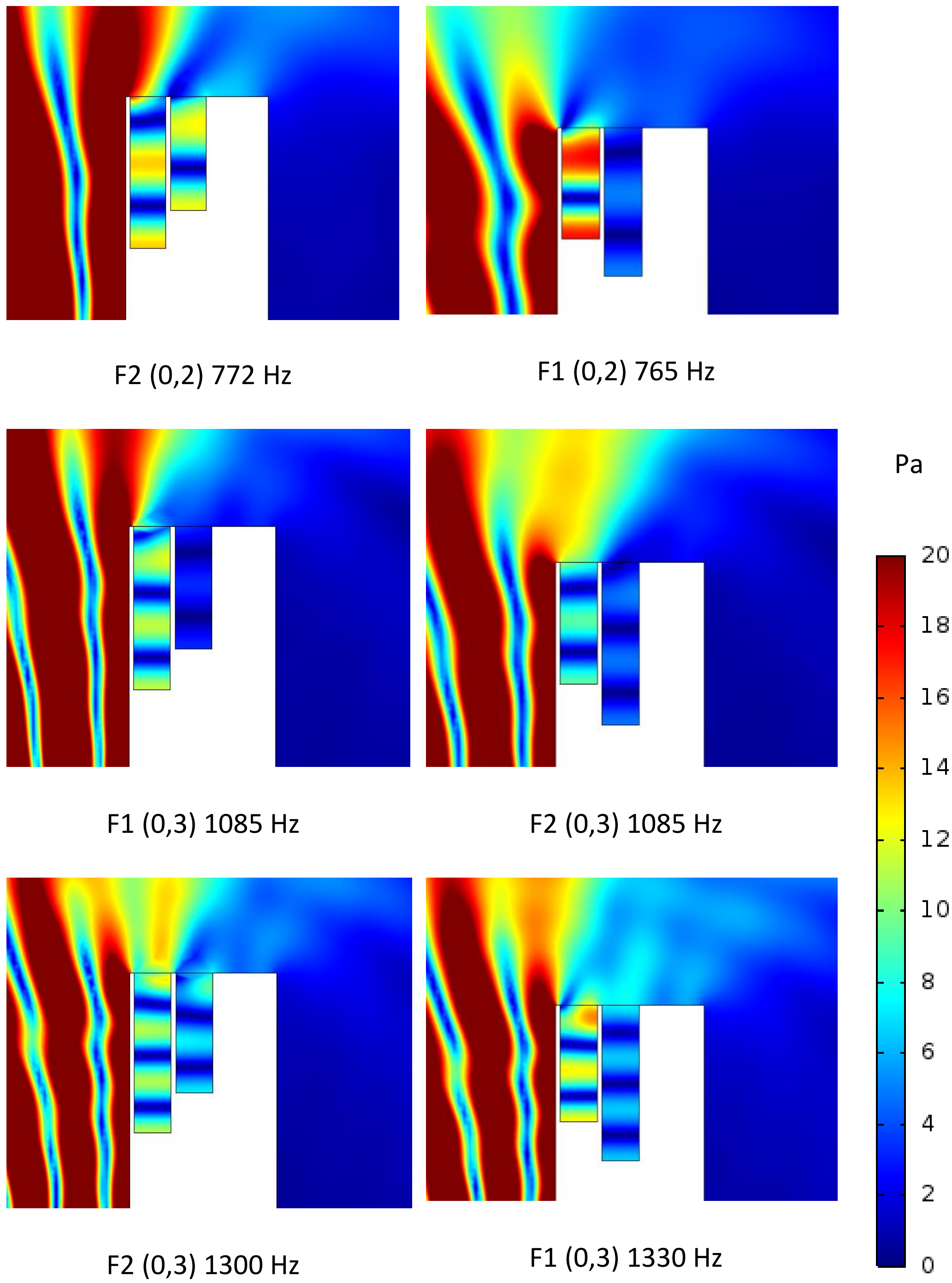
F2 (0,2) 772 Hz
F1 (0,2) 765 Hz
F1 (0,3) 1085 Hz
F2 (0,3) 1085 Hz
F2 (0,3) 1300 Hz
F1 (0,3) 1330 Hz
Pa
20
18
16
14
12
10
8
6
4
2
0

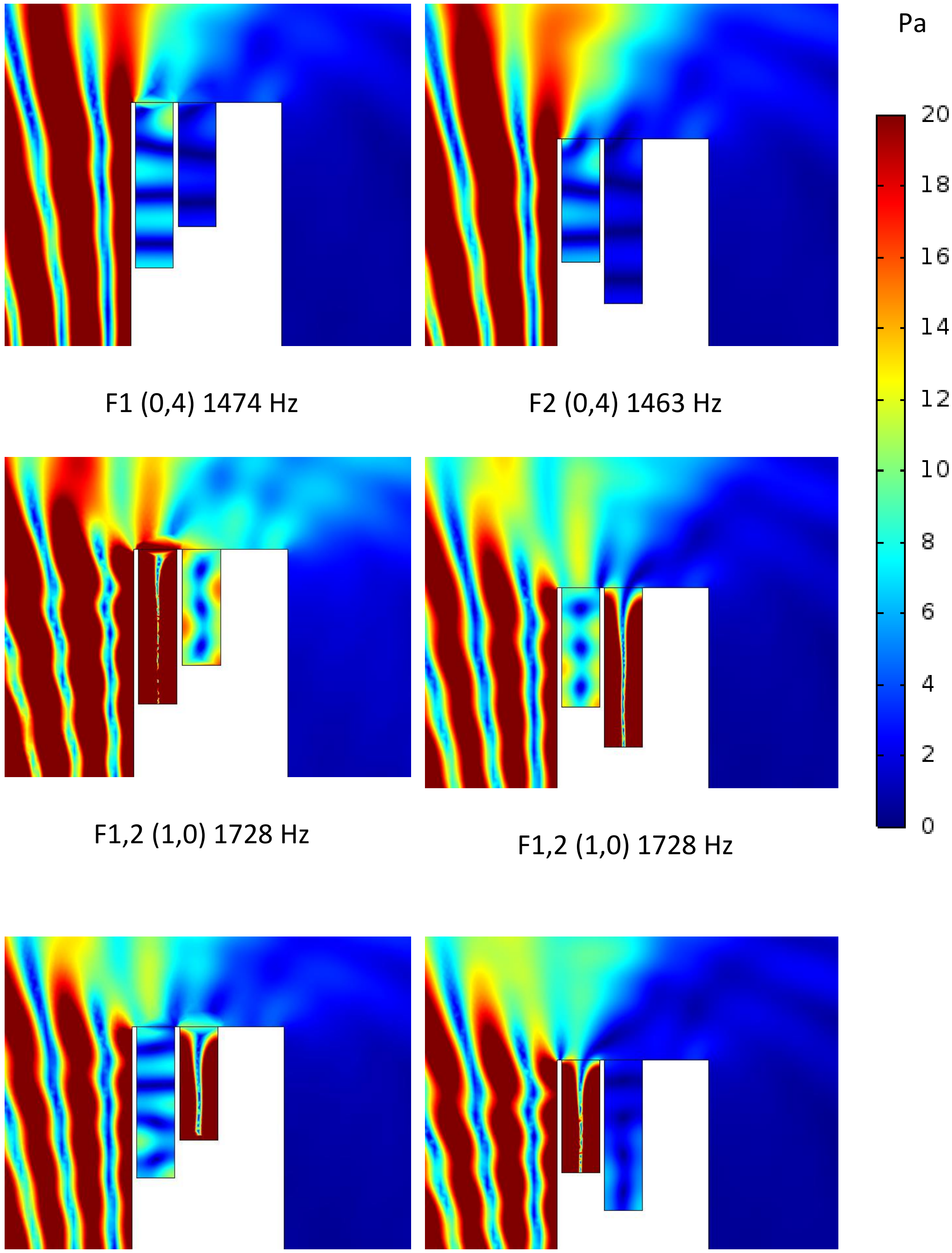

F1 (0,4) 1474 Hz

F2 (0,4) 1463 Hz

F1,2 (1,0) 1728 Hz

F1,2 (1,0) 1728 Hz

F2 (1,1) 1737 Hz

F1 (1,1) 1736 Hz

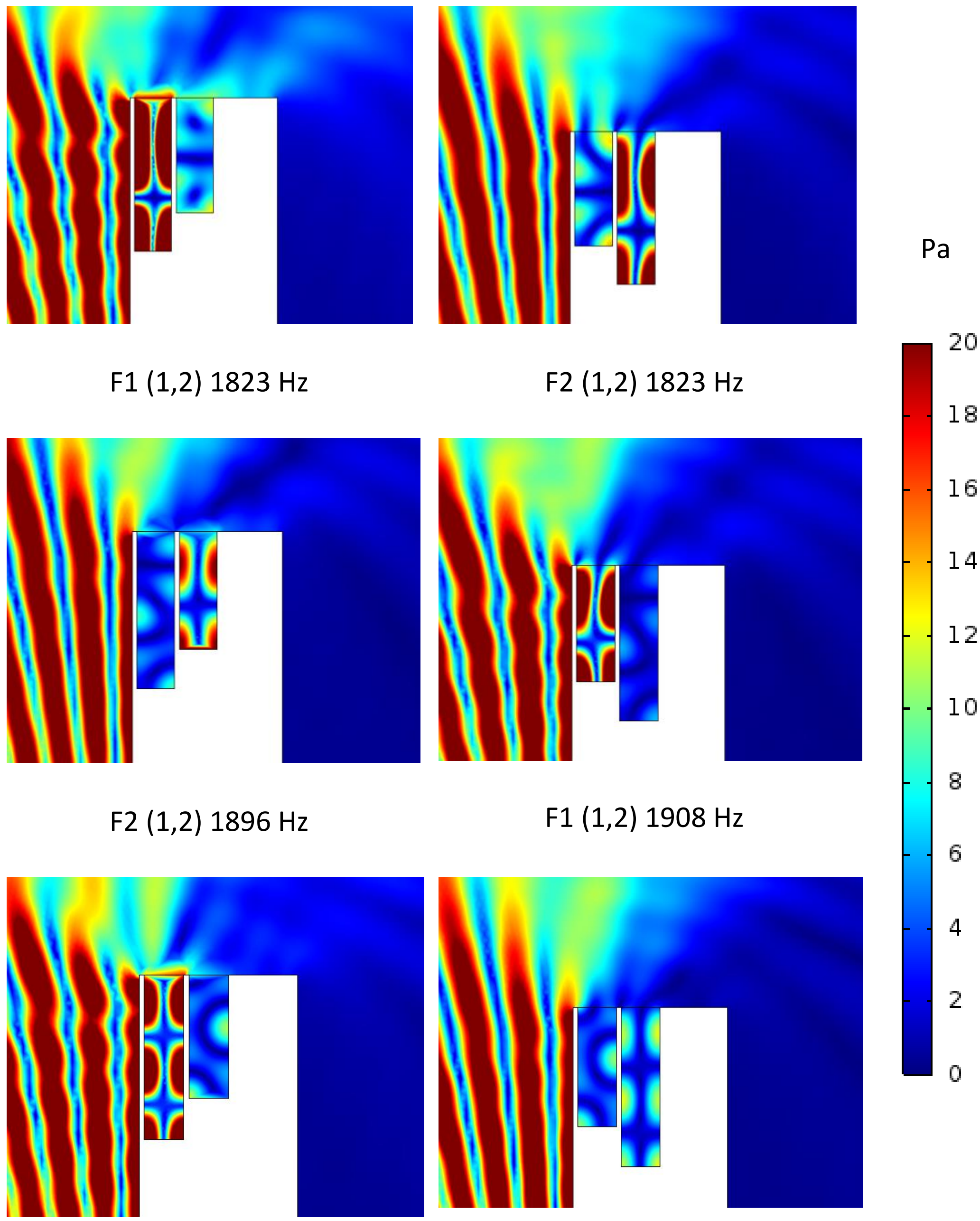

F1 (1,2) 1823 Hz

F2 (1,2) 1823 Hz

F2 (1,2) 1896 Hz

F1 (1,2) 1908 Hz

F1 (1,3) 1998 Hz

F2 (1,3) 1998 Hz

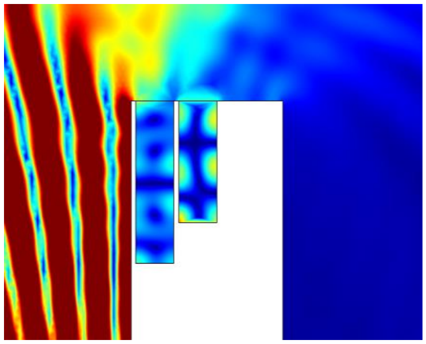

F2 (1,3) 2181 Hz

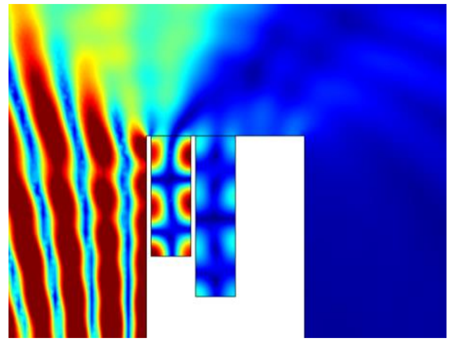

F1 (1,3) 2170 Hz

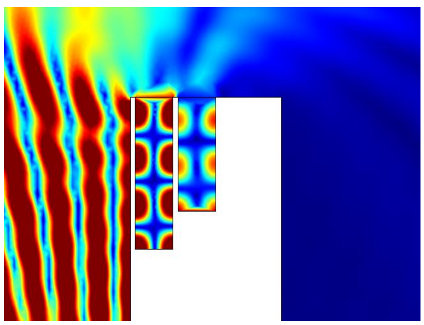

F1 (1,4) 2239 Hz

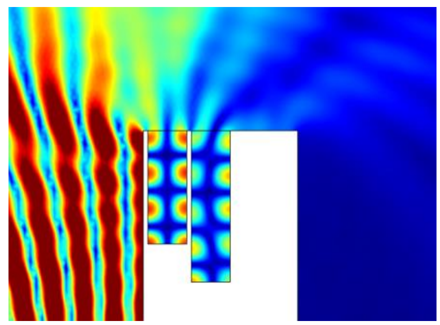

F2 (1,4) 2239 Hz

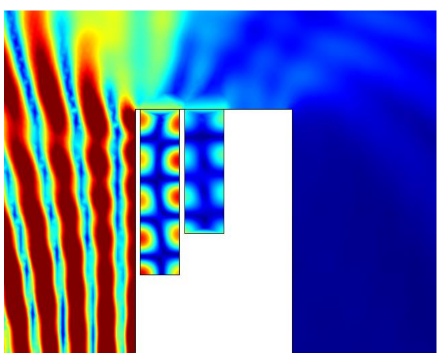

F1 (1,5) 2528 Hz

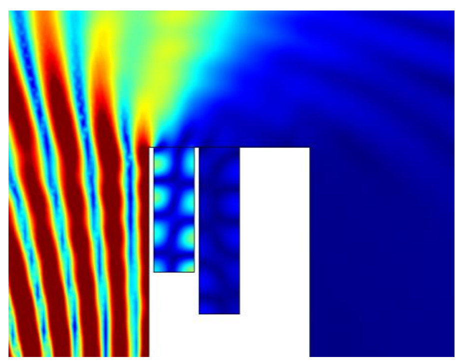

F2 (1,5) 2528 Hz

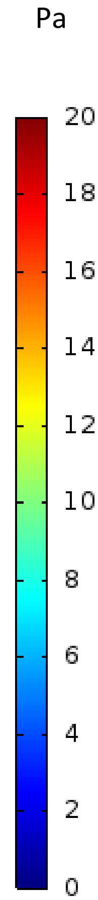

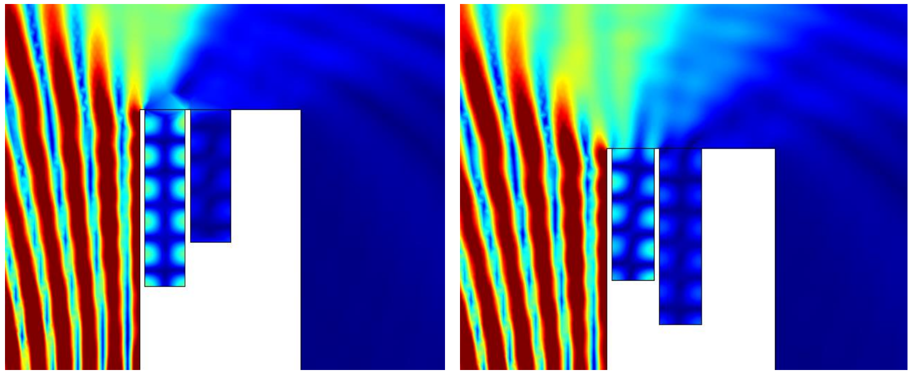

F1 (1,6) 2900 Hz F2 (1,6) 2893 Hz

Figure 4.18 Absolute pressure of sound wave inside cavities of Model D1 and Model D2

4.5.3.2 Summary

Noise barrier with double acoustic cavities (D-Type barrier) on its top surface can provide higher noise attenuation than conventional vertical barrier and even S-Type barrier because of doubling the diffraction edges by the second cavity. The improvement on Insertion Loss is around 2 to 3 dB than conventional vertical barrier and has wider effective frequency range than S-Type barrier. It can also conclude that the resonance frequency of D-Type barrier is the combination of resonance frequency both cavities. Because of the extra peaks than S-Type barrier, D-Type barrier achieve higher noise attenuation than S-Type barrier. Besides that, the resonance frequency of D-Type barrier remains unchanged after swapping the cavities. However, the magnitude of these resonance frequency will change due to the position cavity. The peaks of cavity in first row are always higher than it placed at second row. Thus, the noise attenuation of barrier is dominated by the cavity at first row.

4.5.4 Triple slots barrier (T-Type)

From previous Section, using more cavities will increase barrier noise attenuation performance. Then, more cavities are considered to add on the top surface of barrier to further improve the performance of barrier. These cavities are in different depth so that the resonance frequency can be much wider than D-Type barrier. Test is done by numerical computation with same setting as previous Section. Results are shown as Figure 4.19:

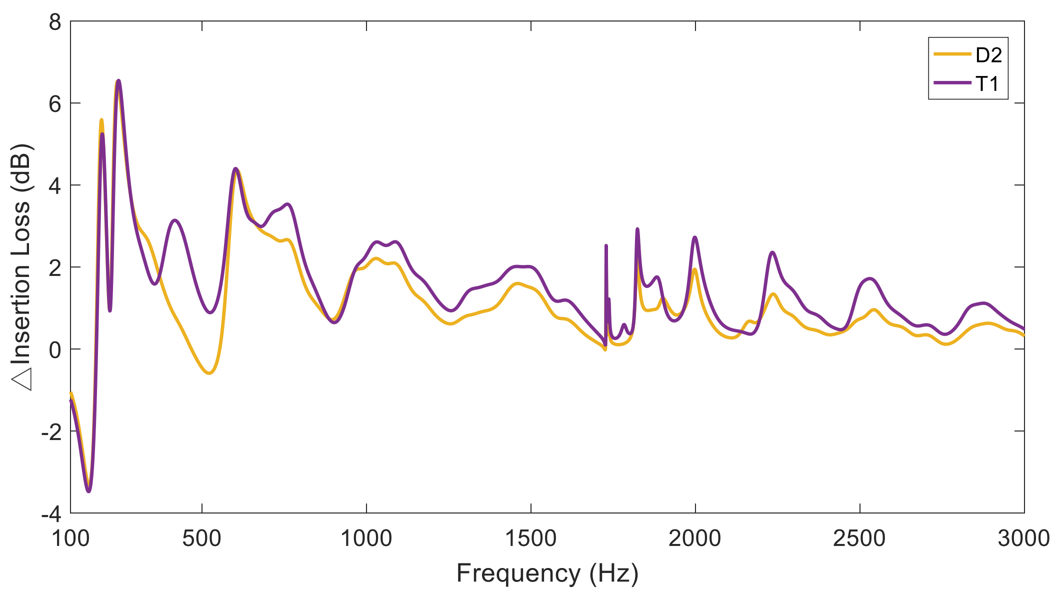

Figure 4.19 Insertion Loss of Model D2 and Model T1

A result obtained from Figure 4.19 has a good agreement to the estimation that more cavities can provide better performance of noise barrier. It is given that the Insertion Loss of Model T1 at low frequency is much higher than Model D2 by 2 dB. Other than that, the effective frequency of Model T1 is wider than of Model D2 at low frequency range where the resonance frequency at high frequency range is almost same as Model D2.

Table 4.6 Resonance frequency of Model D2 and Model T1

Calculated peak frequency	Double slot	Calculated peak frequency	Triple slots
F1(0,1)214	196	F1(0,1)214	197
F2(0,1) 285	245	F2(0,1) 285	245
F1(0,2) 643	610	F3(0,1) 571	427
F2(0,2) 857	765	F1(0,2) 643	600
F1(0,3) 1071	1085	F2(0,2) 857	765
F2(0,3) 1429	1330?	F1(0,3) 1071	1085
F1(0,4) 1500	1479	F2(0,3) 1429	1330
F1,2(0,1) 1715		F1(0,4) 1500	1479
F1(1,1) 1728	1728	F1,2,3(0,1) 1715	
F2(1,1) 1738	1736	F1(1,1) 1728	1728
F1(1,2) 1831	1823	F2(1,1) 1738	1736
F2(1,2) 1917	1908	F3(1,1) 1807	1784
F1(0,5) 1929		F1(1,2) 1831	1824
F2(0,4) 2000		F2(1,2) 1917	
F1(1,3) 2022	1998	F1(0,5) 1929	
F2(1,3) 2232	2170	F2(0,4) 2000	
F1(1,4) 2278	2239	F1(1,3) 2022	2000
F1(0,6) 2358		F2(1,3) 2232	2170
F2(0,5) 2572		F1(1,4) 2278	2237
F1(1,5) 2581	2518	F1(0,6) 2358	
F2(1,4) 2635		F3(1,2) 2425	
F1(0,7) 2786		F2(0,5) 2572	
F1(1,6) 2915	2893	F1(1,5) 2581	2518
		F2(1,4) 2635	
		F1(0,7) 2786	
		F3(0,3) 2858	
		F1(1,6) 2915	2893

The higher order modes of these acoustic cavities are calculated as shown in Table 4.6. By comparing the resonance frequencies of Model T1 and Model D2, it finds that the number of resonance frequencies of Model T1 is more than Model D2. Besides that, only the first transverse mode of third cavity is captured clearly in Model T1. Therefore, the improvement on Insertion Loss is dominated at low frequency where the resonance frequency of third cavity existed. It can be explained that the acoustic energy of high frequency sound is attenuated by the first two cavities so that the performance of the Model T1 and Model D2 at high frequency is same with each other.

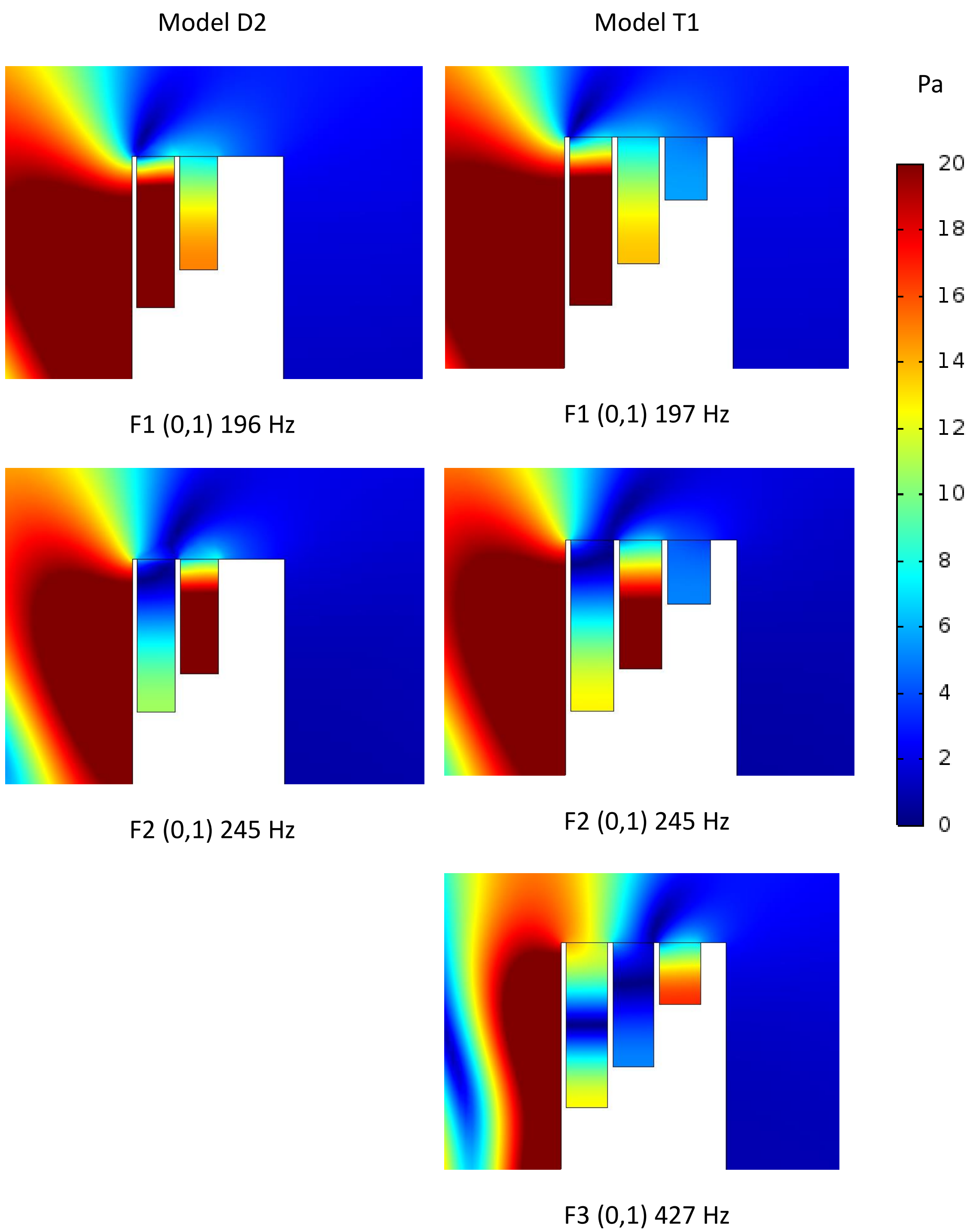

Model D2
Model T1
Pa
20
18
16
14
12
10
8
6
4
2
0
F1 (0,1) 196 Hz
F1 (0,1) 197 Hz
F2 (0,1) 245 Hz
F2 (0,1) 245 Hz
F3 (0,1) 427 Hz

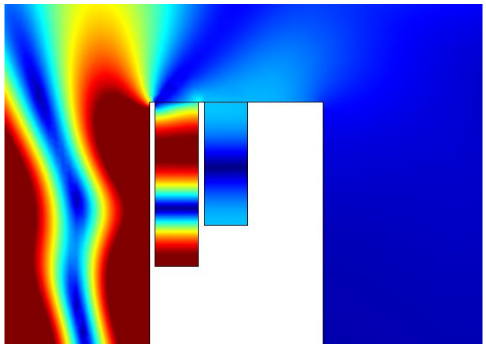

F1 (0,2) 610 Hz

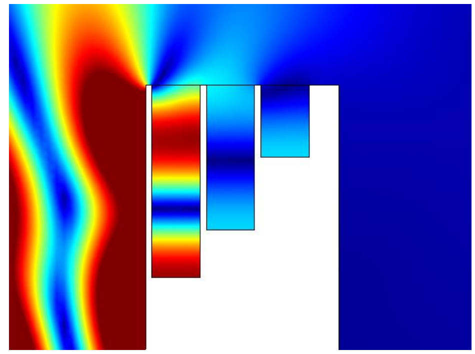

F1 (0,2) 600 Hz

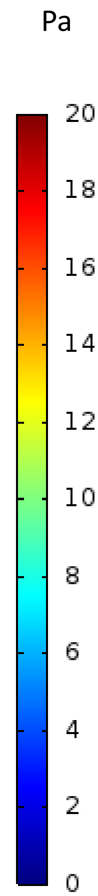

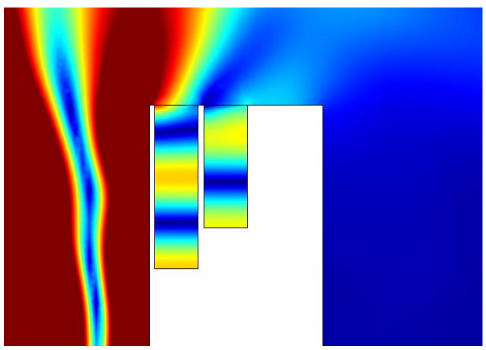

F2 (0,2) 765 Hz

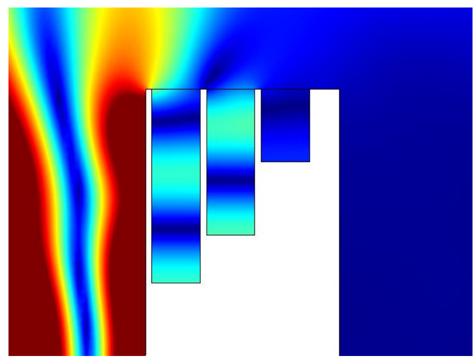

F2 (0,2) 765 Hz

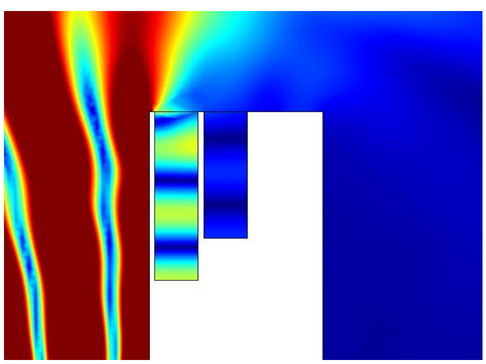

F1 (0,3) 1085 Hz

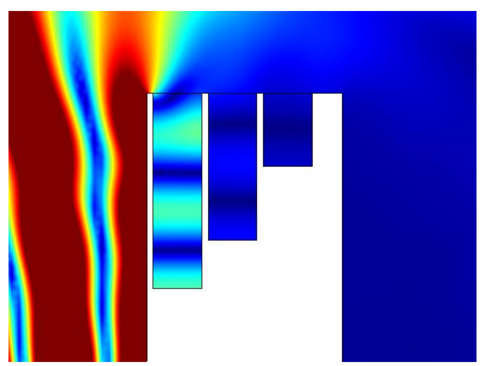

F1 (0,3) 1085 Hz

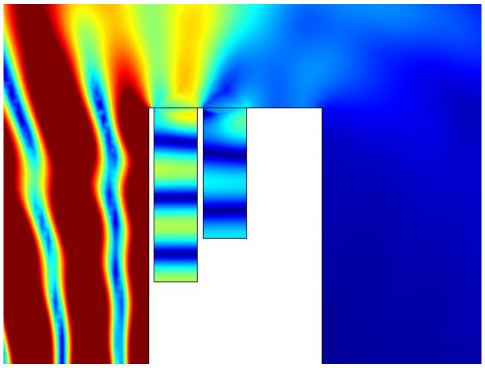

F2 (0,3) 1330 Hz

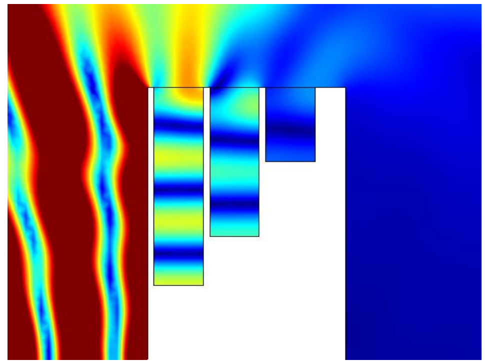

F2 (0,3) 1330 Hz

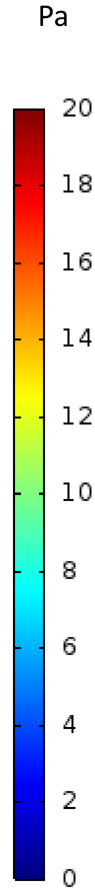

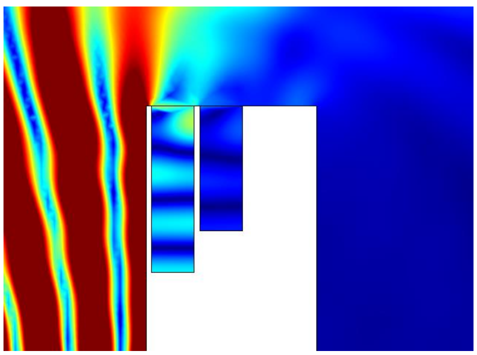

F1 (0,4) 1479 Hz

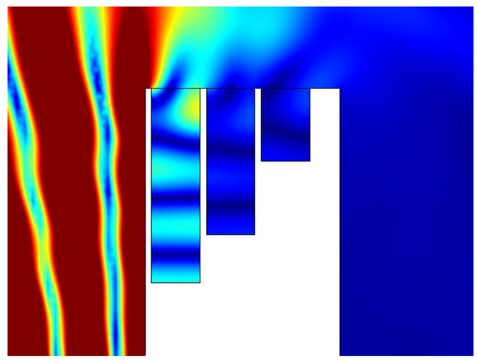

F1 (0,4) 1479 Hz

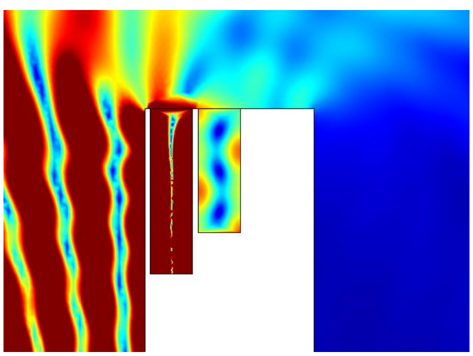

F1 (1,1) 1728 Hz

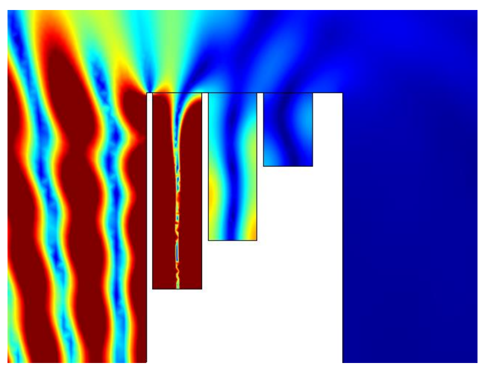

F1 (1,1) 1728 Hz

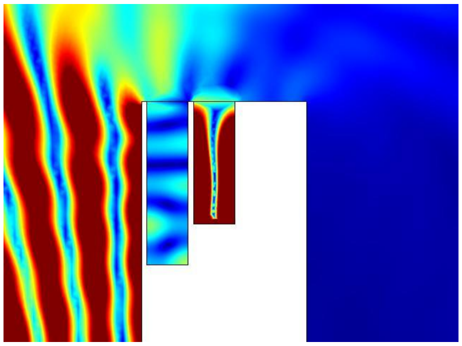

F2 (1,1) 1736 Hz

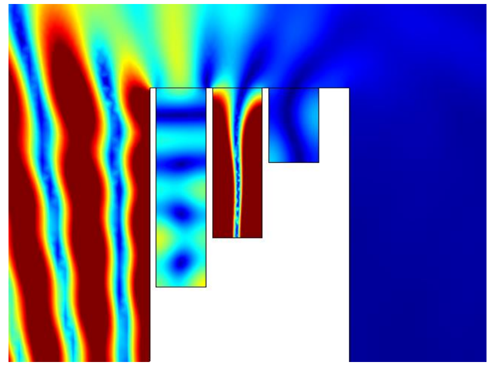

F2 (1,1) 1736 Hz

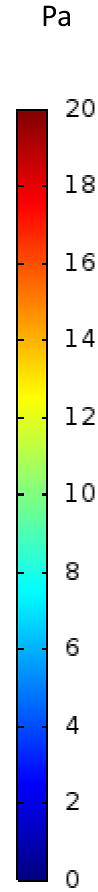

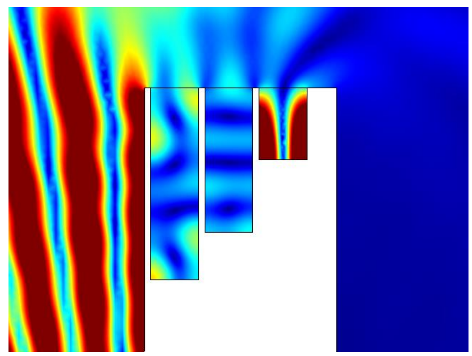

F3 (1,1) 1784 Hz

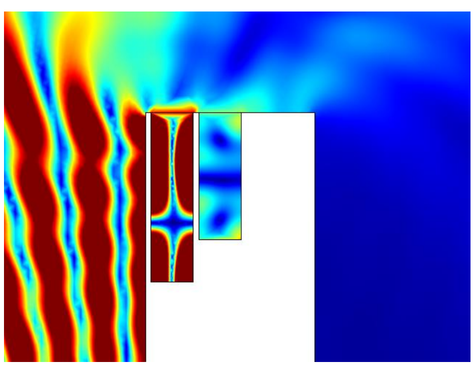

F1 (1,2) 1823 Hz

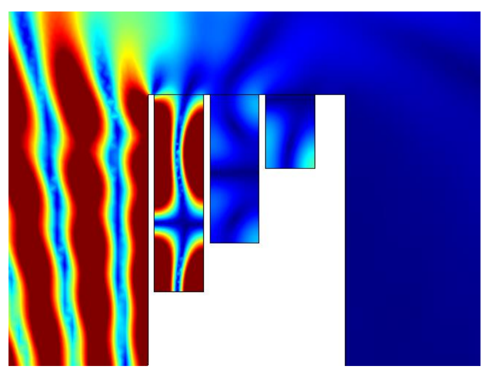

F1 (1,2) 1824 Hz

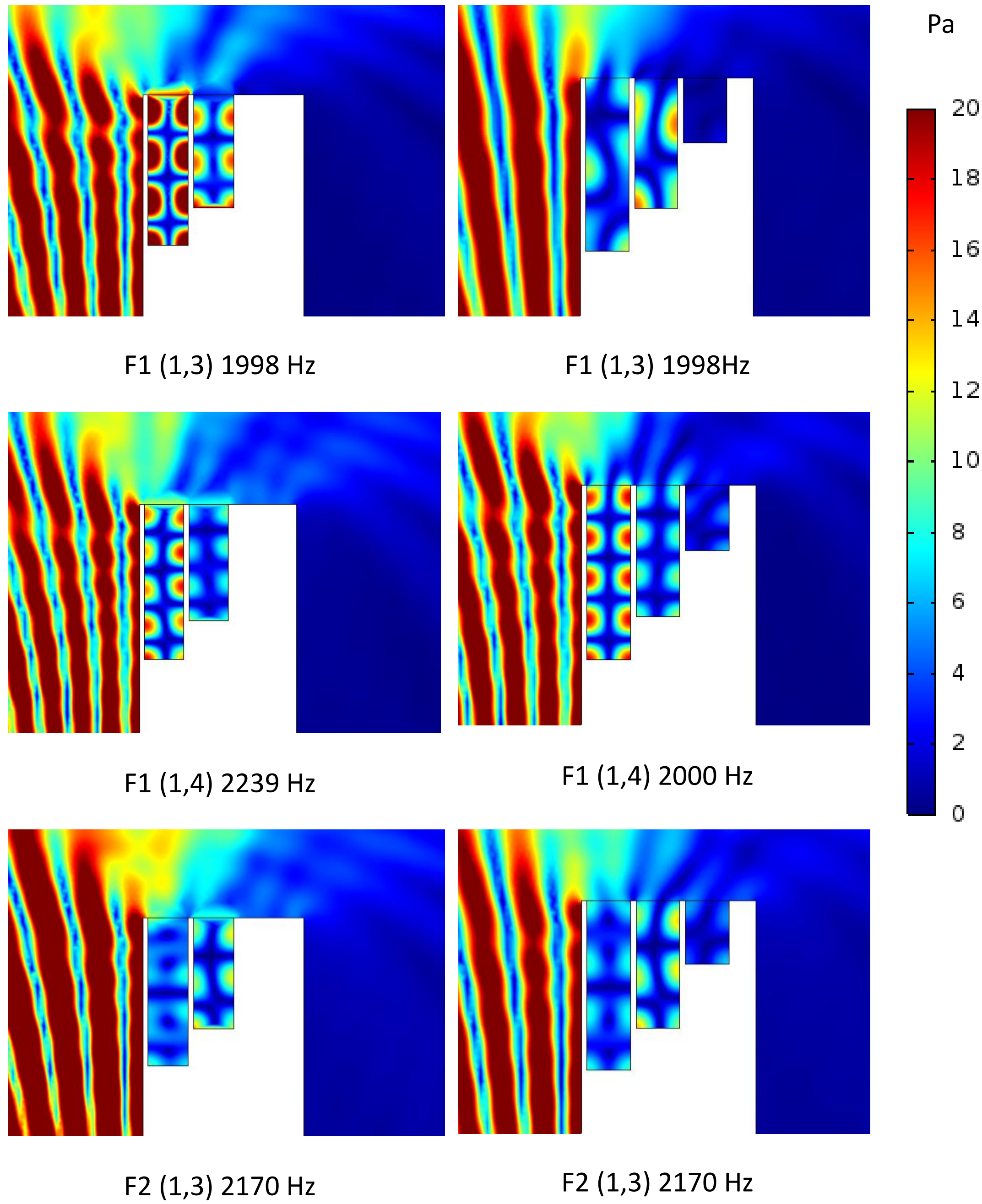

Figure 4.20 Absolute pressure of sound wave of Model D2 and Model T1

From the contour plots on absolute acoustic pressure inside the cavities, the improvement of noise attenuation due to additional cavity (the third one) can be found. The first three rows of Figure 4.20 show the acoustic pressure inside the cavities at the first mode of each cavity respectively. The most important thing to figure out is the magnitude of acoustic pressure in the first and second cavity is almost the same in both Models. Other than that, not only the first peak, nearly all resonance frequencies in these two Models behave same as each other in the first two cavities.

Although a little difference is found on the magnitude of acoustic pressure at some resonance frequencies, the patterns of mode shape are similar. Although the contribution of third cavity on noise attenuation is not good at higher order mode, it can compensate the weakest frequency range at low frequency. Thus, conclusion can be drawn that the present of third cavity can provides improvement on noise attenuation at its first resonance frequency. Moreover, it still contributes to the noise attenuation at other frequency to provide a little higher magnitude of Insertion Loss in whole spectrum.

4.5.5 Summary

Several numerical computations are conducted in this study to determine the effect on Insertion Loss due to the installation of acoustic cavities on top surface of noise barrier. These acoustic cavities are in same width but different depth to provide a different resonance frequency on noise attenuation of noise barrier. Noise attenuation of S-Type barrier is studied in detail at the first part of this chapter. By placing acoustic cavity with different depth at same location, a significant change in resonance frequency is found. And the resonance frequency of each Model is found same as the resonance frequencies of acoustic cavity. Around 2-3 dB improvement on Insertion Loss is observed at low frequency and a little improvement at high frequency because of the high Insertion Loss of conventional vertical barrier at high frequency.

Since diffraction occurred when sound wave propagates towards an obstacle, acoustic energy dissipated at the same time. In the case of sound propagate across barrier, the top edge of barrier performs as a diffraction edge and diffraction occurred. According to the acoustic property of sound wave, the acoustic dissipation of low frequency sound wave by diffraction is less than high frequency sound wave. Thus, when the sound diffracted at the top edge of barrier, a large amount of acoustic energy of high frequency sound wave is loss by diffraction. Then the magnitude of acoustic pressure in high frequency transmit to acoustic cavity becomes lower. The noise reduction effect by acoustic cavity is then decrease at high frequency. In other words, the performance of S-Type barrier at high frequency is dominated by the general noise attenuation property of conventional barrier and the effect of acoustic cavity dominated the noise attenuation of S-Type barrier at low frequency. Acoustic cavity can then be used to solve the noise problem effective at low frequency by adjusting cavity depth for target frequency.

In addition, numerical computation is conducted by changing the location of acoustic cavity. It is found that moving the acoustic cavity to the back of barrier will not have significant change on the resonance frequency of noise barrier performance. Only 10-20 Hz shift to lower frequency of the peak can be obtained in the results. However, it is clearly seen that the noise attenuation efficiency at these resonance frequencies decrease when the location of acoustic cavity far away from the leading edge. Therefore, when the acoustic cavity is far from leading edge, less energy can get into the cavity and the effect of acoustic cavity will decrease at the same time.

Furthermore, the limitation of S-Type barrier is found that it can only provide relatively high noise attenuation at specific resonance frequency but not in the whole frequency range. By considering the general property of sound wave, the acoustic energy of incident wave decreases after diffraction. If the number of diffractions increase, the acoustic energy transmitted to the receiver becomes less. Therefore, more acoustic cavity is used to increase the number of diffractions in result of higher noise attenuation. Results show that more cavity can broaden the effective frequency range since these acoustic cavities provides a higher Insertion Loss at low frequency range. Other than that, the weakness part of one acoustic cavity is compensated by other one so that the effective frequency range at low frequency is enlarged and 2-3 dB improvement on Insertion Loss is found at low frequency range.

The coupling effect between arrangement of acoustic cavity and location of acoustic cavity is also conducted on the D-Type barrier. It can be observed that the resonance frequency keeps unchanged but there is a great effect on the magnitude of Insertion Loss at resonance frequency. The magnitude of Insertion Loss of cavity in second row are lower than that in first row. It is similar to the results by moving the location of acoustic cavity done with S-Type barrier. Then, it can be concluded that the location of acoustic cavity play an important role on the noise attenuation by controlling the magnitude at each resonance frequency. A cavity with suitable depth should be place closer to the leading edge to duel with the most serious noise at certain frequency.

Lastly, one more acoustic cavity is added on the top surface of barrier to further investigate the performance of cavity at third row. It is noticed that the resonance frequency of third cavity is clearly found at low frequency range and there is only a little contribution to the performance of noise barrier at high frequency range. It is because the third cavity is located much closer to the back of barrier, the effectiveness of cavity at third row become relatively low.

Therefore, the main effect of the third cavity becomes achieve a compensation to the weak point of D-Type barrier at low frequency.

In next chapter, experimental study is carried out to determine the performance of barrier with acoustic cavity located on the top edge in three-dimensional. By placing the sound source at different position, the relationship between noise attenuation and incident angle is being tested in a series of scale model experiments. The detail of experimental study is mentioned in following chapter.

Chapter 5: Experiment Results

5.1 Introduction

Scale modeling method is used to determine the noise attenuation performance of acoustic cavity on noise barrier, the scale ratio of these measurements in this study is 1:3. In this chapter, the settings of the measurements include the detail of instruments and network of instrument setup are introduced. At the end of this chapter, an analysis on the experimental results is shown.

5.2 Instrumentations

In order to make validation with the numerical result introduced in Chapter 4, several scale model measurements were carried out in a fully anechoic chamber which sized as 6m x 6m x 4m (height). The cut-off frequency of fully anechoic chamber has been designed as 80 Hz. The source used in these measurements is a point source which assembled by a circular horn with a 1m length and 3 cm internal diameter tube. It was driven by a compression driver PD-30 (Atlas Sound) and powered with a power amplifier LA 1201 (Crest Audio). To capture a full spectrum on Insertion Loss of noise barrier with different top edge design, white noise was generated by NTI 20K Hz signal generator in these measurements. The acoustic response at these receiver points were then taken by pre-polarized free-field ¼" 20 kHz Precision Array microphone 4958(B&K) which connected to 47-channels Pulse Analysis Software with Type 3506D Pulse system(B&K). The whole network of the instruments is shown as Figure 5.1:

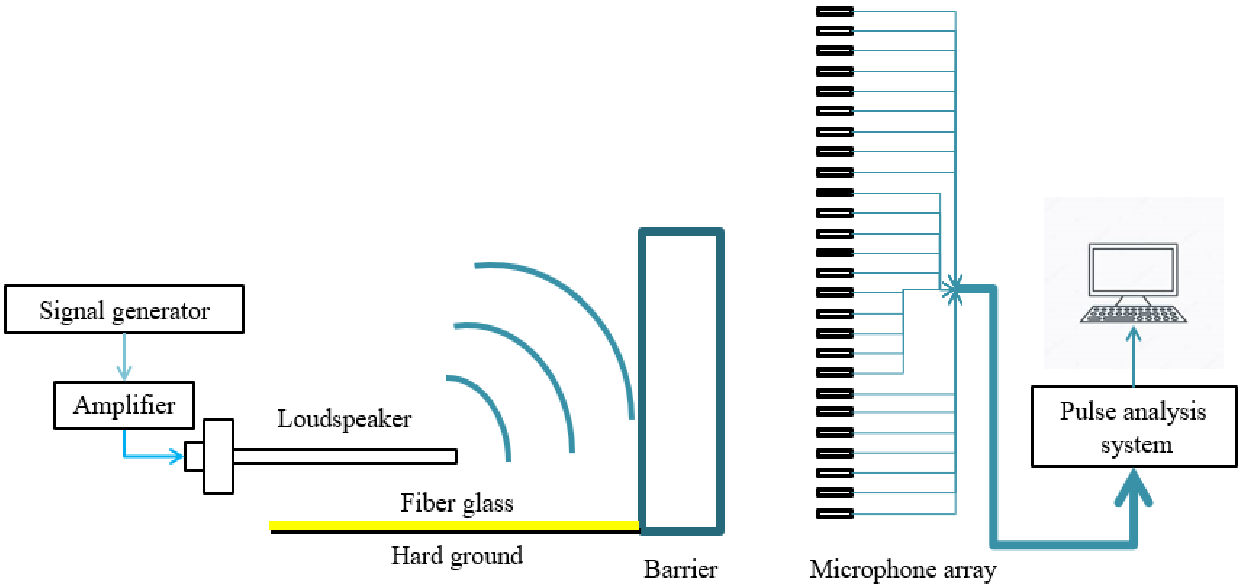

Figure 5.1 Schematic network in measurements

(a) LA 1201 Power Amplifier

Figure 5.2 LA 1201 Power Amplifier

Since the signal voltage generated by signal generator is small, a power amplifier is needed to magnify the power of signal from signal generator to the loudspeaker.

(b) NTI signal generator

Figure 5.3 NTI signal generator

In order to obtain the resonance frequency of different types of noise barrier model tested, up to 20 kHz white noise is generated by NTI signal generator. The signal will then be captured by Pulse in Voltage to ensure the signals generated in these testing cases are consistent.

(c) Loudspeaker

Figure 5.4 Loudspeaker

The loudspeaker with circular horns and tubes is used and it is driven by compression driver PD-30. The designed operating spectrum of this compression driver is around 300-9000 Hz which is 100-3000 Hz in the actual case of this scale model test. The noise source can be assumed as a point source at the outlet of the tube therefore the directivity problem can be neglected during analysis.

(d) Array microphone 4958

Figure 5.5 Array microphone 4958

28 Bruel and Kjaer(B&K) pre-polarized free-field ¼" array microphones (type 4958) are used in these measurements to measure the pressure field behind noise barrier simultaneously with frequency range from 20 Hz-20 kHz. This type of microphone provides a greater sensitivity and frequency range and it is also well suited to general sound measurements requiring frequency analysis.

(e) Pulse Analysis Software with Type 3506D Pulse system

Figure 5.6 Pulse System **Figure 5.7 Pulse Analysis Software**

A 47 channels Pulse system as shown in Figure 5.6 & 5.7 is used for data recording in the present study. Time signal data of 29 receiver points are recorded by the recorder function of Pulse systems in 32768 Hz sampling frequency simultaneously. All time data signals will then convert to readable format by Pulse analyze software and being analysis in software Matlab.

5.3 Experiments on resonance frequency of cavities

Several experiments are conducted to determine the noise attenuation performance of tested barrier. At first, tests on the resonance frequency of acoustic cavities are required to ensure the noise attenuation of acoustic cavity at expected frequency range. The sound pressure level of acoustic cavity in 0.4 m, 0.3 m and 0.15 m depth are tested and compare with the result of normal barrier to indicate the effect on noise attenuation by acoustic cavity but not the diffraction of outer shape of barrier.

5.3.1 Configuration of experiments

The configuration of measurements in this Section is similar to the setting in numerical model. The tested barrier is located at the middle of anechoic chamber. Sound source is placed at the middle of barrier length and 1.3 m away from center of barrier. Only one microphone is used in this measurement which located at 0.5 m above the opening of acoustic cavity.

5.3.2 Resonance frequency of Single acoustic cavity

In this Section, experiments are carried out to determine the resonance frequency of single acoustic cavity used on barrier. The dimension of tested cavities is same as the computational model which is 0.116 m width, 0.3 m length and 0.15 m, 0.3 m, 0.4 m depth respectively.

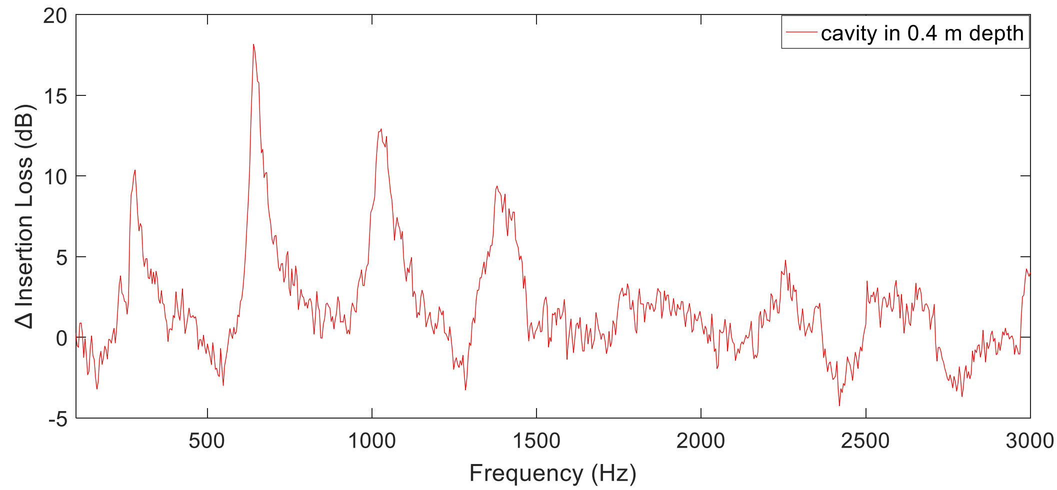

Figure 5.8 Insertion Loss of 0.4 m depth acoustic cavity

In Figure 5.8, Δ Insertion Loss spectrum of 0.4 m depth acoustic cavity is indicated. The peaks of Insertion Loss mean sound pressure vanish at that frequency which also represent the resonance frequency of 0.4 m acoustic cavity. Four sharp peaks are clearly seen below 1500 Hz. For frequency higher than 1500 Hz, no peak can be found which means the noise attenuation performance is weak. The resonance frequency of experiment and calculation by Equation 3.24 is done in Table 5.1. It is found that the four sharp peaks from Figure 5.8 are corresponding to the first four resonance frequencies which are also the first four transverse modes. Other than that, the other two peaks are also found but they are not obvious in the graph. By compare with calculation, it is also seen that these resonance frequencies are transverse modes of acoustic cavity but not the longitudinal modes.

Table 5.1 Resonance frequency of 0.4 m depth acoustic cavity

Calculated resonance frequencies (Hz)	Resonance frequencies of experimental result (Hz)
214 (0,1)	284
643 (0,2)	664
1071 (0,3)	1048
1500 (0,4)	1396
1715 (1,0)	
1728 (1,1)	
1831 (1,2)	
1929 (0,5)	1912
2022 (1,3)	
2278 (1,4)	
2358 (0,6)	2280
2581 (1,5)	
2786 (0,7)	
2915 (1,6)	

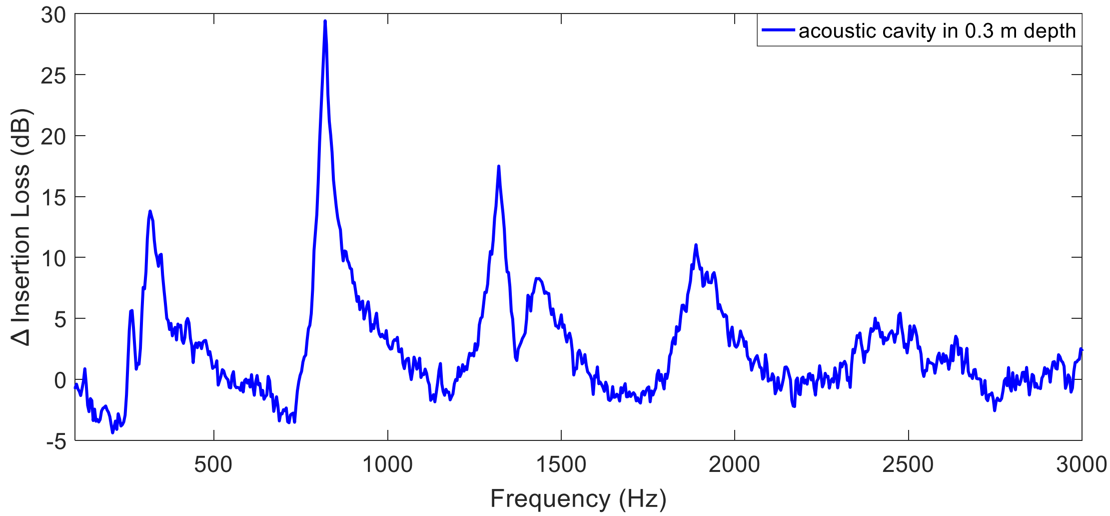

Figure 5.9 Insertion Loss of 0.3 m depth acoustic cavity

In Figure 5.9, Δ Insertion Loss spectrum of 0.3 m depth acoustic cavity is shown. The sharp peaks of Insertion Loss mean sound pressure vanishes at that frequency which is also the resonance frequency of 0.3 m acoustic cavity. Three sharp peaks are clearly seen from Figure 5.9 below 1400 Hz. For frequency higher than 1400 Hz, 4 small peaks are found. Comparison on the resonance frequency of experiment and calculation is done in Table 5.2. It is found that the three sharp peaks from Figure 5.9 are corresponded to the first three resonance frequencies which are also the first three transverse modes. Moreover, 2 of the four small peaks are identified that they are the resonance frequencies by transverse mode of acoustic cavity. Since the other two small peaks are the fourth and fifth mode of cavity, the magnitude of Insertion Loss is low so that peaks cannot be seen clearly.

Table 5.2 Resonance frequency of 0.3 m depth acoustic cavity

Calculated resonance frequencies (Hz)	Resonance frequencies of experimental result (Hz)
285 (0,1)	312
857 (0,2)	820
1429 (0,3)	1320
1715 (1,0)	
1738 (1,1)	
1917 (1,2)	
2000 (0,4)	1948
2232 (1,3)	
2572 (0,5)	2416
2635 (1,4)	

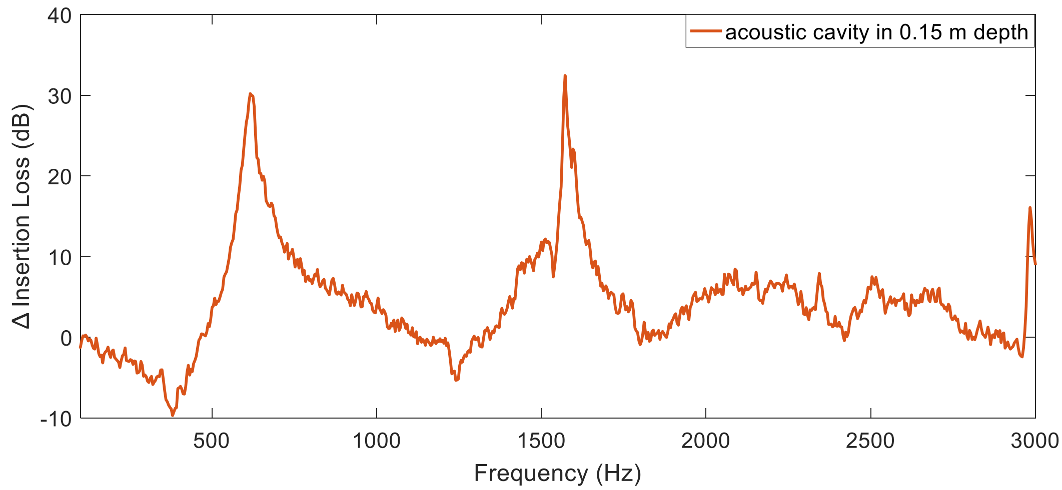

Figure 5.10 Insertion Loss of 0.15 m depth acoustic cavity

In Figure 5.10, Δ Insertion Loss spectrum of 0.15 m depth acoustic cavity is captured. The sharp peaks of Insertion Loss mean sound pressure vanishes at that frequency which is also the resonance frequency of 0.15 m acoustic cavity. Two sharp peaks appear at the frequency below 1600 Hz, many small peaks are observed at high frequency range. Comparison on the resonance frequency of experiment and calculation is done in Table 5.3. It is clearly seen that the two sharp peaks from Figure 5.10 are corresponded to the first two resonance frequencies which is also the first two transverse modes.

Table 5.3 Resonance frequency of 0.15 m depth acoustic cavity

Calculated resonance frequencies (Hz)	Resonance frequencies of experimental result (Hz)
571 (0,1)	616
1715 (1,0)	1572
1807 (0,2)	1968
2425 (0,3)	2272
2858 (1,3)	2580

It is given that the resonance frequency of each acoustic cavity is similar to the calculated result which only has a little shift to left at all resonance frequencies. Same as computational results, the resonance frequency of different acoustic cavity can be observed clearly at low frequency, where the response is too weak to capture clearly at high frequency range. It is also found that when the depth of acoustic cavity increase, the effect by combined mode decrease. It is because the microphone position remains at the same height above the cavity. When cavity depth is change, the distance from microphone to the bottom of cavity also change. The change of distance between microphone and bottom of cavity caused difference in cavity performance at resonance frequency. Therefore, the acoustic cavity used in this experiment is defined as it can provide the expected noise attenuation at resonance frequencies.

5.3.3 Resonance frequency of double acoustic cavity

The results of experimental results and computational results shows good agreement from previous Section, the relationship of coupling effect double cavities is being concerned. Experiments are carried out to investigate the resonance frequency and noise attenuation of using double acoustic cavities. The results are shown as Figure 5.11:

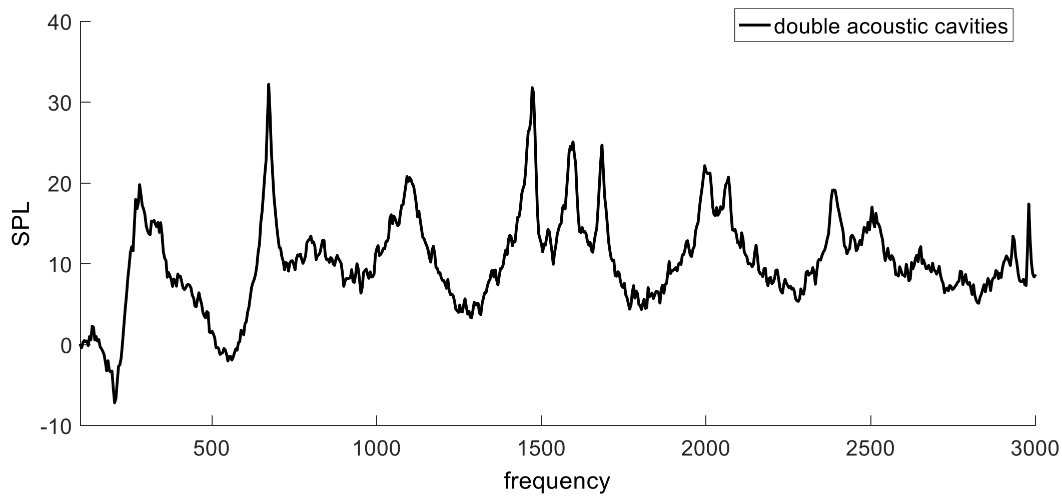

Figure 5.11 Insertion Loss of using double acoustic cavities (Model D1)

In this measurement, the cavity in first row is in 0.3 m depth where the cavity in second row is in 0.4 m depth. Source and receiver are placed at the same position as the test of single acoustic cavity. The Insertion Loss spectrum are shown in Figure 5.11. It can be observed that the Insertion Loss is positive in whole frequency range which means the noise attenuation of double acoustic cavity is better than reference case in whole concerned frequency range. Different from result of single cavity, sharp peak can be found clearly not only at low frequency range, but even at high frequency range.

Table 5.4 Resonance frequency of double acoustic cavities

Calculated resonance frequency (Hz)	Resonance frequency of experimental results (Hz)
F1(0,1)214	280
F2(0,1) 285	324
F1(0,2) 643	460
F2(0,2) 857	672
F1(0,3) 1071	840
F2(0,3) 1429	1040
F1(0,4) 1500	1352
F1,2(1,0) 1715	1476
F1(1,1) 1728	1596
F2(1,1) 1738	1684
F1(1,2) 1831	1824
F2(1,2) 1917	
F1(0,5) 1929	
F2(0,4) 2000	1996
F1(1,3) 2022	2068
F2(1,3) 2232	2112
F1(1,4) 2278	2308
F1(0,6) 2358	2392
F2(0,5) 2572	2528
F1(1,5) 2581	
F2(1,4) 2635	
F1(0,7) 2786	2748
F1(1,6) 2915	2908

From Table 5.4, it can be found that almost all calculated resonance frequencies can be found in whole frequency range. Although the resonance frequency is shifted, the resonance frequency of first four transverse modes can be obtained clearly at low frequency range which is similar to the computation results and results of single acoustic cavity.

In this Section, several measurements are carried out to determine the resonance frequency of acoustic cavity used in following experiments. Results show that almost all the resonance frequencies of each cavity can be captured easily. Although there is a little shift to left on the resonance frequency of these cavities, it does not influence the investigation on noise attenuation level and spatial behavior of acoustic cavities. Thus, the measurements will similar setting will be used in the measurements on noise attenuation in Section 5.4.

5.4. Measurements on noise attenuation of acoustic cavity

In this Section, the noise attenuation level of acoustic cavity is investigated by different experiments. A series of measurements are carried out by changing the number of acoustic cavities used, the length, the width and even the arrangement of acoustic cavity. Results will compare with conventional vertical barrier by Insertion Loss to determine the effect of noise attenuation behind barrier by acoustic cavities.

5.4.1 Configuration of experiments

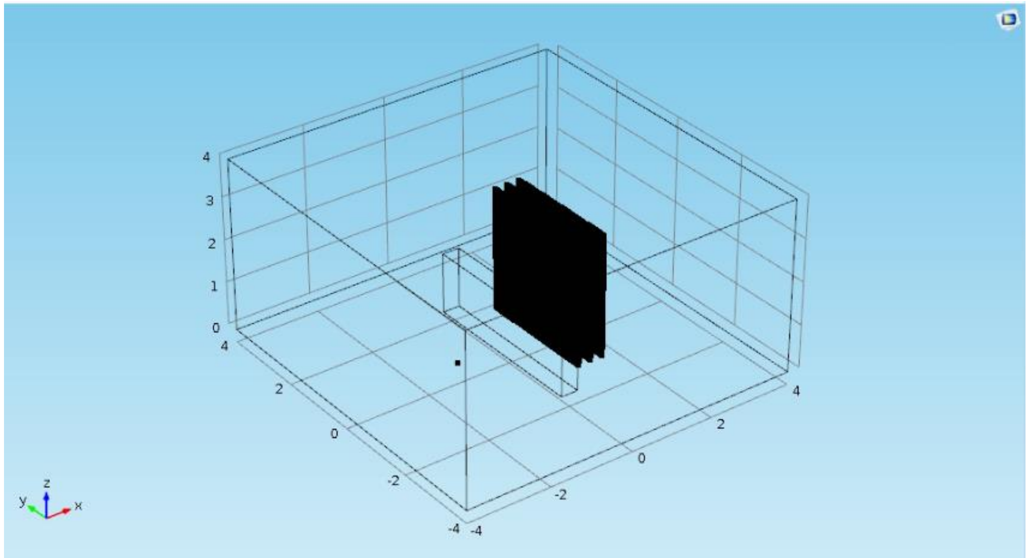

Figure 5.12 Configuration of experiments displayed by 3D CAD drawing

Figure 5.13 Configuration of experiments in anechoic chamber

In this study, in order to investigate the spatial behavior of acoustic cavity and their noise attenuation performance, a large number of receivers are used to capture the whole sound filed behind barrier. As shown in Figure 5.12 and 5.13, source and receivers are located at different side of barrier. The position of loudspeaker is at (-1.3, 0, 0.2) in coordinate system. 1653 receivers are separated into three planes parallel to barrier which located at 0.7 m, 1 m, 1.3 m from barrier. The height of receivers is from 0.1 m to 3 m with interval 0.1 m and the separation of receivers in x-direction is from -1.4 m to 1.4 m with interval 0.05m. Fiber glass is covered on the hard ground at source side to avoid the sound propagate to receiver under the barrier. An automation system is used to move 29 microphones along x direction which is from -1.4 m to 1.4 m. The tested barrier is located at the middle of chamber. The center of barrier is at (0, 0, 0.7) in coordinate system. The dimension of barrier is in 4 m(L) x 0.4 m(W) x 1.4 m(H). Both the barrier and acoustic cavity are made of 12.5 mm thick wooden board which is assumed to be acoustically rigid.

 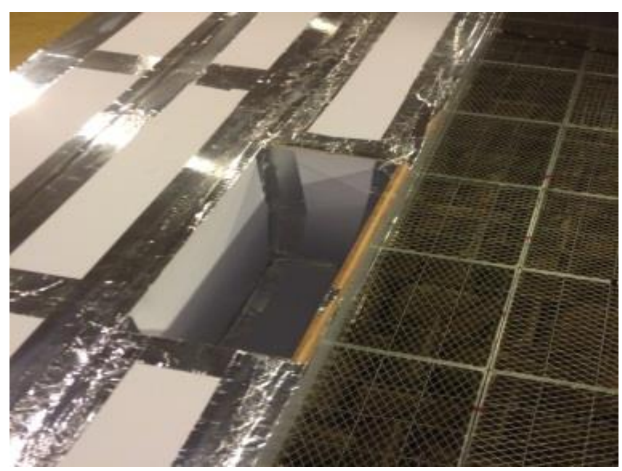

Figure 5.14 Reference barrier and barrier with acoustic cavity

5.4.2 Noise attenuation performance of S-type barrier

In this Section, measurements are carried out to determine the noise attenuation performance of S-type barrier (single acoustic cavity barrier). The noise attenuation of acoustic cavity with various depth are investigated. These results are indicated by using △IL which is the difference of Insertion Loss between reference barrier and tested barrier. The noise attenuation performance caused by acoustic cavity can be observed obviously by △IL. Other than that, the total △IL of these plane and the whole region behind barrier are shown in traffic weighting which mentioned in Chapter 3.

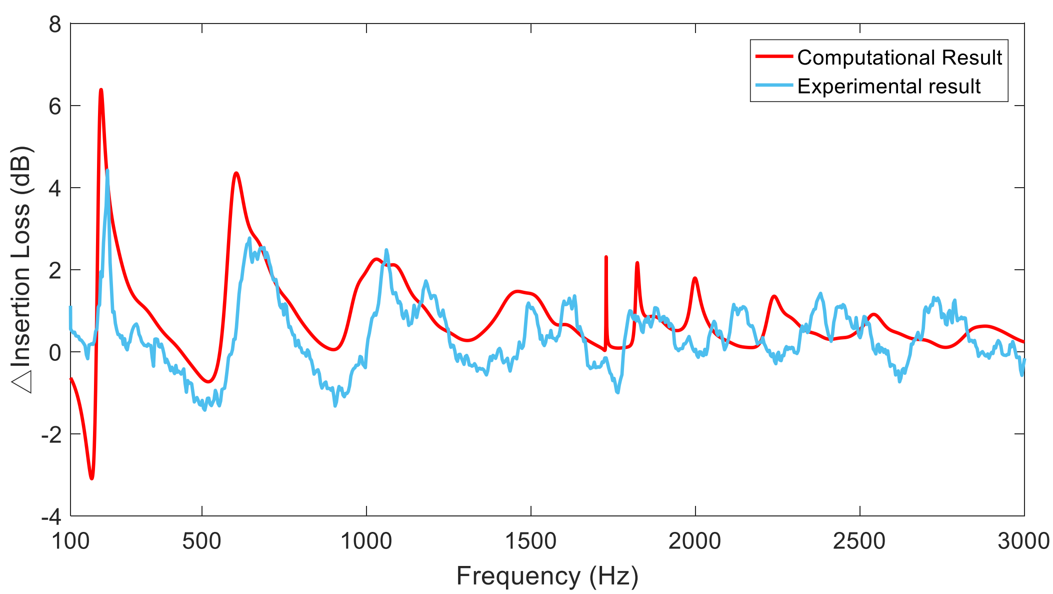

Figure 5.15 Computational results and experimental results of Model S1

In Figure 5.15, Insertion Loss is the ratio of transfer function between reference barrier and tested barrier to show the effect on noise attenuation by different acoustic cavity clearly. If the Insertion Loss is negative which means the noise attenuation is worse than reference barrier at that frequency. By compare with computational results, the patterns of spectrum are nearly the same at low frequency range. Two sharp peaks can be found clearly at around 200 Hz and 500 Hz which are the first two transverse modes of acoustic cavity. After the fourth transverse mode, the magnitude of Insertion Loss is tending to zero which means the effect of acoustic cavity on noise attenuation at high frequency is weak. A comparison on the resonance frequency from calculation and experiment are shown in Table 5.5. It can be found that the frequency shift at first three peaks is very little, but the shift become large after the first longitudinal mode.

Acoustic mode number	Calculated resonance frequency (Hz)	Resonance frequency of experimental results (Hz)
F (0,1)	214	212
F (0,2)	643	644
F (0,3)	1071	1060
F (0,4)	1500	1492
F (1,1)	1728	1632
F (1,2)	1831	1800
F (0,5)	1929	1880
F (1,3)	2022	1876
F (1,4)	2278	2116
F (0,6)	2358	2380
F (1,5)	2581	2448

F (0,7)	2786	2724
F (1,6)	2915	2788

Table 5.5 Resonance frequency of Model S1

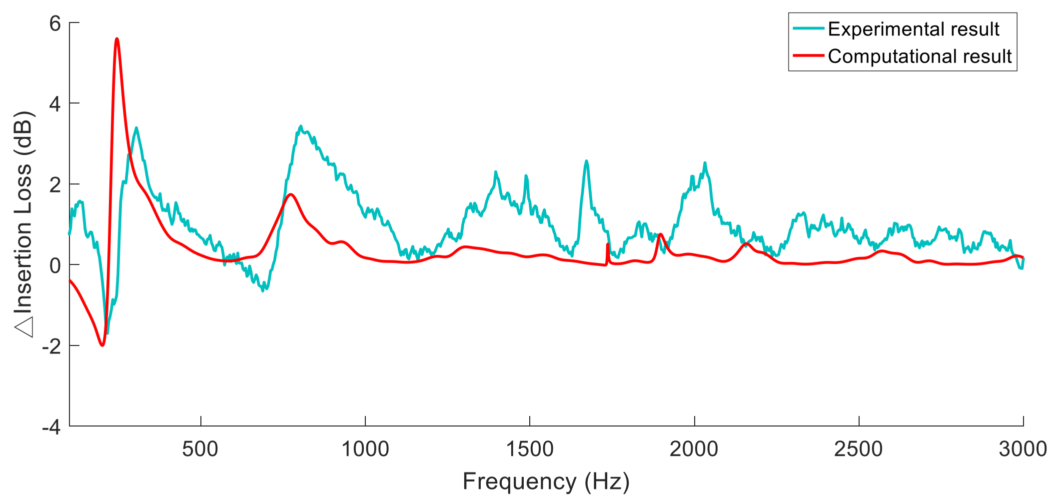

Figure 5.16 Insertion Loss of Model S2

In Figure 5.16, the spectrum of Insertion Loss of Model S2 is indicated. Different from computational result, it can be easily found that there are 5 peaks in experimental result. And these frequencies match the calculated resonance frequency. Two drops are obtained at the lower frequency of first and second resonance frequencies with similar magnitude due to the sudden change in impedance at cavity opening. The decay of peak magnitude is not obvious that only 1 dB – 1.5 dB change from first mode to fourth mode. Comparison is done on the calculated and experimental resonance frequency of Model S2 in Table 5.6.

Table 5.6 Resonance frequency of Model S2

Calculated resonance frequency (Hz)	Resonance frequency of experimental results (Hz)
285	304
857	804
1429	1396
1715	1672
1738	
1917	
2000	2032
2232	
2572	
2635	

In this Section, the noise attenuation performances of S-type barrier are indicated. Results shows that the performances of S-type barrier are poor at high frequency range which make a good agreement to the computational result in Chapter 4. However, unlike computation results, there are significant drops next to the resonance frequencies at low frequency range. The difference between experiment results and computation results is caused by the sound diffraction at the vertical edges of barrier which is neglected at the two-dimensional computation. The maximum Insertion Loss of both cases is located at the first two transverse modes. A sharp peak is always found at around 1700 Hz which is the first longitudinal mode.

5.4.3 Noise attenuation performance of multi-slots barrier

From previous Section, the noise attenuation performance of S-type barrier is discussed. The performance of S-type barrier is good at low frequency due to first transverse mode. However, poor performance is also found at high frequency. To improve the performance of S- type barrier, increasing the number of acoustics cavity is being considered. In this Section, the noise attenuation of D-type (double acoustic cavities) and T-type (Triple acoustic cavities) barrier are investigated. In addition, comparison is also done to the results of S-type barrier to determine the effect of the additional cavities.

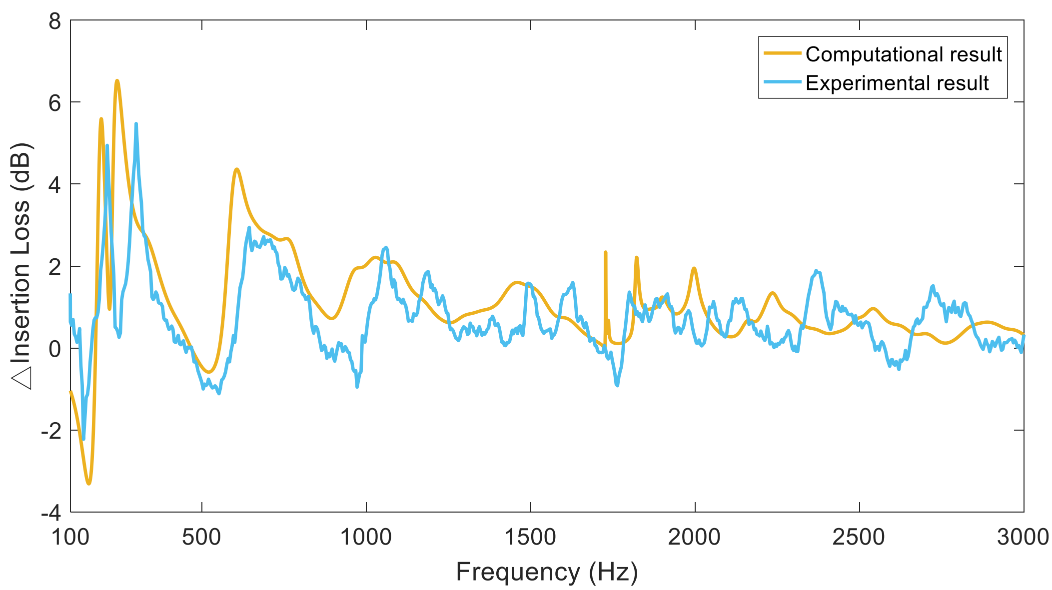

Figure 5.17 Insertion Loss of Model D2

In this measurement, a 0.4 m depth acoustic cavity is located at the first row and a 0.3 m depth acoustics cavity is located at the second row on the barrier top edge. It can be clearly noticed that 3 sharp peaks appear at low frequency with drops at lower frequency. After the third mode appear, the noise attenuation performance of cavity decreases and close to zero at high frequency. The maximum Insertion Loss appears at the first resonance frequency as the first resonance frequency of Model S1. Comparison on resonance frequency of calculated results and experimental results is shown in Table 5.7. It can be observed that the resonance frequency of both acoustic cavities can be captured out clearly with a little shift compare with calculated frequency. Same as the computation results, the first four modes at low frequency range can be captured clearly. The resonance frequencies at high frequency range are not significant to observe since the effect of both cavities on the noise attenuation is too weak at high frequency.

Table 5.7 Resonance frequency of Model D2

Calculated resonance frequency (Hz)	Resonance frequency of experimental results (Hz)
F1(0,1)214	244
F2(0,1) 285	276
F1(0,2) 643	636
F2(0,2) 857	828
F1(0,3) 1071	1048
F2(0,3) 1429	1400
F1(0,4) 1500	1488
F1,2(1,0) 1715	
F1(1,1) 1728	
F2(1,1) 1738	1792
F1(1,2) 1831	1848
F2(1,2) 1917	1964
F1(0,5) 1929	
F2(0,4) 2000	
F1(1,3) 2022	2052
F2(1,3) 2232	2232
F1(1,4) 2278	
F1(0,6) 2358	2344
F2(0,5) 2572	
F1(1,5) 2581	
F2(1,4) 2635	2668
F1(0,7) 2786	
F1(1,6) 2915	

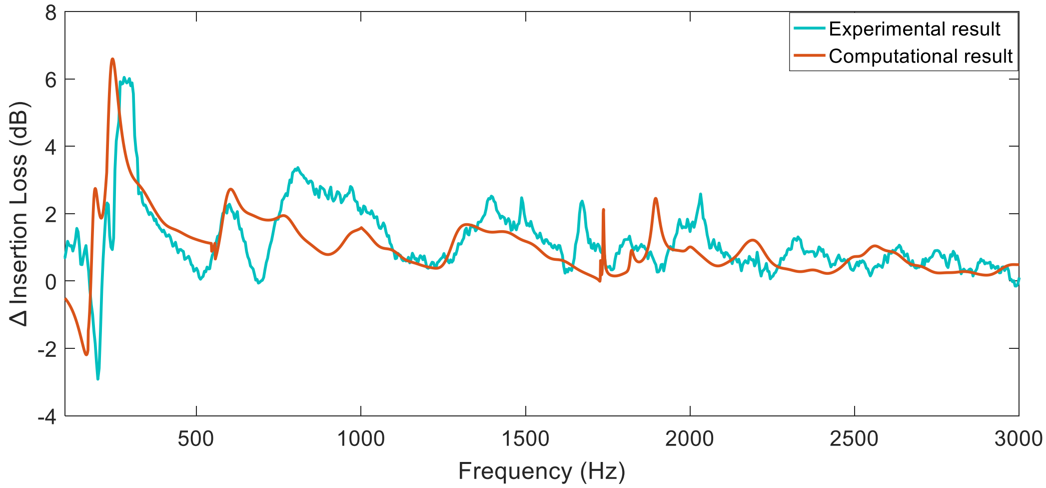

Figure 5.18 Insertion Loss of Model D1

The Insertion Loss of Model D1, which includes a 0.3 m depth acoustic cavity on first row and 0.4 m depth acoustic cavity on second row, is indicated in Figure 5.18. A large drop is found at low frequency which is closed to the first mode of 0.4 m depth cavity. Same as the result of Model D2, the maximum Insertion Loss occurred at the first mode and the magnitude decrease during the order of mode increase. Besides that, a sharp peak is located at around 1700 Hz which is first longitudinal mode. In addition, the performance of D-type barrier is similar to S-type barrier which is also poor at high frequency (0.5 dB improvement). Comparison on the calculated resonance frequency and experimental resonance frequency of Model D1 is made in Table 5.8.

Table 5.8 Resonance frequency of Model D1

Calculated resonance frequency (Hz)	Experimental resonance frequency (Hz)
F1(0,1)214	228
F2(0,1) 285	280
F1(0,2) 643	600
F2(0,2) 857	808
F1(0,3) 1071	968
F2(0,3) 1429	1396
F1(0,4) 1500	1488
F1,2(1,0) 1715	1672
F1(1,1) 1728	
F2(1,1) 1738	
F1(1,2) 1831	1816
F2(1,2) 1917	
F1(0,5) 1929	
F2(0,4) 2000	
F1(1,3) 2022	2032
F2(1,3) 2232	2232
F1(1,4) 2278	
F1(0,6) 2358	2328
F2(0,5) 2572	
F1(1,5) 2581	
F2(1,4) 2635	2636
F1(0,7) 2786	
F1(1,6) 2915	

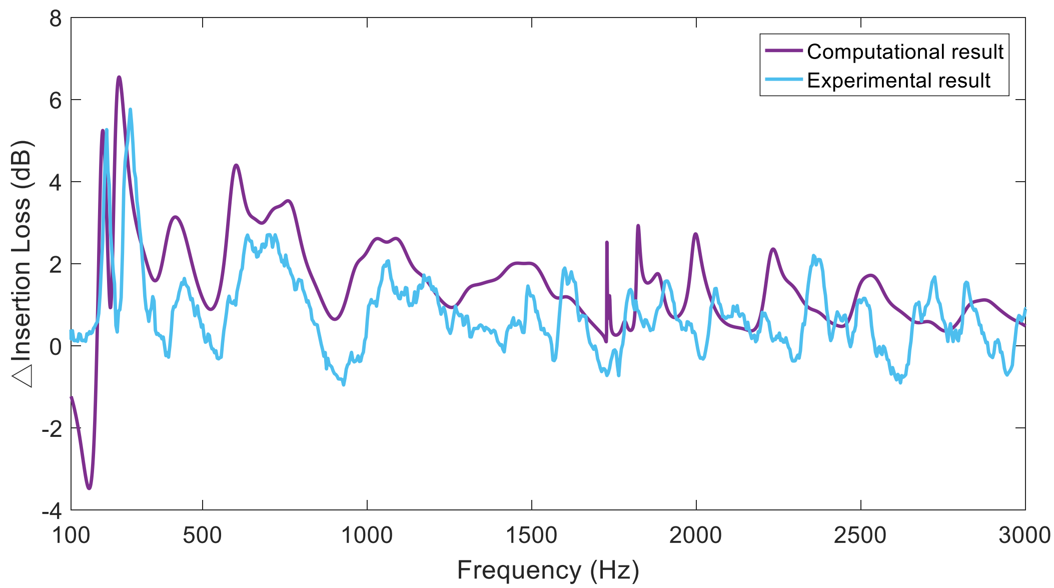

Figure 5.19 Insertion Loss of Model T1

In Figure 5.19, the Insertion Loss of Model T1 is shown. It can be observed that the number of resonance frequencies is much more than S-type and D-type barrier. The magnitude of maximum Insertion Loss is also the highest one. Like the spectrum of D-type barrier, the maximum Insertion Loss is located at first peak of cavity in first row. The magnitude of Insertion Loss decreases during mode order increase. A sharp peak can be noticed clearly at around 1700 Hz which is the first longitudinal mode for these cavities. Noise attenuation performance at high frequency is still poor but has a little improvement than S-type and D-type barrier. Comparison is done on the resonance frequency between calculated and experimental result.

Table 5.9 Resonance frequency of Model T1

Calculated resonance frequency (Hz)	Experimental resonance frequency (Hz)
F1(0,1)214	204
F2(0,1) 285	256
F3(0,1) 571	480
F1(0,2) 643	628
F2(0,2) 857	744
F1(0,3) 1071	1036
F2(0,3) 1429	1488
F1(0,4) 1500	1592
F1,2,3(1,0) 1715	1772
F1(1,1) 1728	
F2(1,1) 1738	
F3(1,1) 1807	1772
F1(1,2) 1831	
F2(1,2) 1917	1964
F1(0,5) 1929	
F2(0,4) 2000	
F1(1,3) 2022	2048
F2(1,3) 2232	2132
F1(1,4) 2278	
F1(0,6) 2358	2340
F3(1,2) 2425	
F2(0,5) 2572	2508

F1(1,5) 2581	
F2(1,4) 2635	2668
F1(0,7) 2786	
F3(0,3) 2858	2856
F1(1,6) 2915	2984

In this Section, the Insertion Loss of D-type and T-type barrier are discussed. Results show that the additional cavity located on the top edge of barrier can improve the noise attenuation at certain frequency, especially in low frequency where the first mode of cavity is located. The maximum Insertion Loss always locates at the first peak of cavity in first row. However, the performance of acoustic cavity decreases when mode order increase and very less improvement on noise attenuation at high frequency for each cavity added on the top edge of barrier. It can be observed that the first longitudinal mode of cavity always appears at around 1700Hz in all types of barriers tested in previous Sections.

Other than the Insertion Loss spectrum analysis on different arrangement on acoustic cavities, Relative Insertion Loss in traffic weighting are also calculated for each barrier type to determine the noise attenuation applied in actual cases. The results are shown in Table 5.10:

	Model S2	Model S1	Model D1	Model D2	Model T1
Plane1	0.53 dB	0.52 dB	0.53 dB	0.55 dB	0.63 dB
Plane2	0.54 dB	0.54 dB	0.56 dB	0.58 dB	0.66 dB
Plnae3	0.58 dB	0.56 dB	0.58 dB	0.59 dB	0.69 dB

Table 5.10 Traffic weighted Insertion Loss of all barrier type

The traffic weighted Insertion Loss of all type barriers is shown in Table 5.10. It can be found that the traffic weighted Insertion Loss of these cases are almost the same. From the results of previous Sections, T-type barrier performs well due to a large number of resonance frequencies and highest magnitude of Insertion Loss at the first peak of cavities. Although T-type barrier can provide up to 5dB improvement on Insertion Loss then reference barrier, the Insertion Loss in these planes are not high at all. The Insertion Loss of D-type barrier is higher than S-type barrier due to noise attenuation is contributed by the cavity in second row.

Correction of traffic weighting is done in low frequency and high frequency much more than frequency around 1000Hz. Therefore, the improvement by resonance frequency are eliminated in result of low traffic weighted Insertion Loss. In contrast, frequency peak of cavity in 0.3 m depth is near 1000 Hz. The frequency range of that peak is wide and the magnitude of Insertion Loss at that peak is high, as a result, the Insertion Loss of Model S2 is higher than others.

5.4.4 Summary

From the results, agreement is made on the effect of noise attenuation by acoustic cavity between computation results and experimental results. First, the depth of acoustic cavity is related to the resonance frequency because of the resonance frequency of acoustic cavity. The maximum Insertion Loss of different S-type barrier is higher than a normal reference barrier for 3.5 dB at the first resonance frequency. The Insertion Loss magnitude decrease when the frequency increases due to the poor performance of acoustic cavity at high modes and the high noise attenuation level of conventional vertical barrier leading edge.

Results show that additional acoustic cavity can improve the performance of noise barrier not in the magnitude of Insertion Loss but in a wider effective frequency range. Since the first peak of cavity is always at low frequency, the Insertion Loss can be improved by around 1 to 2 dB at low frequency range. However, the improvement of Insertion Loss at resonance frequency also leads to an extra reduction on Insertion Loss at around 100 Hz to 200 Hz for 2 dB. Traffic weighted Insertion Loss on each plane behind barrier are presented to reflect the noise attenuation level of cavity in actual environment. Results show that the improvement caused by acoustic cavity is not significant or even low in traffic weighted Insertion Loss. It is because the improvements of acoustic cavity on noise attenuation are always at low frequency range where correction of traffic weighting is made. Therefore, the improvement of cavity reduces significantly.

Conclusion can be drawn by the results that additional cavity can improve the traffic weighted Insertion Loss slightly. To improve the traffic weighted Insertion Loss dramatically, cavity which have resonance frequency around 1000 Hz can contribute a lot to the Insertion Loss. Therefore, suitable selection on cavity depth should be done to provide a good performance on noise attenuation at low frequency and also traffic weighted Insertion Loss.

5.5 Measurements on noise attenuation of long acoustic cavity

In previous Section, the noise attenuation performance of acoustic cavity is investigated. The arrangement of cavity, the depth of cavity and also location of cavity can affect noise attenuation performance in magnitude or resonance frequency. A more important parameter, the length of cavity is considered in this Section. It is assumed that increase the length of acoustic cavity should have an improvement on noise attenuation as using a series of cavities with same depth. Experiments are then conducted to determine the effect on noise attenuation of cavity length.

5.5.1 Configuration of measurement

As same as the configuration in Section 5.4, source and receivers are located at different sides of barrier. The position of loudspeaker is at (-1.3, 0, 0.2) in coordinate system. 1653 receivers are separated into three planes which located at 0.7 m, 1 m, 1.3 m away from barrier. The heights of receivers are from 0.1 m to 3 m with interval 0.1 m and from -1.4 m to 1.4 m in x direction with interval 0.05 m. Fiber glass is used on the hard ground at source side to avoid the sound propagate to receiver under the barrier. An automation system is used to move 29 microphones along x direction. The tested barrier is located at the middle of chamber. The center of barrier is at (0, 0, 0.7) in coordinate system. The dimension of barrier is in 4 m(L) x 0.4 m(W) x 1.4 m(H). The difference to Section 5.4 is that the cavity used in this Section is 4 m long instead 0.3 m long. The models used in this Section are S-type barrier in 4 m length and D-type barrier in 4 m length. The details of these model are shown as Figure 5.20 and Figure 5.21:

Figure 5.20 Acoustic cavities in 4 m length and 0.3 m length

Figure 5.21 Model S2 in 4 m length

5.5.2 Noise attenuation performance of 4m long barrier

Since the tested barrier in previous Section is a finite barrier, the length (z-axis) of acoustic cavity is one of the parameters which will influence the performance of acoustic cavity. Thus, a series of tests are done to investigate the relationship between the length of acoustic cavity and noise attenuation. The result is shown Figure 5.22:

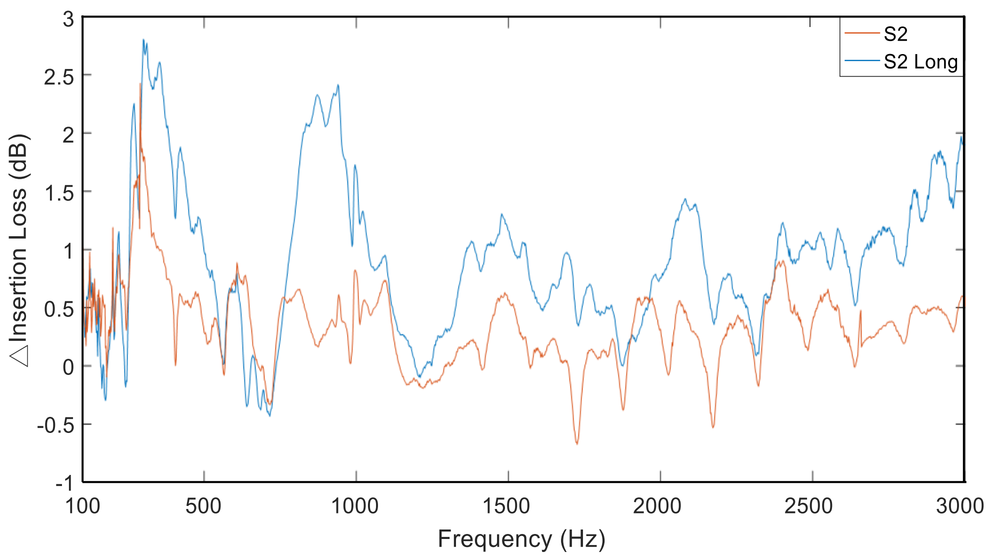

Figure 5.22 Insertion Loss of Model S2 in different length

It can be indicated that the performance of a longer acoustic cavity is better than the shorter one in almost whole frequency range. From Figure 5.22, around 1.5 dB improvement on Insertion Loss is provided by the barrier with 4 m acoustic cavity in low frequency which located at the first to resonance frequency. Moreover, it also gives a good performance at high frequency which is the weakness point of 0.3 m acoustic cavity for 1 dB.

Table 5.11 Resonance frequency of Model S2 in different length

Calculated resonance frequency (Hz)	Experimental resonance frequency of Model S2 (Hz)	Experimental resonance frequency of Model S2 long (Hz)
285	304	300
857	804	872
1429	1396	1378
1715	1672	1768
1738		
1917		
2000	2032	2082
2232		
2572		
2635		

Although the magnitude of Insertion Loss increases in whole frequency, the resonance frequency of Model S2 long is nearly unchanged. From Table 5.11, only a few frequency shifts occur at second resonance frequency. The peak at low frequency is captured easily but the high frequency peak is difficult to found because these of the peaks are hidden by the high noise attenuation of reference barrier.

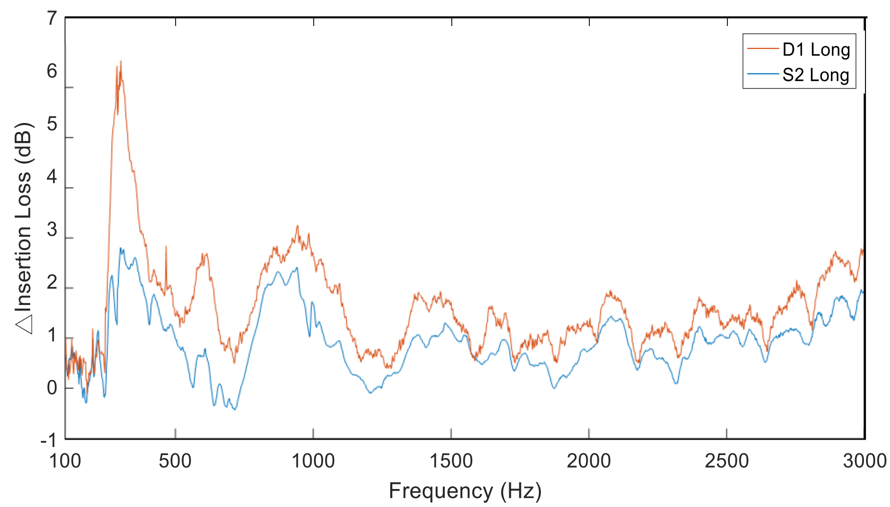

Figure 5.23 Insertion Loss of Model D1 long and Model S2 long

Another experiment is conducted to compare the noise attenuation by a barrier with and without additional 4 m acoustic cavity. In this experiment, 0.3 m depth cavity is located at the first row and 0.4 m depth cavity is located at the second row. It can be observed that the additional cavity provides a higher Insertion Loss than single one in all frequency around 0.5 dB – 1 dB. The length of acoustics cavity can then be concluded that it is proportional to the Insertion Loss of noise barrier. It can provide maximum noise attenuation at the first resonance frequency for 4 dB higher than Model S2 long and even give out at least 0.5 dB improvements in the rest frequency range.

Table 5.12 Resonance frequency Model D1 long and Model S2 long

Calculated resonance frequency (Hz)	Experimental resonance frequency of Model D1 long (Hz)
F1(0,1)214	200
F2(0,1) 285	288
F1(0,2) 643	614
F2(0,2) 857	868
F1(0,3) 1071	1096
F2(0,3) 1429	1382
F1(0,4) 1500	1462
F1,2(1,0) 1715	1698
F1(1,1) 1728	
F2(1,1) 1738	
F1(1,2) 1831	1898
F2(1,2) 1917	
F1(0,5) 1929	
F2(0,4) 2000	
F1(1,3) 2022	2078
F2(1,3) 2232	2232
F1(1,4) 2278	
F1(0,6) 2358	2400
F2(0,5) 2572	
F1(1,5) 2581	
F2(1,4) 2635	

F1(0,7) 2786	2754
F1(1,6) 2915	

Other than the spectrum of Insertion Loss, the noise attenuation of acoustic cavity is observed by traffic weighted Insertion Loss shown as Table 5.13.

Table 5.13 Traffic weighted Insertion Loss of Model D1 long and Model S2 long

	Model S2	Model S2 long	Model D1 long
Plane 1	0.53 dB	0.71 dB	0.77 dB
Plane 2	0.54 dB	0.74 dB	0.81 dB
Plane 3	0.58 dB	0.76 dB	0.86 dB

The noise attenuation of acoustic cavity in traffic weighted is shown in Table 5.13. It can be noticed that the noise attenuation level of Model S2 long is obviously higher than Model S2. Around 0.2 dB difference can be found from both planes. It is because increase the length of cavity is similar to increase the number of cavities used. Although the additional cavity only brings a 0.01 dB or 0.05 dB improvement on the noise attenuation, a 4 m long cavity means it can divide in more than 10 times of cavity used. Therefore, difference can be found between Model S2 and Model S2 long easily. Lastly, different to the results in previous Section. The improvement of additional 4 m long cavity at the second row provides nearly 0.1 dB improvement.

From these results in this Section, conclusion can be drawn that the resonance frequency of cavity is mainly affected by cavity depth but not the cavity length. Therefore, 4 m long cavity have the same resonance frequency as 0.3 m one. Other than that, same as the result in Section 5.4, addition cavity in second row can also improve the noise attenuation level significantly due to the additional resonance frequency of second cavity. At last, the performance of noise attenuation is calculated in traffic weighted Insertion Loss to indicate the performance of barrier in actual environment. It can be observed clearly that long cavity has a better performance than the short one for around 0.2 dB. Further improvement can be achieved by additional cavity in second row. To be concluded, the length of acoustic cavity affects the magnitude of noise attenuation only but with no influence on the resonance frequency on Insertion Loss spectrum.

5.6 Measurements on spatial behavior of acoustic cavity

From Section 5.4 and 5.5, the relation between noise attenuation performance and different cavity parameter are investigated. In this Section, addition experiments are done to study the spatial behavior of acoustic cavity which can also show the diffraction of sound wave after pass over the opening of acoustic cavity.

In this experiment, Model S2 and Model S2 long are used to capture the sound field behind the barrier since the noise attenuation of Model S2 is better than others. The measurement configuration is similar to measurements in Section 5.4 and 5.5. The main difference of configuration is that the number of receivers will reduce to 2 planes instead of 3 planes. Result is shown as Figure 5.24:

Calculated resonance frequency (Hz) | Model S2 | Model S2 long

dB

285

857

1429

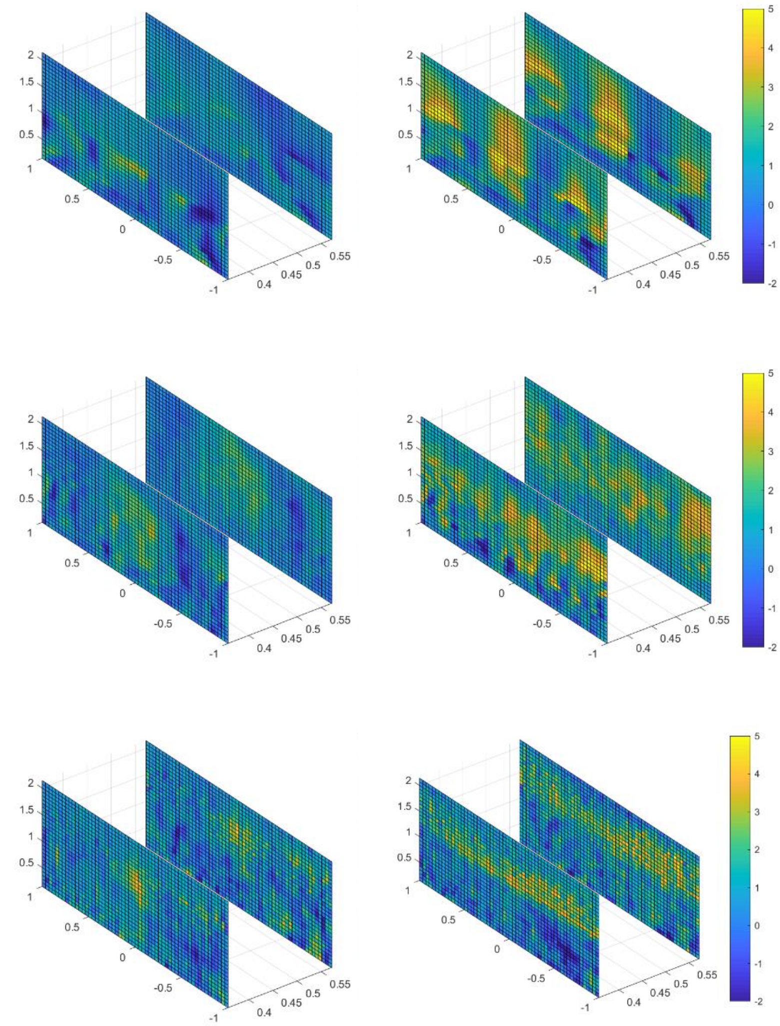

2000

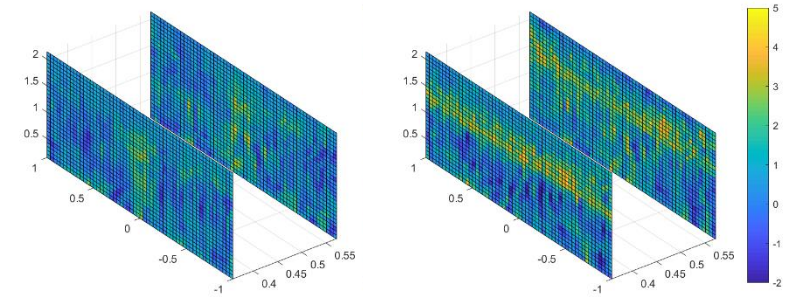

2572

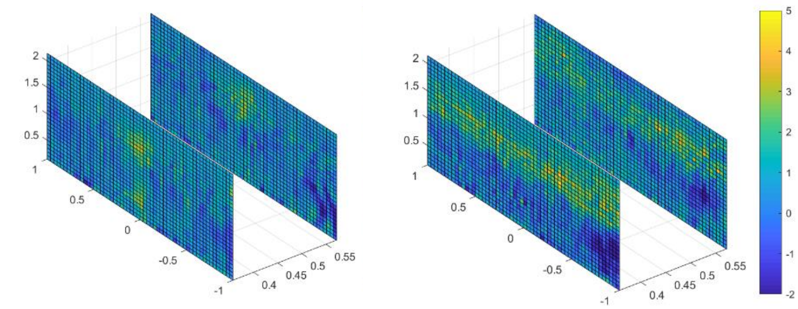

Figure 5.24 Insertion Loss of Model S2 and Model S2 long

Figure 5.24 shows that the Insertion Loss of Model S2 and Model S2 long compare to reference barrier to make obvious result on the spatial behavior of cavities. Therefore, the negative value obtained in these results means that the noise attenuation performance at that point is worse than conventional vertical barrier. Moreover, the X, Y, Z axes are normalized value base on the height of barrier which is 1.4 m and the center of barrier is located at position (0, 0, 0.5).

It can be noticed that when it is at resonance frequency, the Insertion Loss due to acoustic cavity on barrier increase. From Figure 5.24, Insertion Loss can reach 2 dB than reference barrier which same as the results from previous

Sections. At 285 Hz, it can be found that an increase of Insertion Loss appears around the middle part where the barrier top edge in the result of Model S2 is. The maximum Insertion Loss around top edge is 3 dB higher than reference barrier. The width of that region is round 0.125 units and the height of that region is from 0.5 to 2 units. From the result of Model S2 long at 285 Hz, although Insertion Loss of a large region increases, the shape of that region is not matching our prediction which is in rectangular shape. It can be seen that the effective region can divide into 3 parts. The maximum Insertion Loss of these regions provides 5 dB more than reference barrier. The width of these regions is around 0.4 units. The height of middle region is around 1 unit and two side regions are 0.5 unit. Although 0.4 m cavity is located on the whole top edge of barrier, the highest Insertion Loss is only located at the middle of barrier but not along the top edge of barrier uniformly.

From results of 857 Hz, it can be observed that the effective region of 0.3 m cavity become higher and wider. The maximum Insertion Loss is remains in certain level around 3 dB. The width of region becomes 0.3 units and the height of region becomes same as the measurement domain. A large effective region along the barrier top edge is produced by 4 m long cavity. Although the Insertion Loss is not uniform in this region, it is always around 1.5 dB. The Maximum Insertion Loss appears at the right-hand side of measurement domain which is 5 dB higher than reference barrier. The width of that region becomes the whole width of measurement domain and the height becomes 1.5 units.

From the result of 1429 Hz, the width of effective region of 0.3 m long cavity remains unchanged where the height of that region becomes the whole measurement domain. The maximum Insertion Loss located at position at the middle of barrier top edge. The magnitude of this position is around 4 dB. From the other side, a rectangular effective region is formed by 4 m long cavity above the top edge of barrier. The width of that domain remains unchanged where the height reduces to 0.5 units. The position of maximum Insertion Loss moves closer to the middle of barrier, but the magnitude also reduces to 4 dB.

From the results of 2000 Hz, the effective region remains its width and height as in 1429 Hz. However, the magnitude of maximum Insertion Loss reduces to 3 dB. Moreover, the position of maximum Insertion Loss remains located at the middle of barrier top edge. The effective region of 4 m long cavity is similar to that of 0.3 m cavity. The width of effective region and maximum Insertion Loss position remains unchanged. The height of effective region increases to 1 unit above the barrier top edge.

From the figure of 2572 Hz which is the fifth mode of 0.3 m depth cavity. The effective region become difficult to indicate since conventional vertical barrier provides good noise attenuation at this frequency. The width and height of effective region remains no change. The position of maximum Insertion Loss moves upper but still at the middle part of barrier. The magnitude keeps in 3 dB higher than reference barrier. A big difference is found in the result of 4 m long cavity which is the average Insertion Loss in effective region decrease while the width of effective region, the height of effective region and the position of maximum Insertion Loss remains unchanged.

A conclusion can be drawn by the results is that an effective region can be found when resonance frequency appears at that frequency band. Besides that, these effective region and maximum Insertion Loss position are always close to the barrier top edge. It is because the effect of cavity became stronger when it is closer to cavity opening. Moreover, the width and height of effective regions keeps changing until the third mode appear. By the results in Section 5.4, the magnitude of Insertion Loss become smaller after the third mode which also be the reason of no sudden change to the effective region. When the mode order or frequency increase, the Insertion Loss in the effective region and maximum Insertion Loss reduce due to the poor performance of cavity at high frequency. The area of effective region formed by 0.3 m span cavity at resonance frequency is always 0.3 units wide and 0.5-1 unit high where it is always 2 units wide and 0.5 unit high from 4 m long cavity. The spatial behavior of acoustic cavity can then be drawn that the effective region of 0.3 m cavity is around 0.3 units wide and 0.5 unit high. The relation on the length of cavity and the width of effective region is directly proportional to each other.

5.7 Summary

In this chapter, scale model tests are conducted to investigate the effect on noise attenuation level of finite barrier by the aid of acoustic cavity on its top edge. The improvement by acoustic cavity is assessed in various acoustic cavity arrangements. Similar to the results of numerical computation, the performance of acoustic cavity can be indicated by Insertion Loss and resonance frequency compare with conventional vertical barrier (reference barrier in this study.)

To investigate the performance of acoustic cavity on barrier, study is done on acoustic cavity only to ensure they can provide expected noise attenuation at its resonance frequencies. The dimension of the acoustic cavity follows that in the computation and the material of barrier and cavity are wooden board which is assumed acoustically rigid.

At first, the performance of single cavity case is done by changing the depth of cavity. Results show that these cavities can provide a good performance on noise attenuation than reference barrier. Especially at its resonance frequency within the low frequency range, maximum attenuation is always located at the first mode along cavity central axis and the maximum value of insertion loss seems unchanged at around 3.5 dB in all the single cavity cases tested.

Then the performance of additional acoustic cavity is investigated. An additional cavity can provide a better IL than single cavity case by broadening the effective frequency range which is the resonance frequency of additional cavity. Although the performance is improved by enlarging the resonance frequency, the maximum value of Insertion Loss still keeps in the same value. Experiment on triple cavities cases is done to further determined the performance of addition acoustic cavity and result confirm that number of addition cavities can increase the noise attenuation by a wider resonance frequency but not affect to the maximum value of Insertion Loss at resonance frequency.

Based on these results, another parameter is being concerned to increase the Insertion Loss other than broaden resonance frequency of acoustic cavity. Acoustic cavity with longer length is than examined to illustrate the effect on the magnitude of Insertion Loss. Results shows that the resonance frequency is dominated by the depth of acoustic cavity and the magnitude of Insertion Loss even in high frequency is related to the length of acoustic cavity. Further confirmation is done by utilizing the additional cavity with same length as first row, results are similar to the test in previous Section that addition cavity will only improve the performance by a wider effective frequency band.

At the last part of this chapter, measurements are carried out to determine the spatial behavior of cavity on the noise attenuation behind barrier. Model S2 and Model S2 long are chosen to undertake the measurements with 0.3 m cavity depth. Results show that these cavities can form an effective region with higher Insertion Loss at resonance frequency. The magnitude of Insertion Loss at that region becomes lower when the frequency or order of mode increases. The volume of the effective sound reduction region is dependent on frequency until the latter exceeds the third longitudinal mode frequency of the cavity. The area of effective region formed by a 0.3 m span cavity is 0.3 unit wide and 0.5 units high while that formed by a 4 m span cavity is 2 units wide and 0.5 units high. It is further confirmed that the increase in the span of cavity will give rise to a higher noise attenuation.

6. Conclusions

This is the last chapter of this thesis, a summary of all the findings are presented. Other than that, future work is also recommended to investigate the diffraction property of sound pass over the acoustic cavity on the top surface of barrier.

6.1 Summary

Acoustic cavity is a well-known device on noise attenuation. It can provide a significantly high noise attenuation at its resonance frequencies. In this study, acoustic cavities are applied to a conventional vertical barrier. A detailed investigation on Insertion Loss with different cavity installations, such as different cavity depth, different separation between cavity and barrier leading edge, different cavity arrangements and different cavity length, is conducted by two dimensional numerical computations and 1:3 scale model experiments. The main findings are listed as follows:

It is clearly found that the installation of acoustic cavity on barrier top edge can improve the noise attenuation level at the shadow zone by 1 dB. Significant improvement can be observed at the resonance frequencies of cavity. The highest Insertion Loss, which is 3-5 dB higher than that of a conventional vertical barrier, is found at the first resonance frequency which is also the first longitudinal mode of cavity. However, it can also be seen that the improvement on noise attenuation level is decreased with increasing frequency or acoustic mode number because of the high noise attenuation of conventional vertical barrier at high frequencies.

When the separation between barrier leading edge and acoustic cavity is increased, Insertion Loss is decreased. Around 1 dB difference on Insertion Loss can be found when the cavity is placed near the leading and rear edge of barrier. The cavity resonance frequencies are shifted to low frequency side by 10-20 Hz. Thus, acoustic cavity should be placed close to barrier leading edge in order to achieve its highest noise attenuation performance.

Computational and experimental results show that the resonance frequencies of the cavity are affected by the depth of the cavity. The resonance frequencies increase with cavity depth. Although resonance frequencies change with cavity depth, the highest Insertion Loss is still found at the first resonance frequency. A suitable cavity depth should be considered to deal with different traffic noise problems.

In order to broaden the frequency range with high Insertion Loss, extra acoustic cavity with different cavity depth can be installed on the barrier top edge. Various barrier models are tested in this study. It is found that the Insertion Loss level of multiple acoustic cavities barrier is higher than that of a single cavity barrier by around 0.5 dB. Significant improvement of 2-3 dB can be observed at the resonance frequencies of extra cavities. The more these extra cavities are installed on barrier top edge, the higher the Insertion Loss can be achieved. However, the arrangement of acoustic cavities on barrier top edge will affect the Insertion Loss especially at the resonance frequencies of cavities. The cavity in the first row will contribute more to the Insertion Loss because of the effect on separation between barrier leading edge and cavity. The Insertion Loss at the resonance frequencies of the cavities in second and third row is decreased by 0.1- 1 dB and 0.5-2 dB respectively.

The effect of cavity span on noise attenuation level is investigated. To improve the performance of noise barrier, cavity length should be increased. It is because the longer the cavity span, a larger opening surface is provided, and more sound can be diffracted by the acoustic cavity. Even though the Insertion Loss is increased, no resonance frequency shift is found. Around 1.5 dB improvement is found across the whole frequency range of interest by extending the cavity span in both single cavity barrier and multiple cavities barrier cases.

Lastly, spatial behavior of sound at shadow zone is investigated. An effective sound reduction region, a region with higher Insertion Loss (1-2 dB) than the rest of the shadow zone, can be found when acoustic cavity is installed on the top edge of the barrier. The effective sound reduction region is always observed at the cavity resonance frequencies. The center of this region is located at the same height as the barrier top edge and directly behind the center of acoustic cavity opening. The size of this region and even the Insertion

Loss in this region decrease with increasing frequency. The largest effective sound reduction region with the highest Insertion Loss can be obtained at the first resonance frequency. About 2-3 dB improvement of Insertion Loss at sound reduction region can be obtained by extending the cavity span. The size of this region is also increased.

Acoustic cavity gives a significant improvement on barrier noise attenuation level compared to a conventional vertical barrier at its resonance frequencies when it is applied on the top edge of the barrier. In order to achieve the highest barrier noise attenuation performance, long acoustic cavities should be used to provide a higher broadband Insertion Loss.

6.2 Future works and recommendation

Based on the findings obtained during the whole study, future works are recommended for further understanding on the barrier noise attenuation performance with acoustic cavity on its top edge.

First, two dimensional numerical computations are carried out in this study, it is useful for predicting the cavity resonance frequencies and Insertion Loss at these frequencies, but results are different from those in the actual case. Three dimensional computations are recommended to find out the three-dimensional effect, such as the sound diffraction from both vertical barrier side edges, on barrier noise attenuation level.

Moreover, further investigation on the arrangement of acoustic cavity should be done. It is interesting to find out how the barrier noise attenuation level and spatial behavior of sound at shadow zone are affected by installing cavities in other arrangements, such as installing cavities in random positions and installing cavities with different length in same row.

In this study, the position of the sound source is fixed. Further studies can be carried out to observe how the barrier noise attenuation is affected by different sound incidence angles and its effect on the effective sound reduction region.

Ground effect is not considered in this study. However, it is one of the main factors affecting the noise attenuation performance of barrier in actual environment. Investigation should be carried out to observe the barrier noise attenuation performance by the coupling effect between ground and acoustic cavities.

Reference

Andersib, J.S., Bretos-Anerson, M, Noise Its Measurements, Analysis, Rating and Control, ISBN 0 291 39794 8, Published by Avebury Technical, 246-252, 1993.

Alfredson, R.J., Du, X., Special Shapes And Treatment For Noise Barriers, Inter-Noise 95. Newport Beach, CA, USA, 381-384, July 10-12,1995.

Attenborough, K., Understanding and Controlling Acoustics Effects of Outdoor Surfaces, IMechE Seminar Publication 2000-3, Noise and Vibration, Advances in Research and Development, S682/003/99, 29-38, 2000

Born, M.and Wolfm, E., Principles of Optics, Electromagnetics Theory of Propagation, Interference and Diffraction of Light, Pergamon Press , Cambridge, UK,1975.

Boulanger, P., Attenborough, K., Taherzadeh, S., Aters-Fuller, T., Kai, M.L., Ground Effect Over Hard Rough Surfaces, J.Acoust.Soc.Am., 104(3), Pt. 1, 1474-1482, September 1998

BS EN 1793-3, Road traffic noise reducing devices- Test method for determining the acoustic performance. Part 3. Normalized traffic noise spectrum, British Standard, 1998

Carlas, H. S., Diffraction of waves by a wedge of any angle, P. Lond. Math. soc, 18,1291-1306,1920.

Carslaw, H.S., multiform solutions of the partial differential Equations of physical mathematics and their application, P.Lond.Math.soc,30,121-161,1899.

Cannelli, G.B. Traffic noise pollution in Rome. Appl. Acoust., 72, 103-116, 1974.

Chakrabarty,D., Santra, S.C. and Mukherjee, A. Status of road traffic noise in Calcutta metropolis, India. J.Acoust.Soc.Am., 101(2), 943-949,1997.

Copson, E. T., On an integral Equation arising in the theory of diffraction, Q.J.Math, 17,19-34,1946.

Crighton, D.G., Doling, A.P., Flowcs Williams, J.E., Heckl, M., and Leppington, F.G., Modern Methods in Analytical Acoustics Lecture Notes, Springer-Verlag, London, Ch.5,1996.

Daigle, G.A., Diffraction of Sound By A Noise Barrier In The Presence of Atmospheric Turbulence, J.Acoust.Soc.Am., 71(4), 847-854, April 1982.

Embleton, T.F.W., Line integral theory of barrier attenuation in the presence of the ground, J. Acoust. Soc. Am., 71,42-45,1980.

Fehr, R.O., The Reduction of Industrial Machine Noise, Proceedings of Sound Annual Noise Abatement Symposium, 93-103, October 1951.

Fujiwara, K., Hothersall, D.C., Kim, C. Noise Barriers with Reactive Surfaces, Appl. Acoust., 53(4), 255-272, 1998.

Fujiwara, K. and Furuta, N. Sound Shielding Efficiency of a Barrier with a Cylinder at the Edge, Noise Control.Eng.J., 37(1) ,5-11, July-August 1991.

Gharabegian, A. Improving Sound wall Performance Using Route Silent, Inter-Noise 95, Newport Beach, CA, USA, 385-388, JULY 10-12, 1995.

Griffin S, Lane SA, Huybrechts S. Coupled Helmholtz resonators for acoustic attenuation. J. Vib. Acoust. 123,11-17,2001.

Hayek, J.J., and Blaney, C.T., Evaluation of T-Profile Highway Noise Barriers, Transportation Research Record 983, Issues in Transportation Noise Mitigation: Highway and Railway Studies, 8-17, 1984.

Hayek,S.I., Noise Reduction by Absorbent Double Parallel Barriers Over Hard Ground, Inter-noise 85, Munich, 495-498, 18-20 September, 1985.

Hecht, E., Optics, Addison-Wesley Publishing Company, Wokingham, fifth edition ,1998.

Hothersall, D.C. Modelling The Performance of Noise Barriers, Euro symposium 1992, The Migitation of Traffic Noise in Urbam Areas, 247-258, 1992

Hothersall, D.C., Crombie, D.H. and Chandler-Wilde, The performance of T-Profile and Associated Noise Barriers, Appl. Acoust., 32, 269-287, 1991

Hutchins, D.A., Jones, H.W., and Russell, L.T., Model Studies of Barrier Performance in The Presence of Ground Surfaces, Part II- Different Shapes, J.Acoust.Soc.Am., 75(6), 1817-1826, June 1984

Ingard U. On the theory and design of acoustic resonators. J. Acoust. Soc. Am. 25, 1037–1061 ,1953.

Isei, T., Absorptive Noise Barrier on Finite Impedance Ground, J.Acoust.Soc.Jpn. (E), 1, 3-10, 1980.

Ishizuka, T., and Fujiwara, K., “Performance of noise barriers with various edge shapes and acoustical conditions,” Appl. Acoust., 65(2), 125-141, February 2004.

Jin, B.J., Kim, H.S., Kang, H.J., and Kim, J.S., Sound diffraction by a partially inclined noise barrier, Appl. Acoust., 62, 1107-1121,2001.

Jonasson, H.G. Sound Reduction By Barriers On The Ground, J.Sound Vib.,22(1),113-126,1972

Ko, N.W.M. Traffic noise in a high-rise city. Applied Acoustics, 1978, 11(3), 225-239.

Koers, P., Diffraction by An Absorbing Barrier or By an Impedance Transition, Inter-Noise 83, 1983, 31-314.

Koyashu, M. and Yamashita, M., Scale Model Experiments on Noise Reduction By Acoustic Barrier of A Straight Line Source, Appl. Acoust., 6 233-242, 1973

Kryter,K.D. The effects of noise on man. New York: Academic Press, second edition, 1985.

Kurze, U.J. and Anderson, G.S. Sound Attenuation By Barriers, Appl. Acoust., 4, 35- 53, 1971.

L'Esperance, A., Nicolas, J., Daigle, G. A., Insertion loss of absorbent barriers on ground, J. Acoust. Soc. Am., 86(3), 1060-1064, September 1989.

L'Esperance, A., The Insertion loss of finite length barriers on the ground, J. Acoust. Soc. Am., 86(1), 179-183, July 1989.

Lam, Y.M. and ROBERTS, S.C., A simple method for accurate prediction of finite barrier insertion loss, J.Acoust.Soc.Am., 93(3), 1445-1452, March 1993.

Lam, Y.M., Using Maekawa's Chart to Calculate Finite Length Barrier Insertion Loss, Appl. Acoust., 42, 29-40,1994.

Leang, L.K., Yamashita, Y., Matsui, M., Simplified calculation method for noise reduction by barriers on the ground, J.Acoust.Soc.Jpn(E), 11(4), 199-206,1990.

Levine, H. and Schwinger, J., On the theory of diffraction by an aperture in an infinite plane screen. I, Phys.Rev., 74,958-974,1948

Lyon, R.H., and Cann, R.J., Acoustical Modelling in Urban Environments, Inter-noise 74, Washington, D.C.,457-460, September30-October2, 1974

MacDonald, H. M., A class of diffraction problem, P. Lond. Math. soc , 14,410-427,1915.

Maekawa,Z., Noise Reduction by Screens, Appl. Acoust., 1,157-173,1968.

Maekawa,Z., Noise Reduction by screens, Memoirs of The Faculty of Engineering, Kobe University, (11),29-53,1965.

May, D.N. and Osman, M.M., Highway Noise Barriers: New Shapes, J.Sound Vib., 71(1), 73-101, 1980.

Monazzam .M.R., Lam .Y.W., Performance of profiled single noise barriers covered with quadratic residue diffusers. Appl. Acoust., 66,709-730, 2005.

Muradali,A., and Fyfe, K.R., A Study of 2D and 3D Barrier Insertion Loss using Improved Diffraction-based Methods, Appl. Acoust., 53(1-3), 49-75,1998

Menounnou, P., A correction to Maekawa;s curve for the insertion loss behind barriers, J.Acoust.Soc.Am, 110,1828-1838,2001.

Onuu, M.U., Road traffic noise in Nigeria: measurements, analysis and evaluation of nuisance. J.Sound Vib., 233(3), 391-405, 2000.

Piechowicz. J., Sound Wave Diffraction at the Edge of a Sound Barrier, Acta Phys. Pol. A, 119, 1040-1045, 2011.

Priede, T., Origins of automotive vehicle noise. J.Sound Vib., 15(1),61-73,1971.

S. G. Johnson, “Notes on Perfectly Matched Layers (PMLs),” 2010.

Rathe, E.J., Note on to common problems of sound propagation, J.Sound Vib.,10,472-479,1969

Redfearn, S.W., Some acoustical source-observer problems, Philos.Mag.30,223-236,1940.

Salomons, E., Geerlings, A.C., and Duhamel, D., Comparison of a Ray Model and A Fourier – Boundary Element Method for Traffic Noise Situations Acoustics with Multiple Diffractions and Reflections, Acustica – J.Eur.Acoust.Asso., 83(1),35-47,1997

Sandberg, U., A road surface for reduction of tire noise emission. In: Proceeding of Inter-noise 79, Warszawa, Poland, September, 1979

Scholes, W.E., Salvidge, A.C., and Sargent, J.W., Field Performance of A Noise Barrier, J.Sound Vib., 16(4), 627-642, 1971

Seznec, R., Diffraction of Sound Around Barriers: Use if The Boundary Elements Technique, J.Sound Vib., 73(2), 195-209,1980

Skudrzyk, E.J., The Foundations of Acoustics, Springer-Verlag,New York,1971.

Sommerfeld.A, Mathematische Theorie der Diffraktion, Math.Ann., 47,317-341,1896.

Sommerhoff,J., Recuero, M., and Suarez, E., Community noise survey of the city of Valdivia, Chile. Appl. Acoust., 65(7), 643-656, 2004.

Sutherland, L.C., and Daigle, G.A., Atmospheric Sound Propagation, Chapter 28, Handbook of Acoustic, M. J. Crocker(Editor), 305-329,1998

Takagi, K., Hotta, R. and Yamamoto, K., A Simple Method for the Calculation of Noise Attenuation by A Finite Length Barrier, Appl. Acoust., 43, 353-365, 1994.

Tang PK, Sirignano WA. Theory of generalized Helmholtz resonator. J.Sound Vib. 26,247–262,1973.,.

Tatge, R.B. Barrier-wall attenuation with a finite-sized source, J.Acoust.Soc.Am., 53,1317-1319,1973.

Tolstoy, I. Diffraction by a hard truncated wedge and astrip, IEEE J.Ocean Eng., 14,4-16,1989.

Tolstoy, I. Exact, explicit solutions for diffraction by hard sound barriers and seamounts, J.Acoust. Soc. Am., 85,661-669,1989.

Watts, G.R. Acoustics Performance of a Multiple Edge Noise Barrier Profile at Motorway Sites, Appl. Acoust., 47, 47-66, 1996.

Watts, G.R., Crombie, D.H. and Hothersall, D.C. Acoustic Performance of New Designs of Traffic Noise Barriers: Full Scale Tests, J.Sound Vib., 177(3), 289-305, 1994.

Wright, M.C.M., Lecture Notes on the Mathematics of Acoustics, Part II, Ch5, Imperial College Press, London ,2005.

Xu, M.B., Selamet, A., Kim, H. Dual Helmholtz resonator, Appl. Acoust., 71, 822-829 ,2010.

Yamamoto, K., Yamashita, M., Yoshida, Shono, Y., Application of Noise Abatement Devices At The Top of Highway Noise Barrier, Inter-Noise 95, Leuven-Belgium, 1719-1722, August 24-26, 1993.

Yamamoto, K., Taya, K., Tamashita, M., and Katsunori, T., Reduction of Road Traffic Noise by Absorptive Cylinder Adapted at The Top of A Barrier, Inter-noise 89, Newport Beach, Ca, USA,349-352, , December 4-6,1989.

Yamamoto,K. and Takagi,K., Expression of Makekawa's chart for Computation. Appl. Acoust., 37, 75-82, 1992.

Yamashita, M., and Yamamoto, K., Scale Model Experiments for the Prediction of Road Traffic Noise and the Design of Noise Control Facilities, Appl. Acoust., 31, 185-196,1990.